

UNIVERSIDADE ESTADUAL DE MARINGÁ
CENTRO DE CIÊNCIAS BIOLÓGICAS
PROGRAMA DE PÓS-GRADUAÇÃO EM CIÊNCIAS BIOLÓGICAS
ÁREA DE CONCENTRAÇÃO EM BIOLOGIA CELULAR E MOLECULAR

THATIANE RODRIGUES MOTA

**CHEMICAL PRETREATMENTS AND SUPPRESSION OF
BAHD ACYL COA TRANSFERASE ENHANCE THE
PLANT CELL WALL SACCHARIFICATION**

MARINGÁ
PARANÁ - BRASIL

2019

UNIVERSIDADE ESTADUAL DE MARINGÁ
CENTRO DE CIÊNCIAS BIOLÓGICAS
PROGRAMA DE PÓS-GRADUAÇÃO EM CIÊNCIAS BIOLÓGICAS
ÁREA DE CONCENTRAÇÃO EM BIOLOGIA CELULAR E MOLECULAR

THATIANE RODRIGUES MOTA

**CHEMICAL PRETREATMENTS AND SUPPRESSION OF
BAHD ACYL COA TRANSFERASE ENHANCE THE
PLANT CELL WALL SACCHARIFICATION**

Tese apresentada ao Programa de Pós-Graduação em Ciências Biológicas (área de concentração - Biologia Celular e Molecular), da Universidade Estadual de Maringá para a obtenção do grau de Doutora em Ciências Biológicas.

Orientador: Wanderley Dantas dos Santos

MARINGÁ
PARANÁ - BRASIL

2019

Dados Internacionais de Catalogação-na-Publicação (CIP)
(Biblioteca Central - UEM, Maringá - PR, Brasil)

M917c

Mota, Thatiane Rodrigues

Chemical pretreatments and suppression of bahd acyl coa transferase enhance the plant cell wall saccharification / Thatiane Rodrigues Mota. -- Maringá, PR, 2019.
100 f.: il. color., figs., tabs.

Orientador: Prof. Dr. Wanderley Dantas dos Santos.

Tese (Doutorado) - Universidade Estadual de Maringá, Centro de Ciências Biológicas, Departamento de Bioquímica, Programa de Pós-Graduação em Ciências Biológicas (Biologia Celular), 2019.

1. Bioquímica de Plantas. 2. Sacarificação enzimática. 3. Parede celular vegetal. 4. Biomassa lignocelulósica. I. Santos, Wanderley Dantas dos, orient. II. Universidade Estadual de Maringá. Centro de Ciências Biológicas. Departamento de Bioquímica. Programa de Pós-Graduação em Ciências Biológicas (Biologia Celular). III. Título.

CDD 23.ed. 572.82

THATIANE RODRIGUES MOTA

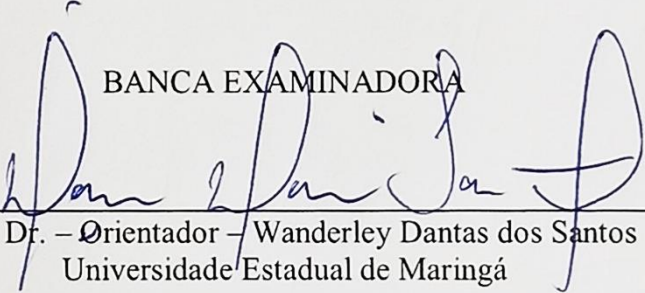
CHEMICAL PRETREATMENTS AND SUPPRESSION OF BAHD ACYL COA
TRANSFERASE ENHANCE THE PLANT CELL WALL SACCHARIFICATION

Tese apresentada ao Programa de Pós-
Graduação em Ciências Biológicas (área de
concentração – Biologia Celular e
Molecular), da Universidade Estadual de
Maringá para a obtenção do grau de
Doutora em Ciências Biológicas.

Aprovada em:

31, 10, 19

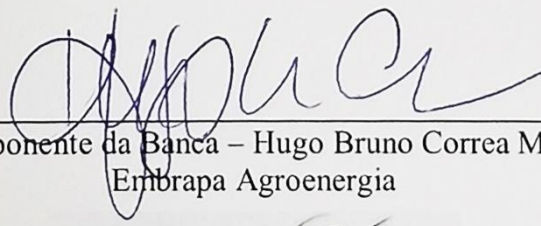
BANCA EXAMINADORA



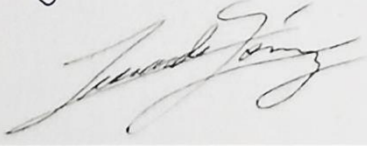
Prof. Dr. – Orientador – Wanderley Dantas dos Santos
Universidade Estadual de Maringá



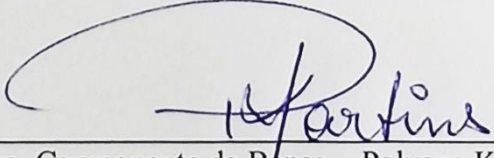
Profª. Dra. Componente da Banca – Emy Luiza Ishii Iwamoto
Universidade Estadual de Maringá



Dr. Componente da Banca – Hugo Bruno Correa Molinari
Embrapa Agroenergia



Dr. Componente da Banca – Leonardo Gomez
University of York



Dra. Componente da Banca – Polyana Kelly Martins
GDM Genética do Brasil

BIOGRAFIA

Thatiane Rodrigues Mota nasceu em Altamira, Pará em 23/01/1989. Possui graduação em Ciências Biológicas pela Universidade Estadual de Maringá (UEM-2012) e Mestrado em Ciências Biológicas pelo Programa de Pós-Graduação em Ciências Biológicas (UEM-2014). Atualmente está concluindo o Doutorado (UEM-2015/2019) pelo mesmo Programa de Pós-Graduação, onde desenvolveu a sua tese em bioquímica de plantas sob a supervisão do professor Wanderley Dantas dos Santos.

Em 2017, realizou estágio na Embrapa Agroenergia em Brasília, DF, sob a supervisão de Hugo Bruno Correa Molinari, onde trabalhou com biotecnologia vegetal, transformação genética de plantas e caracterização química da parede celular de *Setaria viridis* silenciadas por RNA de interferência. O foco deste projeto foi compreender como as alterações moleculares dos genes silenciados estão envolvidos na modificação da parede celular e como elevar os níveis de açúcares produzidos durante a sacarificação, visando aumento na produtividade de bioetanol de cana-de-açúcar, o que culminou em resultados inéditos na literatura. De 2018 a 2019 realizou o doutorado sanduíche pelo Programa de Doutorado Sanduíche no Exterior (CAPES-PDSE) na *University of York*, York, Reino Unido, sob a supervisão de Simon McQueen-Mason e Leonardo Dario Gomez, onde trabalhou com plataformas robóticas e metodologias *high throughput* para caracterização da parede celular de biomassas vegetais submetidas a distintos pré-tratamentos, visando a otimização do processo de sacarificação para aplicação em indústrias de bioetanol. Também realizou um treinamento em análise de polissacarídeos na *University of Cambridge* – Cambridge, Reino Unido, sob orientação de Paul Dupree.

Desenvolveu seus conhecimentos em diferentes aspectos da biossíntese, estrutura e degradação da parede celular plantas, principalmente gramíneas, buscando compreender a organização e dinâmica da parede celular e, para isso, utilizou duas abordagens distintas, porém complementares: caracterização de plantas silenciadas por RNAi e pré-tratamento da biomassa lignocelulósica. Seus estudos resultaram em descobertas e publicações de artigos científicos em revistas científicas internacionais, seja como primeira autora dos trabalhos ou colaboradora científica em outras publicações. Tem experiência na área de Bioquímica de Plantas, atuando principalmente nos seguintes temas: bioquímica e fisiologia molecular de plantas, caracterização da parede celular, metabolismo de lignina, pré-tratamento de biomassas, sacarificação enzimática e aplicação de técnicas de alto rendimento para análise de parede celular vegetal.

AGRADECIMENTOS

Agradeço a Coordenação de Aperfeiçoamento de Pessoal de Nível Superior (CAPES), pela concessão da bolsa de doutorado e a CAPES-PDSE pela concessão da bolsa de doutorado sanduíche no exterior.

Ao meu esposo, Dyoní Matias de Oliveira, pela parceria, incentivo, compreensão, paciência, companheirismo, incentivo e apoio incondicional às minhas decisões. Obrigada por estar sempre ao meu lado!

Aos meus pais, Valquiria Laurindo Mota e Laércio Rodrigues Mota, pela segurança que sempre me proporcionaram, pelo amor, por todo o esforço que dedicaram às minhas conquistas, pelo apoio, exemplos de vida e perseverança. Obrigada por sempre confiarem em mim!

As minhas irmãs, Christiane e Sandra, sobrinhos e cunhados, pelos momentos alegres, de descontração, amizade e confiança depositadas em mim.

Ao Professor Dr. Wanderley Dantas dos Santos, pela confiança, convivência, oportunidade, apoio para seguir na carreira científica e supervisão para o desenvolvimento da tese.

Aos Professores Dr. Osvaldo Ferrarese-Filho e Dr. Rogério Marchiosi pela parceria e convivência ao longo desses quatro anos no Laboratório de Bioquímica de Plantas (BIOPLAN).

Ao Dr. Hugo Bruno Correa Molinari, da Embrapa Agroenergia (Brasília, DF, Brasil), pela oportunidade de realizar o estágio no laboratório de Genética e Biotecnologia de plantas.

Ao Professor Dr. Simon J. McQueen-Mason e Dr. Leonardo D. Gomez, da *University of York* (York, UK) pela oportunidade de realizar o doutorado sanduíche no CNAP (*Center of Novel Agricultural Products*) e pelos conselhos acadêmicos e discussões científicas.

A Professora Dra. Camila Alves de Rezende, da Universidade de Campinas (UNICAMP, Campinas, SP), pelas discussões científicas.

Aos colegas de laboratório da Embrapa Agroenergia, em especial o Dr. Wagner R. de Souza, que me auxiliaram e contribuíram para o desenvolvimento do trabalho.

Aos colegas de laboratório do BIOPLAN e CNAP.

Aos técnicos do Laboratório de Bioquímica de Plantas da UEM (BIOPLAN) Aparecida Maria Dantas e Fabiano Rodrigo.

A Rachael Hallam, Julia Crawford, Alexandra Lanot, Mônica Bandeira, Clare Steele-King e Caragh Whitehead pelo auxílio técnico no CNAP.

A secretária do PBC, Érica, pelo auxílio nas documentações.

A todos os pesquisadores que figuraram como coautores dos trabalhos, que colaboraram com análises experimentais, discussões dos dados e no processo de escrita dos artigos científicos.

A Deus e a todas as boas energias do Universo!

Meus sinceros agradecimentos.

When we focus on what matters, we can build the lives we want in the time we've got!
(Laura Vanderkam)

“Vá em busca de seus sonhos”.

ÍNDICE

Biografia	04
Agradecimentos	05
Apresentação	09
Resumo geral	11
General abstract	12
Chapter 1. Plant cell wall composition and enzymatic deconstruction	13
Abstract	14
1. Introduction	15
2. Structure of lignocellulose	17
2.1. Cellulose	17
2.2. Hemicellulose	18
2.3. Pectin	20
2.4. Lignin.....	20
3. Enzymatic breakdown of lignocellulose	22
3.1. Cellulases.....	22
3.2. Hemicellulases.....	23
3.3. Pectinases.....	24
3.4. Ligninases	24
4. Pretreatments of lignocellulosic biomass.....	25
5. Conclusions	27
References	28
Chapter 2. Hydrogen peroxide-acetic acid pretreatment increases the saccharification and enzyme adsorption on lignocelulose	38
Abstract	39
1. Introduction	40
2. Material and methods	41
2.1. Raw material and chemicals	41
2.2. HPAC pretreatment	41
2.3. Determination of furfurals	42
2.4. Cell wall preparation and lignin determination	42
2.5. Monosaccharide composition	42
2.6. Enzymatic hydrolysis.....	42
2.7. ATR-FTIR spectroscopy	42
2.8. Adsorption isotherms.....	43
3. Results and discussion	43
3.1. HPAC pretreatment alters biomass composition	43
3.2. HPAC pretreatment improves the enzymatic hydrolysis	46
3.3. HPAC pretreatment enhances the enzyme adsorption	47
3.4. HPAC pretreatment avoids the production of furfurals	49
4. Conclusions	50
References	52

Chapter 3. Suppression of a BAHD acyltransferase decreases <i>p</i>-coumaroyl on arabinoxylan and improves biomass digestibility in the model grass <i>Setaria viridis</i>	55
Significance statement	56
Summary	57
1. Introduction	58
2. Results	61
2.1. Generation of <i>SvBAHD05</i> silencing lines in <i>Setaria viridis</i>	61
2.2. <i>SvBAHD05</i> silencing lines present reduced content of ester-linked <i>p</i> CA and <i>p</i> CA linked to the AX	62
2.3. Composition of cell wall polysaccharides in RNAi silencing lines	64
2.4. Effects of <i>SvBAHD05</i> suppression on lignin content and structure	65
2.5. Molecular dynamics simulations of BAHD05 and BdAT1	66
2.6. Saccharification, plant biomass, and seed yield of <i>SvBAHD05</i> RNAi plants ...	69
3. Discussion	71
4. Experimental procedures	74
4.1 Growth conditions for <i>Setaria viridis</i>	74
4.2 Plasmid construct and generation of transgenic plants	74
4.3 Determination of transcript abundance	75
4.4 Determination of <i>p</i> CA, FA, <i>p</i> CA-Araf, FA-Araf and DiFA	75
4.5 Transcriptome analysis of transgenic <i>SvBAHD05</i>	77
4.6 Monosaccharide composition	77
4.7 Cell wall characterization by solution-state 2D NMR	77
4.8 Lignin quantification and monomers composition	78
4.9 Computational details of protein modeling	79
4.10 Pretreatment and enzymatic saccharification assay	80
4.11 Biomass and seed measurement	81
4.12 Statistical Analyses	81
4.13 Gene identifiers	81
References	83
Supporting material	89

APRESENTAÇÃO

Esta tese de Doutorado é composta de três artigos científicos. Em consonância com as regras do Programa de Pós-Graduação em Ciências Biológicas, os artigos foram redigidos de acordo com as normas de publicação dos respectivos periódicos. Nos quais foram submetidos e publicados.

O **capítulo 1** é um artigo de revisão, publicado em 2018 e intitulado '*Plant cell wall composition and enzymatic deconstruction*', que descreve os principais avanços biotecnológicos na compreensão da arquitetura e fisiologia da parede celular de plantas. O artigo descreve os componentes da parede celular e discute as estratégias para superar a recalcitrância da biomassa lignocelulósica e a geração de açúcares fermentáveis a partir da biomassa lignocelulósica.

Outro projeto desenvolvido durante o doutorado é apresentado no **capítulo 2**, intitulado '*Hydrogen peroxide-acetic acid pretreatment increases the saccharification and enzyme adsorption on lignocellulose*'. Este artigo de pesquisa descreve os efeitos de um método de pré-tratamento baseado em peróxido de hidrogênio e ácido acético. Este pré-tratamento apresenta uma alta eficiência na deslignificação da biomassa, elevando a adsorção enzimática aos polissacarídeos e promovendo grande aumento no rendimento da sacarificação, com potencial para aplicação a nível industrial.

Como parte majoritária do período de doutorado, foi realizado um estudo aprofundado sobre mudanças composicionais da parede celular de uma planta modelo de cana-de-açúcar, que resultou no **capítulo 3** '*Suppression of a BAHD acyltransferase decreases p-coumaroyl on arabinoxylan and improves biomass digestibility in the model grass Setaria viridis*'. Este capítulo descreve a caracterização de um novo gene responsável pela adição de ácido *p*-cumárico ao arabinoxilano, com a caracterização da parede celular da planta modelo *Setaria viridis* após o silenciamento gênico via RNA de interferência. Adicionalmente, a hidrólise enzimática foi realizada antes e após pré-tratamento com ácido sulfúrico, utilizado para melhorar a sacarificação da biomassa lignocelulósica.

1. **Thatiane R. Mota**, Dyoni M. Oliveira, Rogério Marchiosi, Osvaldo Ferrarese-Filho, Wanderley D. dos Santos (2018) Plant cell wall composition and enzymatic deconstruction. *AIMS Bioengineering*, 5 (1): 63-77.

2. **Thatiane R. Mota**, Dyoni M. Oliveira, Gutierrez R. de Moraes, Rogério Marchiosi, Marcos S. Buckeridge, Osvaldo Ferrarese-Filho, Wanderley D. dos Santos (2019) Hydrogen peroxide-acetic acid pretreatment increases the saccharification and enzyme adsorption on lignocellulose. *Industrial Crops and Products*, 140: 111657.

JCR: 4.191.

3. **Thatiane R. Mota**, Wagner R. de Souza, Dyoni M. Oliveira, Polyana K. Martins, Bruno L. Sampaio, Felipe Vinecky, Ana P. Ribeiro, Karoline E. Duarte, Thályta F. Pacheco, Norberto K. V. Monteiro, Raquel B. Campanha, Rogério Marchiosi, Davi S. Vieira, Adilson K. Kobayashi, Patrícia A. O. Molinari, Osvaldo Ferrarese-Filho, Rowan A. C. Mitchell, Hugo B. C. Molinari, Wanderley D. dos Santos. Suppression of a BAHD acyltransferase decreases *p*-coumaroyl on arabinoxylan and improves biomass digestibility in the model grass *Setaria viridis*. Submitted to 'The Plant Journal'. Under review.

JCR: 5.726.

RESUMO GERAL

A biomassa lignocelulósica é uma fonte renovável e de baixo custo para a produção de biocombustíveis que podem substituir os combustíveis fósseis e reduzir as emissões de gases de efeito estufa. O grande desafio da tecnologia de bioconversão é o alto custo para superar a recalcitrância da biomassa para a conversão de polissacarídeos em açúcares fermentáveis. Considerando as diversas maneiras de superar a recalcitrância da biomassa lignocelulósica à digestão enzimática, minha tese está organizada em três capítulos, que abordam: a composição e organização da biomassa vegetal; um estudo com pré-tratamento químico para elevar a sacarificação da biomassa lignocelulósica e, por fim, o uso de engenharia genética para produzir plantas com sacarificação elevada. O primeiro capítulo é um artigo de revisão no qual descrevo as informações básicas sobre a composição química da biomassa lignocelulósica e o arsenal enzimático para a desconstrução da lignocelulose em açúcares fermentáveis. No segundo capítulo, um método eficaz de deslignificação foi utilizado para o pré-tratamento de materiais lignocelulósicos, utilizando solução de peróxido de hidrogênio e ácido acético (HPAC). O pré-tratamento da palha de milho, bagaço de cana-de-açúcar e casca de eucalipto com HPAC removeu de 45–75% da lignina e aumentou a adsorção enzimática de ~2,5 a 7 vezes. Como consequência, o pré-tratamento com HPAC aumentou em até 21 vezes a eficiência da sacarificação enzimática. Adicionalmente, descobrimos que a solução HPAC remove os furfurais do meio hidrolítico, o que pode contribuir para uma fermentação mais eficiente do etanol. Este método pode ser uma alternativa para melhorar a sacarificação de biomassas, reduzir custos e aumentar a produção de bioetanol de segunda geração. Visando aprofundar os estudos de parede celular, no terceiro capítulo, eu investiguei a modificação de um gene envolvido na biossíntese da parede celular da gramínea modelo *Setaria viridis*. Gramíneas possuem um alto conteúdo de ácidos hidroxicinâmicos ligados ao arabinosilano. Neste estudo, caracterizamos um gene BAHD acil-coenzima A transferase, demonstrando que ele realiza a adição de ácido *p*-cumárico (*pCA*) à parede celular de *S. viridis*. As linhagens silenciadas por RNA de interferência (*SvBAHD05*) apresentaram reduções de até 42% nos níveis de *pCA* esterificados à parede celular, de forma consistente ao longo de 3 gerações. As biomassas de plantas *SvBAHD05* exibiram aumento de até 30% na sacarificação enzimática após o pré-tratamento com ácido sulfúrico e nenhuma alteração no teor de lignina total. Os estudos de dinâmica molecular sugeriram que o *SvBAHD05* é uma *p*-coumaroil-coenzima A transferase envolvida na adição de *pCA* nas unidades arabinofuranosil do arabinosilano em *S. viridis*. Nossos resultados fornecem a primeira forte evidência de que a *p*-coumarilação do arabinosilano é promovida pela aciltransferase traduzida do gene *BAHD05* nas paredes celulares de monocotiledôneas. Assim, o *SvBAHD05* é um alvo biotecnológico promissor para a engenharia de culturas agrícolas visando a melhoria da sacarificação enzimática de biomassas vegetais para a produção de etanol celulósico.

PALAVRAS-CHAVE: Celulose, hemicelulose, hidroxicinamatos, HPAC, lignocelulose, parede celular de plantas, pré-tratamento de biomassa, proteínas BAHD, sacarificação.

GENERAL ABSTRACT

Lignocellulosic biomass is a low-cost renewable source for biofuel production that can replace fossil fuels and thus reduce greenhouse gas emissions. The main challenge for bioconversion technology is the high cost to overcome biomass recalcitrance for the conversion of polysaccharides into fermentable sugars. Considering the various ways to overcome the recalcitrance of lignocellulosic biomass, my thesis is organized in three chapters, which consists in an introductory chapter about the composition and organization of plant biomass; a study with a chemical pretreatment to increase saccharification of lignocellulosic materials and, finally, the use of genetic engineering to produce plants with enhanced saccharification. The first chapter is a review article, in which I describe the basic information about the chemical composition of lignocellulosic biomass and the enzymatic arsenal for lignocellulose deconstruction in fermentable sugars. In the second chapter, an effective delignification method was used for the pretreatment of lignocellulosic materials using hydrogen peroxide and acetic acid (HPAC) solution. Pretreatment of maize straw, sugarcane bagasse and eucalyptus bark with HPAC removed 45–75% of lignin and increased enzymatic adsorption by ~2.5-to 7-fold. As a result, HPAC pretreatment increased the efficiency of enzymatic saccharification up to 21-fold. Additionally, we found that HPAC removes furfurals from hydrolytic solution, which may contribute to more efficient ethanol fermentation. The method can be a useful alternative for improving biomass saccharification, reducing the costs and increasing the second-generation bioethanol production. For a further investigation of plant cell walls, in the third chapter I investigated the modification of a gene involved in the cell wall biosynthesis of the model grass *Setaria viridis*. Grasses have high contents of hydroxycinnamic acids bound to arabinoxylan. In this study, we characterized a BAHD gene of acyl-coenzyme A transferase responsible for the addition of *p*-coumaric acid (*p*CA) in the cell walls of *S. viridis*. Silenced lines by RNA interference (*SvBAHD05*) presented up to 42% of decrease in ester-linked *p*CA consistently across 3 generations. Biomass of *SvBAHD05* RNAi silencing plants exhibited up to 30% of increase in saccharification after sulfuric acid pretreatment and no significant changes in the total lignin content. Molecular dynamics analyses have suggested that *SvBAHD05* is a *p*-coumaroyl coenzyme A transferase involved in the addition of *p*CA to the arabinofuranosyl units of arabinoxylan in *S. viridis*. Our data provide the first strong evidence of arabinoxylan *p*-coumaroylation promoted by *BAHD05* acyltransferase gene in cell walls of monocots. Thus, *SvBAHD05* is a promising biotechnological target to engineering crops for improved biomass saccharification of plant biomass and cellulosic ethanol production.

KEYWORDS: BAHD protein, biomass pretreatment, cellulose, hemicellulose, HPAC, hydroxycinnamates, lignocellulose, plant cell wall, saccharification.

CHAPTER 1

Plant cell wall composition and enzymatic deconstruction

Thatiane R. Mota^{1,*}, Dyoni M. Oliveira¹, Rogério Marchiosi¹, Osvaldo Ferrarese-Filho¹ and Wanderley D. dos Santos¹

¹ Department of Biochemistry, Laboratory of Plant Biochemistry, State University of Maringá, PR, Brazil.

***Corresponding author:**

Thatiane R. Mota

E-mail: thatianermota@gmail.com

Type of chapter:

Review article

Journal:

AIMS Bioengineering

Volume/issue, pages:

5 (1): 63–77

Date of publication:

March 2018

DOI:

10.3934/bioeng.2018.1.63

Abstract

Cellulosic ethanol is one the most prominent technologies capable of replacing the use of fossil fuels in an observable horizon of technological development. The complexity of plant biomass, however, continues to challenge our ability to convert it into biofuels efficiently. Highly complex and cross-linked polysaccharides, hydrophobic and protein adsorbent polymers, and crystalline structures comprise some of the structures that shield the plant cell contents (and the shield structures themselves) against predators. In response, a sophisticated enzymatic weaponry, with its associated chemical and physical mechanisms, is necessary to overcome this recalcitrance. Here we describe basic information about chemical composition of lignocellulosic biomass and the enzymatic arsenal for lignocellulose deconstruction into fermentable sugars.

Keywords

Biomass; cellulose; enzymatic hydrolysis; hemicellulose; lignin; lignocellulose; saccharification.

Abbreviations

Ara: arabinose; FA: ferulic acid; Fuc: fucose; Gal: galactose; Glc: glucose; GlcA: glucuronic acid; Man: mannose; Xyl: xylose.

1. Introduction

Currently, our energy is mainly derived from oil reserves. These fossil resources are finite and therefore our economy is unsustainable in the long term. Besides, the intensive and increasing burning of fossil reserves since the industrial revolution has introduced an excessive amount of CO₂ into the atmosphere and increased the temperature of the planet. These factors demand the development of technologies that allow us to exploit sustainable energy sources to ensure sustainable economic development [1,2]. Lignocellulosic biomass is the most abundant renewable raw material in nature. The production of plant biomass in the world is about 200×10^9 tons per year and over 90% of this biomass is lignocellulose [3,4] and has the potential to replace oil in a reasonable scenario of technological development [5]. Currently, sugarcane and maize are the main crops used in the production of ethanol [6] starting from soluble carbohydrates as sucrose and starch [7].

Due to its long history of sugarcane production, Brazil is prominent in the use of biomass to produce ethanol [8]. Bioethanol can be an alternative to gasoline [9]. The United States is currently the main producer of ethanol in the world, primarily using corn starch, while Europe uses wheat starch and sugar beet. In 2013, the total production of ethanol by the United States was 50.3 billion liters [9]. The global production of biofuels was 18.2 billion liters in 2000, 60.6 billion liters in 2007 and 85 billion liters in 2011 [3]. Therefore, almost all ethanol produced in the world today comes from soluble carbohydrates such as sucrose and starch [7].

The global demand for biofuels quadrupled between 2000 and 2008. In 2000, the production of biofuel was 400 petajoule (PJ) per year and in 2008 was nearly 1800 PJ per year [10], justifying investments in the development of technologies to increase ethanol production [11,12,13]. The bioethanol production from sugar feedstock is called “first generation ethanol”. Second generation ethanol is made by saccharification of lignocellulosic feedstock as agricultural wastes [3].

In sugarcane plants, after extraction of the soluble carbohydrates, the residual biomass is burned to sustain the energy demands of the industry [14]. Surplus of

biomass is usually converted into electricity and sold to distributors or, less commonly, used as cattle feed [15]. As this residual biomass is essentially composed of carbohydrates, it could be partially converted into ethanol, contributing to increased productivity, without competing with food production [16]. Therefore, different sources of lignocellulosic biomass have high potential for bioenergy, mainly monocots plants—rice, wheat, sorghum, tall fescue, giant reed and elephant grass; and some eudicots—poplar, eucalyptus and rapeseed [17].

However, in contrast to the processing of sucrose and starch, degradation of lignocellulosic biomass demands a sophisticated set of enzymes. The complexity of the carbohydrate polymers and their cross-linkages with lignin demands a complex set of enzymes in order to allow the access of polysaccharidases and release fermentable sugars [18]. Lignocellulose is basically composed of plant cell wall components. The recalcitrance of cell walls to enzyme digestion is the result of long-range co-evolution among plants and their predators [19].

Microorganisms and herbivores promote the enzymatic degradation of lignocellulose via multiple carbohydrate-active, lignin-active and accessory enzymes, which typically act together with complementary and synergistic activities [20]. The industrial conversion of lignocellulosic materials into ethanol typically involves: (i) physical or chemical pretreatments to disrupt polymer interactions and make cellulose and hemicellulose more accessible for enzymatic hydrolysis; (ii) saccharification of pretreated biomass by enzyme complexes including cellulases, hemicellulases and accessory enzymes; (iii) fermentation of monosaccharides to produce ethanol or other platform chemicals [21].

However, the technology to produce cellulosic ethanol is still under development and to make the process competitive in terms of cost, it is necessary to improve the efficiency of lignocellulosic degradation [22]. We therefore need to enhance our knowledge about cell wall organization and its enzymatic breakdown. The review describes the basic information about chemical composition of lignocellulosic

biomass and the enzymatic arsenal for lignocellulose deconstruction into fermentable sugars.

2. Structure of lignocellulose

Lignocellulose biomass can be divided into polysaccharide - cellulose, hemicellulose and pectin - and non-polysaccharide fractions - lignin, phenolic compounds and proteins [23]. Plant tissues vary widely in structure and composition. The composition and architecture of cell walls vary according to species, cell type, tissue, developmental stage and cell wall layer [24,25]. During plant growth and cell elongation, plant cells produce a primary cell wall, which typically contains cellulose, hemicellulose, pectin and proteins [26]. The primary cell walls of grasses and eudicots share some similarities (i.e. a cellulose fraction embedded in a non-cellulosic fraction) with differences in the abundance and type of different components (Figure 1). After cell elongation, some tissues produce a secondary cell wall, which is deposited inside the primary cell wall, displacing it outwards. The secondary cell wall is a prominent feature of fibers, such as xylem and sclerenchyma. Secondary cell walls are composed of cellulose, hemicellulose and lignin [27,28].

2.1 Cellulose

Cellulose, the most abundant biopolymer, consists of D-glucose units connected to each other by glycoside β -1,4 linkages, with cellobiose as the fundamental repeating unit (Figure 1a), synthesized by cellulose synthase complex [29]. Cellulose chains show an exceptionally high degree of polymerization, with lengths of 2,000 to 25,000 glucose residues [16,30]. These cellulose molecules are interconnected in parallel by hydrogen bonds, generating microfibrils comprising 30 to 36 linear chains, which have a high degree of mechanical resistance and recalcitrance against enzyme attack [31].

2.2 Hemicellulose

The cellulose microfibrils are cross-linked by hemicellulose molecules (also known as cross-linking glycans; Figure 1b–1e). Hemicellulose also impedes the collapse of cellulose microfibrils, preventing the microfibrils from sliding over each other [32]. Finally, the cellulose-hemicellulose network is embedded in a matrix of pectin that may contain lignin [29]. Hemicelluloses are the second major polysaccharide fraction of the cell wall [33].

Compared with cellulose, hemicelluloses are of lower molecular weight, comprising 100 to 200 monomeric units. The backbone of hemicellulose is mainly composed of hexoses (such as D-glucose and D-mannose) or pentoses (such as D-xylose) connected to each other by β -1,4 linkages. Except for β -1,3; β -1,4 mixed linkage glucans found exclusively in grasses, hemicelluloses are heteropolysaccharides presenting different monosaccharides (such as D-galactose, D-fucose, arabinose and D-glucuronic acid) attached to the backbone core [28].

Xyloglucan is the main hemicellulose in eudicots and non-commelinid monocots. It consists of a β -1,4-D-glucose backbone regularly branched by α -(1,6)-linked xylosyl residues, which may be further connected to galactosyl, arabinosyl and fucosyl residues, formally named fucogalactoxyloglucans (Figure 1b) [34].

The main hemicelluloses in eudicots are xyloglucans, xylans and mannans [16]. Xylan is a major hemicellulosic component in grasses, consisting of a β -1,4-linked D-xylose backbone exhibiting different patterns of branching with arabinose and glucuronic acid (Figure 1c). Glucuronoarabinoxylan (GAX) may present hydroxycinnamic acids such as ferulic acid and *p*-coumaric acid, ester-linked to arabinosyl residues of the GAX structure [35].

Mixed-linkage glucans, also simply called β -glucans, are unbranched homopolymers of glucose, alternating short sequences of β -1,4-glucan with single β -1,3-glucans (Figure 1d). β -Glucans are unique to the cell walls of grasses (family Poaceae) and a few related families from the order Poales [28]. The content of β -

2.3 Pectin

Pectin is the most complex class of structural polysaccharides, consisting of branched heteropolysaccharides presenting acidic sugars (galacturonic and glucuronic acid) and neutral sugars (rhamnose, galactose and arabinose). Abundant in the middle lamella and in primary plant cell walls [38], it is involved in intercellular adhesion, confers charge and preserves the water content of plant cell walls. Pectin also contributes to the integrity and rigidity of plant tissues and is important in defense mechanisms against pathogens [39]. Pectin is used in the food, cosmetic and drugs industries, e.g. in paper substitutes and biodegradable films [40]. Plant primary cell walls contain approximately 30% pectin in dicotyledonous and non-commelinid monocot plants, while lower levels (2%–10%) are found in grasses and other commelinid plants [39,40].

Pectin contains different monosaccharides, the most abundant being galacturonic acid [38]. Homogalacturonan (HG) is the most abundant pectic polysaccharide. It consists of a linear homogeneous polymer of α -1,4 linked galacturonic acid [40]. Other abundant types of pectin are xylogalacturonan, apiogalacturonan, rhamnogalacturonan I and rhamnogalacturonan II [39].

2.4 Lignin

Lignin is the most abundant non-polysaccharide fraction of lignocellulose and the second most abundant biopolymer, after cellulose. It consists of a complex phenolic polymer linked to cellulose and hemicellulose [41]. Corresponding to 15% - 40% of dry weight [42], lignin is present in the plant secondary cell walls of specialized tissues (fibers, vessel, cortex and so on), where it interacts with cellulosic microfibrils, interrupting cell growth and providing mechanical strength to the plant and chemical resistance against pathogens, herbivores and abiotic stresses [43,44].

Lignin is produced by the phenylpropanoid pathway [45], which begins in the cytosol with the deamination of L-phenylalanine to produce cinnamic acid, a reaction catalyzed by phenylalanine ammonia-lyase [46,47]. Afterwards, hydroxylation of the

aromatic ring produces *p*-coumaric acid, the first phenylpropanoid in the pathway. Following further hydroxylations and methoxylations at C-3 and C-5 of the aromatic ring, and reduction of the carboxylic acid to an alcohol, these intermediates are converted to three different hydroxycinnamyl alcohols: *p*-coumaryl, coniferyl and sinapyl alcohols, see Figure 2 [48–50].

Specific cell wall peroxidases promote an oxidative polymerization of monolignols resulting in a highly hydrophobic matrix of C-C and C-O-C. The monolignol residues in lignin polymers may be identified by their ring decoration, and are referred to as *p*-hydroxyphenyl (H), guaiacyl (G) and syringyl (S) units, respectively [51,52]. The incorporation of monolignols H, G and S in a growing lignin polymer occur via mutual coupling and cross-coupling of monolignols by inter-linkage β -O-4 (β -ether), β -5 phenylcoumaran, β - β resinol and 4-O-5 biphenyl ether [48].

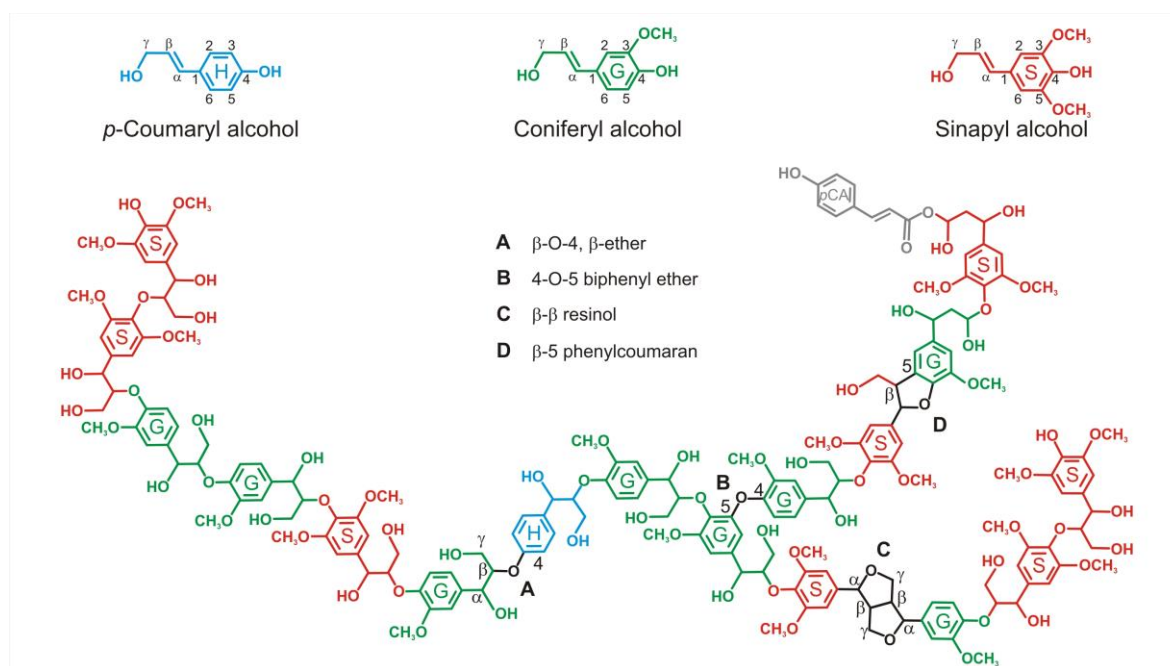


Figure 2. Structural components of lignin polymers. The biosynthetic precursors, coniferyl (blue), coniferyl (green) and sinapyl (red) alcohols are shown, as well as *p*-coumarate ester conjugated lignin (gray). The linkages specifically formed by radical coupling reactions are shown in bold and labeled with the type of unit produced in the polymer.

3. Enzymatic breakdown of lignocellulose

Different types and large quantities of enzymes are necessary to release fermentable sugars from cell wall components. Table 1 presents different types of enzymes used for the breakdown of cellulose and hemicellulose [53]. Enzymes that modify complex carbohydrates are known as Carbohydrate-Active EnZymes (CAZymes). Collectively they are organized into families: Glycoside hydrolases (GHs), glycosyl transferases (GT), polysaccharide lyases (PL), carbohydrate esterases (CE), and auxiliary activities (AA). The latter group includes oxidative enzymes, such as cellobiose dehydrogenase (CDH) and lytic polysaccharide monooxygenase (LPMO) that are involved in polysaccharide degradation [54,55]. Many CAZymes are modular proteins, consisting of catalytic modules and non-catalytic carbohydrate-binding modules (CBMs) [56,57]. CBMs have an important role in crystalline cellulose degradation and are also found in enzymes that act on glucans, xylans, mannans and glucomannans [57]. CBMs promote the association of enzymes with substrates, potentiating the action of cellulolytic enzymes on insoluble substrates [58–60].

3.1 Cellulases

Cellulases are the primary enzymes used for cellulose hydrolysis. Deconstruction of cellulose is achieved by three predominant activities: Cellobiohydrolase (also called exoglucanase), endoglucanase and β -glucosidase. They act synergistically in the hydrolysis of the cellulose, which reduces problems of product inhibition [21]. Endoglucanases (EC 3.2.1.4) cleave the glycosidic internal bonds of the non-crystalline cellulose portion [61]. Cellobiohydrolases and exoglucanases (EC 3.2.1.91 and EC 3.2.1.176) remove glucose dimers (cellobiose) from the reducing and non-reducing ends of cellulose chains, respectively [62]. The main distinction between cellobiohydrolase and exoglucanase is that cellobiohydrolase releases cellobiose from crystalline cellulose [63]. Finally, β -glucosidases (EC 3.2.1.21) cleave cellobiose into two glucose molecules [64].

3.2 Hemicellulases

The β -1-4-D-glucose backbone of xyloglucans can be hydrolyzed by the cellulases described above, after elimination of the branches containing xylose, galactose and fucose. Enzymes responsible for the hydrolysis of the xyloglucan backbone are xyloglucan endo- β -1,4-glucanases, EC 3.2.1.151 [65]. Different classes of xyloglucanases present affinities for xyloglucans with different degrees of branching [62].

Degradation of xylan backbones requires at least two different enzymes: 1) endoxylanases (EC 3.2.1.8) hydrolyze glycoside linkages from the xylan chain releasing xylooligosaccharides; 2) β -xylosidases (EC 3.2.1.37) hydrolyze xylobiose and xylooligosaccharides from the non-reducing end. The xylanase group of enzymes have different specificities for xylan backbones depending on the kind and degree of branching [66]. α -Arabinofuranosidases (EC 3.2.1.55) act on α -glycosidic bonds of arabinofuranoses (Araf) branching from the xylan backbone [67,68], while α -glucuronidases (EC 3.2.1.139) hydrolyze xylan linked with glucuronic acid [69]. Acetyl xylan esterases (EC 3.1.1.72) remove acetyl groups [70,71], and feruloyl esterases (EC 3.1.1.73) hydrolyze ester-linked ferulic and *p*-coumaric acids attached to Araf branches in xylan chains and pectin [72,73]. Feruloyl esterases present synergistic actions with xylanase, β -glucosidase, arabinofuranosidase and other accessory enzymes in the degradation of cell walls [74,75]. These synergies may reduce the quantity of enzyme necessary for saccharification and reduce the costs of bioethanol production from lignocellulosic biomass [76,77]. The enzymatic saccharification system using feruloyl esterase combined with accessory enzymes could contribute to the production of fermentable sugars for bioethanol production [35].

The structurally heterogeneous nature of mannans requires associations and synergistic actions among a variety of cleaving enzymes such as endo- β -mannanase (EC 3.2.1.78), exo- β -mannosidase (EC 3.2.1.25), β -glucosidase (EC 3.2.1.21), acetyl mannan esterases (EC 3.1.1.6), and α -galactosidase (EC 3.2.1.22) for efficient enzymatic hydrolysis [37]. Endo- β -mannanases, also referred to simply as mannanases, hydrolyze

the endo- β -(1,4)-glucose-mannose backbone of galacto(gluco)mannans, releasing predominantly mannobiose and mannotriose. β -Mannosidases hydrolyze β -(1,4)-glucose-mannose, releasing mannose from the non-reducing end of manno-oligosaccharides [37].

Degradation of mixed linked β -glucans is catalyzed by linkage specific β -glucanases. Depending on the type of glycosidic linkage they cleave, β -glucanase is grouped into four main categories, namely β -1,3;1,4-glucanases (lichenases; EC 3.2.1.73), endoglucanases (cellulases; EC 3.2.1.4), β -1,3-glucanases (laminarinases, EC 3.2.1.39) and β -1,3(4)-glucanases (EC 3.2.1.6) [62].

3.3 Pectinases

Pectinases or polygalacturonases (pectin depolymerases) form a heterogeneous group of enzymes with the capacity to hydrolyze α -1,4-glycosidic linkages of pectate present in plant cell walls [78]. Pectins are extremely important for cell wall growth and extension [79]. Pectinases have a potential application in improving ethanol production from various feedstocks, as pectinase treatment requires less energy and produces no inhibitory factors [80–82].

3.4 Ligninases

Ligninases are laccase, lignin peroxidase and manganese peroxidase. These enzymes are able to hydrolyze the lignin fraction, improving polysaccharide degradation by glycosyl hydrolases, and reducing the recalcitrance of lignocellulosic biomass, as well as decreasing the adsorption of lignin to enzymes [83].

Laccases (EC 1.10.3.2) are copper-containing enzymes with four copper atoms in the catalytic center [84]. They catalyze the oxidative cleavage of phenolic compounds, producing radicals [12]. Lignin peroxidase (EC 1.11.1.7) and manganese peroxidase (EC 1.11.1.7) are the two largest classes of glycoproteins in the peroxidase group. They present a heme group that requires hydrogen peroxide as an oxidant [12]. Laccases play an important role in lignin biosynthesis. Plant cells secrete peroxidases

and laccases into the apoplast for the polymerization of monolignols by radicals [85], while fungi and bacteria secrete them for lignin depolymerization [86].

Table 1. The main enzymes required to degrade cellulose and hemicellulose to monomers.

Group of enzymes	Enzymes	Linkages breakdown
Cellulases	Cellobiohydrolase	β -(1,4)-Glc
	Endoglucanase	Endo- β -(1,4)-Glc
	β -Glucosidase	β -(1,4)-Glc
Hemicellulases	Endoxylanase	Endo- β -(1,4)-Xyl
	β -Xylosidase	β -(1,4)-Xyl
	β -Glucanase/lichenase	β (1,3)-Glc, β (1,4)-Glc
	Feruloyl esterase	Ester linkage FA-Ara
	<i>p</i> -Coumaroyl esterase	Ester linkage <i>p</i> CA-Ara
	Arabinofuranosidase	α -(1,2)-Ara, α -(1,3)-Ara
	Glucuronidase	α (1,2)-GlcA
	4-O-Glucuronoyl methylesterase	α -(1,2)-4-O-metil- α -glucuronic
	Xyloglucanase	Endo- α -(1,4)-Glc
	Fucosidase	α -(1,2)-Fuc
	α -Galactosidase	α -(1,3)-Gal, α -(1,6)-Gal
	Mannanase	Endo- β -(1,4)-Glc-Man
	β -Mannosidase	β -(1,4)-Glc-Man
Acetyl xylan esterase	α -(1,2)-Xyl	

4. Pretreatments of lignocellulosic biomass

Lignocellulosic biomass presents several features that confer recalcitrance, such as crystalline cellulose which precludes decomposition by enzymes [87]; highly complex hemicelluloses and pectin, which demands a huge number of enzymes; the high degree of lignin adsorption to proteins that inhibits enzymatic activity [88]; and the complex cross-linkages between phenolic and polysaccharide components [35,89]. Biological, chemical and physical pretreatments can reduce the crystallinity of lignocellulose and break various linkages, drastically reducing its complexity [17].

Biological pretreatments have been widely studied and have demonstrated some advantages over chemical and physical pretreatments such as a low demand for energy, environmental friendliness and low levels of toxic products [90]. Biological pretreatments include in vivo application of microorganisms [91], for example, brown, white and soft rot fungi that produce hydrolytic enzymes such as laccase and manganese peroxidase that degrade lignin [92].

Chemical pretreatments strongly improve the biodegradability of cellulose [93]. In alkali pretreatments, biomass is mixed with bases such as sodium or potassium hydroxides. These pretreatments promote modifications in the cell wall structure and increase enzyme accessibility for saccharification [94]. Acid hydrolysis mostly employs sulfuric acid, but phosphoric acid, hydrochloric acid and nitric acid are also used to remove lignin [95]. In addition, microwave energy has been applied to facilitate alkaline and acid pretreatments [96]. Pretreatments that use organic solvents are known as organosolv and utilize aliphatic alcohols, polyols (e.g. glycerol), acetone or phenol as solvents to promote delignification. Organic solvents improve removal of lignin content and reduce the viscosity of the pretreatment medium [97].

Physical pretreatments are used to enhance lignocellulosic porosity. Milling procedures are the most traditional physical pretreatment used in laboratories [98]. Although effective, milling is energy intensive and only mild milling procedures have been shown to be industrially viable. Ultrasonic pretreatment induces mechanical vibrations and cavitations that help to disrupt tissues [99]. One of the most promising pretreatment methods is steam explosion. It consists of compression and fast decompression of the biomass to increase the porosity of the lignocellulosic material and facilitate the access of hydrolytic enzymes. The process has been demonstrated to be efficient for biomasses containing low amounts of lignin [7,94].

The extraction of lignin by pretreatments improves saccharification [100]. Although in principle these treatments are feasible, they still require a substantial technological development to become cost and energy efficient enough for industrial application [7,101].

5. Conclusions

Lignocellulose has a complex and varied composition that, although reasonably well known, is still a challenge for efficient conversion in biorefineries. Development of technologies that improve the efficiency of generation of biofuels and platform chemicals from lignocellulose has been the focus vigorous scientific efforts. While bioethanol has real potential as an oil replacement, considerable technological advances are necessary to reduce financial and energetic costs and make the biochemical conversion of lignocellulose into biofuels a commercial reality.

Acknowledgments

This work was supported by grants from the Coordenação de Aperfeiçoamento de Pessoal de Nível Superior (CAPES) and Conselho Nacional de Desenvolvimento Científico e Tecnológico (CNPq). T. R. Mota is recipient of CAPES and D. M. Oliveira is recipient from CNPq. O. Ferrarese-Filho and W. D. dos Santos are research fellows of CNPq.

Conflict of interest

All authors declare no conflicts of interest in this paper.

References

1. Santos WDD, Gómez ED, Buckeridge MS, (2011) Bioenergy and the Sustainable Revolution, In: Buckeridge MS, Goldman GH. *Routes to Cellulosic Ethanol*. Springer Science and Business Media, LCC, 1 Ed., New York, 15–26.
2. Jaiswal D, Souza APD, Larsen S, et al. (2017) Brazilian sugarcane ethanol as an expandable green alternative to crude oil use. *Nat Clim Change* 7: 788–792.
3. Saini JK, Saini R, Tewari L (2015) Lignocellulosic agriculture wastes as biomass feedstocks for second-generation bioethanol production: Concepts and recent developments. *Biotech* 5: 337–353.
4. Buckeridge MS, Dos Santos WD, Mas T, et al. (2016) The cell wall architecture of sugarcane and its implications to cell wall recalcitrance, In: Lam E, Carrer H, Da Silva JA, et al. *Compendium of Bioenergy Plants: Compendium of Bioenergy Plants*, Boca Raton, FL: CRC Press, 31–50.
5. Poovaiah CR, Nageswara-Rao M, Soneji JR, et al. (2014) Altered lignin biosynthesis using biotechnology to improve lignocellulosic biofuel feedstocks. *Plant Biotechnol J* 12: 1163–1173.
6. Torres AF, Visser RGF, Trindade LM (2015) Bioethanol from maize cell walls: Genes, molecular tools, and breeding prospects. *GCB Bioenergy* 7: 591–607.
7. Balat M (2011) Production of bioethanol from lignocellulosic materials via the biochemical pathway: A review. *Energ Convers Manage* 52: 858–875.
8. Souza APD, Leite DCC, Pattathil S, et al. (2013) Composition and structure of sugarcane cell wall polysaccharides: Implications for second-generation bioethanol production. *BioEnergy Res* 6: 564–579.
9. Gupta A, Verma JP (2015) Sustainable bio-ethanol production from agro-residues. *Renew Sust Energ Rev* 41: 550–567.
10. Sims REH, Mabee W, Saddler JN, et al. (2010) An overview of second generation biofuel technologies. *Bioresource Technol* 101: 1570–1580.
11. Amorim HV, Lopes ML, Oliveira JVC, et al. (2011) Scientific challenges of bioethanol production in Brazil. *Appl Microbiol Biotechnol* 91: 1267–1275.

12. Verardi A, Blasi A, Molino A, et al. (2016) Improving the enzymatic hydrolysis of *Saccharum officinarum* L. bagasse by optimizing mixing in a stirred tank reactor: Quantitative analysis of biomass conversion. *Fuel Process Technol* 149: 15–22.
13. Limayem A, Ricke SC (2012) Lignocellulosic biomass for bioethanol production: Current perspectives, potential issues and future prospects. *Prog Energy Combust Sci* 38: 449–467.
14. Goldemberg J, Coelho ST, Guardabassi P (2008) The sustainability of ethanol production from sugarcane. *Energ Policy* 36: 2086–2097.
15. Rocha GJM, Gonçalves AR, Oliveira BR, et al. (2013) Steam explosion pretreatment reproduction and alkaline delignification reactions performed on a pilot scale with sugarcane bagasse for bioethanol production. *Ind Crop Prod* 35: 274–279.
16. Buckeridge MS, Santos WDD, Souza AP, (2010) Routes for cellulosic ethanol in Brazil, In: Cortez LAB. *Sugarcane Bioethanol, R&D for productivity and sustainability*, Blucher, 992.
17. Kou L, Song Y, Zhang X, et al. (2017) Comparison of four types of energy grasses as lignocellulosic feedstock for the production of bio-ethanol. *Bioresource Technol* 241:434–429.
18. Álvarez C, Manuel RF, Bruno D (2016) Enzymatic hydrolysis of biomass from wood. *Microb Biotechnol* 9: 149–156.
19. Malinovsky FG, Fangel JU, Willats WGT (2014) The role of the cell wall in plant immunity. *Front Plant Sci* 5: 178.
20. Payne CM, Knott BC, Mayes HB, et al. (2015) Fungal cellulases. *Chem Rev* 115: 1308–1448.
21. Khare SK, Pandey A, Larroche C (2015) Current perspectives in enzymatic saccharification of lignocellulosic biomass. *Biochem Eng J* 102: 38–44.
22. Jørgensen H, Kristensen JB, Felby C (2007) Enzymatic conversion of lignocellulose into fermentable sugars: Challenges and opportunities. *Biofuels Bioprod Biorefin* 1: 119–134.

23. Le GH, Florian F, Jean-Marc D, et al. (2015) Cell wall metabolism in response to abiotic stress. *Plants* 4: 112–166.
24. Pauly M, Keegstra K (2008) Cell-wall carbohydrates and their modification as are source for biofuels. *Plant J* 54: 559–568.
25. Höfte H, Voxeur A (2017) Plant cell walls. *Curr Biol* 27: R865–R870.
26. Carpita NC, Gibeaut DM (1993) Structural models of primary cell walls in flowering plants: Consistency of molecular structure with the physical properties of the walls during growth. *Plant J* 3: 1–30.
27. Chundawat SPS, Beckham GT, Himmel ME, et al. (2011) Deconstruction of lignocellulosic biomass to fuels and chemicals. *Annu Rev Chem Biomol Eng* 2: 121–145.
28. Meents MJ, Watanabe Y, Samuels AL (2018) The cell biology of secondary cell wall biosynthesis. *Ann Bot*.
29. Turner S, Kumar M (2018) Cellulose synthase complex organization and cellulose microfibril structure. *Philos Trans* 376: 20170048.
30. Himmel ME, Ding SY, Johnson DK, et al. (2007) Biomass recalcitrance: Engineering plants and enzymes for biofuels production. *Science* 315: 804–807.
31. Carpita NC, Mccann MC, (2000) The cell wall, In: Buchanan BB, Gruissem W, Jones RL, *Biochemistry and molecular biology of plants*. Rockville: IL: American Society of Plant Physiologists, 1367.
32. Abramson M, Shoseyov O, Shani Z (2010) Plant cell wall reconstruction toward improved lignocellulosic production and processability. *Plant Sci* 178: 61–72.
33. Van dWT, Dolstra O, Visser RG, et al. (2017) Stability of cell wall composition and saccharification efficiency in miscanthus across diverse environments. *Front Plant Sci* 7: 2004.
34. Pauly M, Keegstra K (2016) Biosynthesis of the plant cell wall matrix polysaccharide xyloglucan. *Annu Rev Plant Biol* 67: 235–259.

35. Oliveira DM, Finger-Teixeira A, Mota TR, et al. (2016). Ferulic acid: A key component in grass lignocellulose recalcitrance to hydrolysis. *Plant Biotechnol J* 13: 1224–1232.
36. Kozlova LV, Ageeva MV, Ibragimova NN, et al. (2014) Arrangement of mixed-linkage glucan and glucuronoarabinoxylan in the cell walls of growing maize roots. *Ann Bot* 114: 1135–1145.
37. Srivastava PK, Kapoor M (2017) Production, properties, and applications of endo- β -mannanases. *Biotechnol Adv* 35: 1–19.
38. Biswal AK, Atmodjo MA, Li M, et al. (2018) Sugar release and growth of biofuel crops are improved by downregulation of pectin biosynthesis. *Nat Biotechnol*.
39. Voragen AGJ, Coenen GJ, Verhoef RP, et al. (2009) Pectin, a versatile polysaccharide present in plant cell walls. *Struct Chem* 20: 263–275.
40. Mohnen D (2008) Pectin structure and biosynthesis. *Curr Opin Plant Biol* 11: 266–277.
41. Nguyen TN, Son S, Jordan MC, et al. (2016) Lignin biosynthesis in wheat (*Triticum aestivum* L.): Its response to waterlogging and association with hormonal levels. *BMC Plant Biol* 16: 1–16.
42. Ragauskas AJ, Beckham GT, Biddy MJ, et al. (2014) Lignin valorization: Improving lignin processing in the biorefinery. *Science* 344: 1246843.
43. Santos WDD, Ferrarese MDLL (2008) Ferulic acid: An allelochemical troublemaker. *Funct Plant Sci Biotechnol* 2: 47–55.
44. dos Santos WD, Ferrarese ML, Nakamura CV, et al. (2008) Soybean (*Glycine max*) root lignification induced by ferulic acid the possible mode of action. *J Chem Ecol* 34: 1230–1241.
45. Liu Q, Luo L, Zheng L (2018) Lignins: Biosynthesis and Biological Functions in Plants. *Int J Mol Sci* 19: 335.
46. Salvador VH, Lima RB, dos Santos WD, et al. (2013) Cinnamic acid increases lignin production and inhibits soybean root growth. *PLoS One* 8: e69105.

47. Oliveira DMD, Finger-Teixeira A, Freitas DLD, et al. (2017) Phenolic Compounds in Plants: Implications for Bioenergy, In: Buckeridge MS, de Souza AP, *Advances of Basic Science for Second Generation Bioethanol from Sugarcane*, Springer Int Publishing, 39–52.
48. Boerjan W, Ralph J, Baucher M (2003) Lignin biosynthesis. *Annu Rev Plant Biol* 166: 63–71.
49. Moreira-Vilar FC, Siqueira-Soares RC, Finger-Teixeira A, et al. (2014) The acetyl bromide method is faster, simpler and presents best recovery of lignin in different herbaceous tissues than klason and thioglycolic acid methods. *PLoS One* 9: e110000.
50. Santos WDD, Marchiosi R, Vilar FCW, et al. (2014) Polyvalent Lignin: Recent Approaches in Determination and Applications, In: Lu F, *Lignin: Structural analysis, applications in biomaterials and ecological significance*, New York: Nova Publishers, 1–26.
51. Fornalé S, Rencoret J, Garcíacalvo L, et al. (2017) Changes in cell wall polymers and degradability in maize mutants lacking 3'- and 5'-O-methyltransferases involved in lignin biosynthesis. *Plant Cell Physiol* 58: 240–255.
52. Lima RB, Salvador VH, dos Santos WD, et al. (2013) Enhanced lignin monomer production caused by cinnamic acid and its hydroxylated derivatives inhibits soybean root growth. *PLoS One* 8: e80542.
53. Saritha M, Arora A, Lata (2012) Biological Pretreatment of Lignocellulosic Substrates for Enhanced Delignification and Enzymatic Digestibility. *Indian J Microbiol* 52: 122–130.
54. Henrissat B, Bairoch A (1993) New families in the classification of glycosyl hydrolases based on amino acid sequence similarities. *Biochem J* 293: 781–788.
55. Lombard V, Ramulu HG, Drula E, et al. (2014) The carbohydrate-active enzymes database (CAZy). *Nucleic Acids Res* 42: D490–D495.
56. Bourne Y, Henrissat B (2001) Glycoside hydrolases and glycosyltransferases families and functional modules. *Curr Opin Struc Biol* 11: 593–600.

57. Hashimoto H (2006) Recent structural studies of carbohydrate-binding modules. *Cell Mol Life Sci* 63: 2954–2967.
58. Boraston AB, Bolam DN, Gilbert HJ, et al. (2004) Carbohydrate-binding modules: Fine-tuning polysaccharide recognition. *Biochem J* 382: 769–781.
59. Davies G, Henrissat B (1995) Structures and mechanisms of glycosyl hydrolases. *Structure* 3: 853–859.
60. Terrapon N, Lombard V, Drula E, et al. (2017) The CAZy Database/the Carbohydrate-Active Enzyme (CAZy) Database: Principles and Usage Guidelines, In: Aoki-Kinoshita K (eds), *A Practical Guide to Using Glycomics Databases*. Springer, Tokyo, 117–131.
61. Segato F, Dias B, Berto GL, et al. (2017) Cloning, heterologous expression and biochemical characterization of a non-specific endoglucanase family 12 from *Aspergillus terreus* NIH2624. *BBA* 1865: 395–403.
62. Segato F, Damásio AR, de Lucas RC, et al. (2014) Genomics review of holocellulose deconstruction by aspergilli. *Microbiol Mol Biol Rev* 78: 588–613.
63. Olsen JP, Alasepp K, Kari J, et al. (2016) Mechanism of product inhibition for cellobiohydrolase Cel7A during hydrolysis of insoluble cellulose. *Biotechnol Bioeng* 113: 1178–1186.
64. Grange DC, Haan R, Zyl WH (2010) Engineering cellulolytic ability into bioprocessing organisms. *Appl Microbiol Biotechnol* 87: 1195–1208.
65. Damásio ARL, Rubio MV, Gonçalves TA, et al. (2017) Xyloglucan breakdown by endo-xyloglucanase family 74 from *Aspergillus fumigatus*. *Appl Microbiol Biotechnol* 101: 2893–2903.
66. Dodd D, Cann IKO (2009) Enzymatic deconstruction of xylan for biofuel production. *GCB Bioenergy* 1: 2–17.
67. Damásio ARDL, Pessedela BC, Segato F, et al. (2012) Improvement of fungal arabinofuranosidase thermal stability by reversible immobilization. *Process Biochem* 47: 2411–2417.

68. Wilkens C, Andersen S, Dumon C, et al. (2017) GH62 arabinofuranosidases: Structure, function and applications. *Biotechnol Adv* 35: 792–804.
69. Wu L, Jiang J, Kallemeijn W, et al. (2017) Activity-based probes for functional interrogation of retaining β -glucuronidases. *Nat Chem Biol* 13: 867–873
70. Bornscheuer UT (2002) Microbial carboxyl esterases: Classification, properties and application in biocatalysis. *FEMS Microbiol Rev* 26: 73–81.
71. Krastanova I, Guarnaccia C, Zahariev S, et al. (2005) Heterologous expression, purification, crystallization, X-ray analysis and phasing of the acetyl xylan esterase from *Bacillus pumilus*. *BBA* 1748: 222–230.
72. Wong DWS (2006) Feruloyl esterase, a key enzyme in biomass degradation. *Appl Biochem Biotechnol* 133: 87–111.
73. Dilokpimol A, Mäkelä MR, Aguilarpontes MV, et al. (2016) Diversity of fungal feruloyl esterases: Updated phylogenetic classification, properties, and industrial applications. *Biotechnol Biofuels* 9: 231.
74. Faulds CB, Mandalari G, Curto RBL, et al. (2006) Synergy between xylanases from glycoside hydrolase family 10 and 11 and a feruloyl esterase in the release of phenolic acids from cereal arabinoxylan. *Appl Microbiol Biotechnol* 71: 622–629.
75. Wong DWS, Chan VJ, Liao H, et al. (2013) Cloning of a novel feruloyl esterase gene from rumen microbial metagenome and enzyme characterization in synergism with endoxylanases. *J Ind Microbiol Biotechnol* 40: 287–295.
76. Pérezrodríguez N, Moreira CD, Torrado AA, et al. (2016) Feruloyl esterase production by *Aspergillus terreus* CECT 2808 and subsequent application to enzymatic hydrolysis. *Enzyme Microb Tech* 91: 52–58.
77. Oliveira DM, Salvador VH, Mota TR, et al. (2016) Feruloyl esterase from *Aspergillus clavatus* improves xylan hydrolysis of sugarcane bagasse. *AIMS Bioeng* 4: 1–11.
78. Garg G, Singh A, Kaur A, et al. (2016) Microbial pectinases: An ecofriendly tool of nature for industries. *Biotech* 6: 47.

79. Kant S, Vohra A, Gupta R (2013) Purification and physicochemical properties of polygalacturonase from *Aspergillus niger* MTCC 3323. *Protein Expres Purif* 87: 11–16.
80. Chen Q, Jin Y, Zhang G, et al. (2012) Improving production of bioethanol from duckweed (*Landoltia punctata*) by pectinase pretreatment. *Energies* 5: 3019–3032.
81. Kataria R, Ghosh S (2011) Saccharification of Kans grass using enzyme mixture from *Trichoderma reesei* for bioethanol production. *Bioresource Technol* 102: 9970–9975.
82. Oberoi HS, Vadlani PV, Nanjundaswamy A, et al. (2011) Enhanced ethanol production from Kinnow mandarin (*Citrus reticulata*) waste via a statistically optimized simultaneous saccharification and fermentation process. *Bioresource Technol* 102: 1593–1601.
83. Shanmugam VK, Gopalakrishnan D (2016) Screening and partial purification for the production of ligninase enzyme from the fungal isolate *Trichosporon asahii*. *Braz Arch Biol Technol* 59: e160220.
84. Vrsanska M, Voberkova S, Langer V, et al. (2016) Induction of laccase, lignin peroxidase and manganese peroxidase activities in white-rot fungi using copper complexes. *Molecules* 21: E1553.
85. Pan L, Zhao H, Yu Q (2017) miR397/Laccase gene mediated network improves tolerance to fenoxaprop-*P*-ethyl in *Beckmannia syzigachne* and *Oryza sativa*. *Front Plant Sci* 23: 879.
86. Kameshwar AKS, Qin W (2016) Recent developments in using advanced sequencing technologies for the genomic studies of lignin and cellulose degrading microorganisms. *Int J Biol Sci* 12: 156–171.
87. Rastogi M, Shrivastava S (2017) Recent advances in second generation bioethanol production: An insight to pretreatment, saccharification and fermentation processes. *Renew Sust Energ Rev* 80: 330–340.
88. Huang R, Su R, Qi W, et al. (2011) Bioconversion of lignocellulose into bioethanol process intensification and mechanism research. *BioEnergy Res* 4: 225–245.

89. Lygin AV, Upton J, Dohleman FG, et al. (2011) Composition of cell wall phenolics and polysaccharides of the potential bioenergy crop—*Miscanthus*. *Global Change Biol Bioenergy* 3: 333–345.
90. Wei Y, Li X, Yu L, et al. (2015) Mesophilic anaerobic co-digestion of cattle manure and corn stover with biological and chemical pretreatment. *Bioresource Technol* 198: 431–436.
91. Balat M, Balat H (2009) Recent trends in global production and utilization of bio-ethanol fuel. *Appl Energ* 86: 2273–2282.
92. Cianchetta S, Maggio BD, Burzi PL, et al. (2014) Evaluation of selected white-rot fungal isolates for improving the sugar yield from wheat straw. *Appl Biochem Biotechnol* 173: 609–623.
93. Behera S, Arora R, Nandhagopal N, et al. (2014) Importance of chemical pretreatment for bioconversion of lignocellulosic biomass. *Renew Sust Energ Rev* 36: 91–106.
94. Safari A, Karimi K, Shafiei M (2017) Dilute alkali pretreatment of softwood pine: A biorefinery approach. *Bioresource Technol* 234: 67–76.
95. Rabemanolontsoa H, Saka S (2016) Various pretreatments of lignocellulosics. *Bioresource Technol* 199: 83–91.
96. Zhu Z, Simister R, Bird S, et al. (2015) Microwave assisted acid and alkali pretreatment of *Miscanthus* biomass for biorefineries. *AIMS Bioeng* 2: 446–468.
97. Tang C, Shan J, Chen Y, et al. (2017) Organic amine catalytic organosolv pretreatment of corn stover for enzymatic saccharification and high-quality lignin. *Bioresource Technol* 232: 222–228.
98. Silva ASD, Inoue H, Endo T, et al. (2010) Milling pretreatment of sugarcane bagasse and straw for enzymatic hydrolysis and ethanol fermentation. *Bioresource Technol* 101: 7402–7409.
99. Chemat S, Lagha A, AitAmar H, et al. (2004) Comparison of conventional and ultrasound-assisted extraction of carvone and limonene from caraway seeds. *Flavour Frag J* 19: 188–195.

100. Sipponen MH, Rahikainen J, Leskinen T, et al. (2017) Structural changes of lignin in biorefinery pretreatments. *Nord Pulp Pap Res J* 32: 547–568.
101. Fang H, Zhao C, Song XY, et al. (2013) Enhanced cellulolytic enzyme production by the synergism between *Trichoderma reesei* RUT-30 and *Aspergillus niger* NL02 and by the addition of surfactants. *Biotechnol Bioprocess Eng* 18: 390–39.

CHAPTER 2

Hydrogen peroxide-acetic acid pretreatment increases the saccharification and enzyme adsorption on lignocellulose

Thatiane R. Mota^{1,*}, Dyoni M. Oliveira¹, Gutierrez R. Morais², Rogério Marchiosi¹, Marcos S. Buckeridge³, Osvaldo Ferrarese-Filho¹, Wanderley D. dos Santos^{1,*}

¹ Department of Biochemistry, State University of Maringá, Maringá, PR, Brazil.

² Department of Physics, State University of Maringá, Maringá, PR, Brazil.

³ Department of Botany, Institute of Biosciences, University of São Paulo, São Paulo, SP, Brazil.

***Corresponding author**

Thatiane R. Mota

Wanderley D. dos Santos

E-mail: thatianermota@gmail.com.br; wdsantos@uem.br

Type of chapter:	Research article
Journal:	Industrial Crops and Products
Impact factor:	4.191
Volume/issue, pages:	140: 111657
Date of publication:	November 2019
DOI:	10.1016/j.indcrop.2019.111657

Abstract

Biomass delignification is a crucial condition for the effective production of fermentable sugars from lignocellulosic materials. Here, an effective method was used to pretreat lignocellulosic materials using hydrogen peroxide-acetic acid (HPAC) solution. The pretreatment of maize straw, sugarcane bagasse and eucalyptus bark with HPAC removed 45 to 75% of lignin and improved from 2.1 to 20.8-fold the saccharification process. Delignification caused by HPAC increased the enzyme adsorption capacities of pretreated substrates from 2.6 to 7.1-fold. The HPAC treatment clearly removes furfurals of the hydrolytic medium, contributing to more efficient ethanol fermentation. The applied method can be a useful alternative to improve biomass saccharification, reduce costs and increase the production of second-generation bioethanol.

Keywords

Biomass feedstock; cell wall; enzymatic hydrolysis; HPAC pretreatment, lignin.

1. Introduction

Two companies in Brazil that are using sugarcane bagasse residues (Raízen and GranBio) and one in the USA using maize residues (Poet-DSM consortium) are close to commercializing cellulosic ethanol with economic viability (Gírio et al., 2017). Although these industrial plants are already producing and selling cellulosic ethanol, they still require further reduction of the production cost. The main obstacles include the efficient removal of lignin from lignocellulosic biomass, the high cost to produce hydrolytic enzymes, and the low efficiency of yeasts to ferment pentoses (Marques, 2018). Pretreatment prior to enzymatic hydrolysis disrupts the recalcitrant structure of lignocellulosic biomass, enhancing the access of enzymes to the polysaccharides (Amorim et al., 2011; Oliveira et al., 2015; Mota et al., 2018). Several pretreatment procedures have been reported, including physical, biological and chemical methods, and their industrial applications can reduce the downstream operating costs for biofuel production (Alvira et al., 2010).

The hydrolysis rate is related to the number of enzymes adsorbed onto biomass (Kumar and Wyman, 2009; Lin et al., 2018). However, the relationship between cellulase adsorption kinetics and lignin removal in pretreated biomasses is not fully understood (Pareek et al., 2013). During enzymatic hydrolysis, enzymes tend to bind on the lignin-rich surfaces, inhibiting the enzymatic hydrolysis and harming the enzyme recycling (Pareek et al., 2013; Rahikainen et al., 2013; Lin et al., 2018), and finally, demanding higher enzyme loadings and increasing the costs of the process (Ko et al., 2015).

Ideally, a pretreatment method ought to present a low cost, efficient delignification of different lignocellulosic materials, minimum cellulose degradation and non-significant production of inhibitors for the subsequent enzymatic saccharification and fermentation (Gatt et al., 2018). Some strategies are being developed to decrease the content of inhibitory compounds, as furfural and 5-hydroxymethylfurfural (HMF) produced during the pretreatments. An efficient strategy is to use mild conditions like lower temperature and shorter times of pretreatment (Jönsson & Martin, 2016). By and large, hydrogen peroxide-acetic acid (HPAC) pretreatment meets these criteria because it efficiently removes lignin, using mild temperatures and weak acids (Wi et al., 2015). Previous studies revealed that HPAC pretreatment is quite effective for the delignification of pine and oak woods (Wi et al., 2015), sugarcane bagasse (Tan et al., 2010) and Jerusalem artichoke stalk (Song et al., 2016).

Together with sugarcane bagasse and maize straw, eucalyptus bark is a residue considered an interesting lignocellulosic material for cellulosic ethanol production (Lima et al. 2013; Reina et al. 2016). The large cultivated area of these plants generates a high amount of residues, with high potential for lignocellulosic biofuels. In addition, eucalyptus is widely used in building and paper industries. Based on the principle that HPAC efficiently removes lignin from different lignocellulosic sources, herein we evaluated the saccharification of HPAC-pretreated maize straw (MS, *Zea mays*), sugarcane bagasse (SCB, *Saccharum* sp.) and eucalyptus bark (EB, *Eucalyptus grandis*). Maize and sugarcane are important crops for food and ethanol. After HPAC pretreatment, the chemical modifications and structural features of lignocellulosic materials were characterized by attenuated total reflectance Fourier transform infrared (ATR-FTIR) spectroscopy. The enzyme adsorption capacity on pretreated substrates and the degradation of furfurals were also evaluated.

2. Material and methods

2.1. Raw materials and chemicals

Maize straw, sugarcane bagasse and eucalyptus bark were air-dried, ball-milled to a fine powder and stored at room temperature. All chemicals used in this work were of analytical grade. Acetic acid and hydrogen peroxide were purchased from Nuclear (Brazil). Novozymes (Araucaria, Brazil) kindly donated cellulase complex NS22086, β -glycosidase complex NS22118 and Cellic[®] HTec2.

2.2. HPAC pretreatment

Each lignocellulosic material source was treated using the HPAC method described by Wi et al. (2015) with modifications. The HPAC solution was prepared by mixing hydrogen peroxide and acetic acid (1:1; v/v). One gram of lignocellulosic biomass was homogenized into a screw-capped plastic tube containing 10 mL of HPAC solution and incubated at 80 °C for 2 h. The HPAC-pretreated material was filtered to separate the liquor from the solid residue, and the solids were washed with distilled water and dried at 50 °C for 72 h.

2.3. Determination of furfurals

The liquor fraction obtained from HPAC pretreatment, with furfural (FURF) and 5-hydroxymethylfurfural (HMF) standards, were filtered through a 0.45- μm disposable syringe filter and analyzed by High-Performance Liquid Chromatography system (HPLC) (Moreira-Vilar et al., 2014).

2.4. Cell wall preparation and lignin determination

The dry matter of untreated or HPAC-pretreated biomasses was subjected to successive extractions with 80% ethanol (*v/v*) as described by Oliveira et al. (2016). The remaining solid material was defined as the alcohol insoluble residue (AIR). For lignin determination, AIR was subsequently washed with different solutions to obtain the protein-free cell wall fraction (Ferrarese et al., 2002) and quantified by the acetyl bromide method (Moreira-Vilar et al., 2014).

2.5. Monosaccharide composition

Five mg of AIR were hydrolyzed in 1 mL of 2 M trifluoroacetic acid (TFA) for 1 h at 100 °C, and the monosaccharides released were analyzed by High-Performance Anion Exchange Chromatography with Pulsed Amperometric Detection (HPAEC-PAD). The parameters used and the patterns obtained with standards for the monosaccharide separation are described by Pagliuso et al. (2018).

2.6. Enzymatic hydrolysis

The reaction mixtures were prepared with 15 mg of AIR, enzyme extract containing 5 U/mL cellulase and 30 U/mL xylanase, 0.02% sodium azide (*v/v*) and 50 mM sodium acetate buffer pH 5.0 at 50 °C (Oliveira et al., 2016). The reducing sugars were analyzed by DNS method (3,5-dinitrosalicylic acid) (Miller, 1959).

2.7. ATR-FTIR spectroscopy

ATR-FTIR spectroscopy was performed on a Bruker Vertex 70 FTIR Spectrometer equipped with an Attenuated Total Reflectance accessory and was carried out on AIR samples with 128 scans per sample at a 400 to 4000 cm^{-1} range with a resolution of 2 cm^{-1} .

2.8. Adsorption isotherms

Adsorption isotherms of proteins on lignocellulosic substrates were evaluated by varying the protein concentrations of the enzyme complex from 75 to 6,000 µg/mL (5–400 mg protein/g AIR) according to the methods of Ko et al. (2015) with modifications. The concentration of non-adsorbed proteins in the supernatant was measured according to the Bradford method. Adsorbed protein data were fitted into the following Langmuir equation:

$$P_{ads} = (P_{max} \times K_p \times P_{free}) / (1 + K_p \times P_{free}) \quad (1)$$

where P_{ads} is the amount of adsorbed protein (mg protein/g AIR), P_{free} is the amount of non-adsorbed protein in the supernatant (mg protein/mL), P_{max} is the maximum protein adsorption capacity (mg protein/g AIR), K_p is the Langmuir constant (mL/mg protein) and the equation is a measurement for the adsorption affinity. Adsorption parameters were determined by non-linear regression of experimental data using GraphPad Prism (version 5.00 for Windows).

3. Results and discussion

3.1. HPAC pretreatment alters biomass composition

After 2 h of pretreatment, the total recovery of solids from maize straw (MS), sugarcane bagasse (SCB) and eucalyptus bark (EB) were 67%, 63% and 59%, respectively, and were similar to pinewood, oak wood and rice straw, which ranged from 59 to 75% (Wi et al., 2015). The decrease in HPAC-insoluble solids was mainly due to the solubilization of lignin-derived compounds and pectin-derived monosaccharides (**Table 1**). HPAC pretreatment removed 45%, 70% and 75% of lignin from MS, SCB and EB, respectively. In contrast, crystalline cellulose increased from 34% to 53% after pretreatment, and the hemicellulose content was barely reduced only in SCB (–8%), with no significant differences in MS and EB. The increased cellulose content together with the reduced lignin content resulted in an increased cellulose/lignin ratio in HPAC-pretreated materials. Due to the varied compositional features, different lignocellulosic materials can influence the pretreatment effectiveness and cell wall recalcitrance to hydrolysis in different ways (Alvira et al., 2010; Oliveira et al., 2019a).

The analysis of non-cellulosic monosaccharides by HPAEC-PAD revealed significant differences in the lignocellulosic materials pretreated with HPAC. Neutral monosaccharides released from hemicelluloses and pectin of MS, SCB and EB showed a high proportion of pentoses, before and after HPAC pretreatment. The higher content of xylose and arabinose in SCB and MS, when compared to EB, is related to the high content of arabinoxylan typical of grasses (de Souza et al., 2012; Lima et al. 2014; Oliveira et al., 2019b). EB presented a higher amount of rhamnose (2.27 mg/g AIR) in comparison to MS (0.36 mg/g AIR) and SCB (0.16 mg/g AIR), indicating higher proportions of pectin in EB. Hexose contents of hemicelluloses were significantly changed (**Table 1**). HPAC pretreatment removed 68% and 55% of glucose from MS and SCB hemicelluloses, respectively. Differently from eucalyptus, sugarcane and maize cell walls contain significant quantities of mixed linkage (β -1,4 and β -1,3) glucans (Mota et al., 2018). Our results suggest that HPAC pretreatment partially removed the mixed linkage glucans, modulating the hemicellulose composition. Although pentose fermentation is considerably less efficient than hexose, conversion of pentoses after enzymatic hydrolysis can be achieved using engineered or natural fermenting microorganisms (Almeida et al., 2011).

Changes in specific bands of ATR-FTIR spectroscopy were analyzed after HPAC pretreatment (**Fig. 1A**) and were based on previous studies (Bekiaris et al., 2015; Pereira et al., 2016). Except for bands at 1633 and 1660 cm^{-1} in EB, bands at 1465, 1510, 1600 and 1633 cm^{-1} assigned to lignin decreased considerably after pretreatment, in concordance with the lignin removal data determined by the acetyl bromide method (**Table 1**). The band assignment at 1735 cm^{-1} , usually attributed to the presence of acetyl groups of hemicellulose, did not change in any sample (**Fig. 1B**). Similar results were observed in pinewood, oak wood and rice straw (Wi et al., 2015). Bands at 1053, 1160, 1375, 2910 and 3450 cm^{-1} assigned to crystalline cellulose (Bekiaris et al., 2015), and the band at 898 cm^{-1} assigned to amorphous cellulose were similar in untreated and HPAC-pretreated materials, demonstrating that HPAC pretreatment did not degrade cellulose (**Fig. 1B**).

The ratio of the peaks between 1510 and 898 cm^{-1} was used to calculate the lignin/cellulose ratio after HPAC pretreatment. In MS, the ratio reduced from 1.17 (before pretreatment) to 0.62 (after HPAC pretreatment). In SCB, the pretreatment reduced from

Table 1. Chemical composition of untreated and HPAC-pretreated materials (expressed in mg/g AIR).

Samples	Lignin	Cellulose	Hemicellulose	Cellulose/Lignin ratio	Arabinose	Xylose	Fucose	Galactose	Glucose	Mannose	Rhamnose
MS	191.12 ± 4.28	283.53 ± 18.68	197.48 ± 15.55	1.48	32.36 ± 3.07	124.10 ± 5.98	0.53 ± 0.06	8.52 ± 0.75	30.22 ± 2.56	1.39 ± 0.09	0.36 ± 0.05
MS-HPAC	105.38 ± 1.89	380.27 ± 7.82	185.38 ± 6.57	3.61	31.37 ± 1.21	137.57 ± 5.74	0.21 ± 0.01	6.32 ± 0.30	9.55 ± 0.35	0.39 ± 0.01	0.17 ± 0.02
<i>P</i> -value	< 0.001	0.022	0.271		0.352	0.078	0.001	0.039	0.006	0.001	0.022
SCB	262.78 ± 8.84	395.34 ± 20.51	141.42 ± 0.45	1.50	13.79 ± 0.24	117.24 ± 1.45	0.55 ± 0.04	2.75 ± 0.07	5.66 ± 0.53	1.26 ± 0.02	0.16 ± 0.01
SCB-HPAC	79.64 ± 1.93	594.86 ± 40.50	130.36 ± 2.09	7.47	13.69 ± 0.22	112.27 ± 1.32	0.06 ± 0.01	1.59 ± 0.06	2.55 ± 0.20	0.14 ± 0.01	0.06 ± 0.01
<i>P</i> -value	< 0.001	0.009	0.004		0.387	0.027	< 0.001	< 0.001	0.001	< 0.001	< 0.001
EB	241.96 ± 7.04	307.22 ± 9.37	77.91 ± 2.51	1.27	14.58 ± 0.47	47.03 ± 1.58	1.14 ± 0.05	9.42 ± 0.40	2.60 ± 0.15	0.86 ± 0.05	2.27 ± 0.07
EB-HPAC	61.44 ± 3.56	468.89 ± 23.49	74.87 ± 1.62	7.63	2.58 ± 0.07	61.89 ± 1.30	1.20 ± 0.03	5.59 ± 0.15	2.74 ± 0.07	0.47 ± 0.01	0.39 ± 0.01
<i>P</i> -value	< 0.001	0.001	0.174		< 0.001	< 0.001	0.200	< 0.001	0.214	< 0.001	< 0.001

Mean values ± SEM ($n = 3$ to 4). *P*-values ≤ 0.05 that are statistically significant are showed in bold (unpaired two-sided *t* test).

1.09 to 0.51, and in EB, the ratio decreased from 1.51 to 0.87. These findings strongly suggest that HPAC reacts preferentially with the lignin fraction.

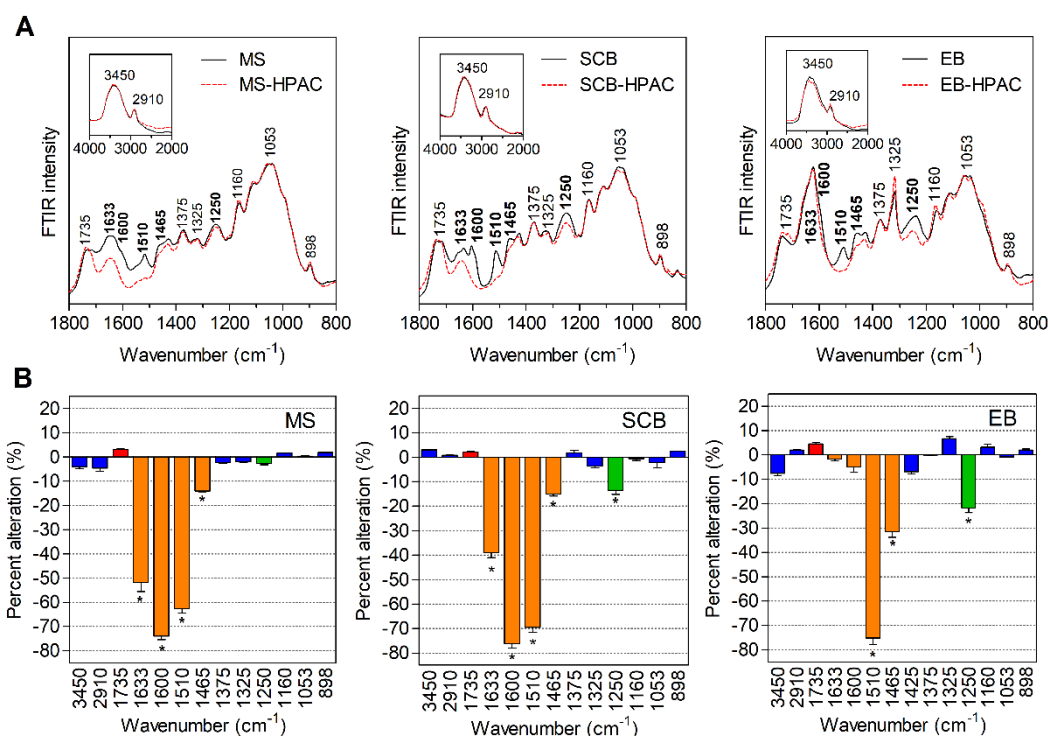


Fig. 1. ATR-FTIR spectra (A) and percent alterations in bands comparing the untreated and HPAC-pretreated substrates (B). Bands at 1465, 1510, 1600 and 1633 cm⁻¹ correspond to lignin (orange bars), 1735 cm⁻¹ corresponds to acetyl groups (red bar), 1250 cm⁻¹ corresponds to xylan (green bar), bands at 898, 1058, 1160, 1325, 1375, 2910 and 3450 cm⁻¹ correspond to cellulose (blue bars). Mean values \pm SEM ($n = 3$). * $P < 0.05$, unpaired two-sided t test.

3.2 HPAC pretreatment improves the enzymatic hydrolysis

The HPAC pretreatment positively affected the saccharification in the different lignocellulosic materials (**Fig. 2A**). The amount of reducing sugars released from HPAC-pretreated MS increased 2.1-fold, from 6.03 to 12.58 g/L, at 50 °C for 96 h of hydrolysis. The enzymatic hydrolysis of SCB increased 7.1-fold the release of reducing sugars, raising it from 2.25 to 15.89 g/L, and in EB it increased 20.8-fold, from 0.59 to 12.24 g/L. In fact, these results indicate that HPAC pretreatment is a highly efficient process for improving biomass saccharification.

To better understand the relationships between cell wall components, enzymatic hydrolysis and protein adsorption, we constructed a heatmap of pairwise Pearson's correlations coefficients (r) comparing all lignocellulosic materials. The lignin contents

of untreated and pretreated samples were negatively correlated with enzymatic hydrolysis at 96 h ($r = -0.95$; $P = 0.0032$). The high sugar yield after enzymatic hydrolysis obtained in HPAC-pretreated materials indicates that cellulose and hemicellulose became more accessible to enzymes.

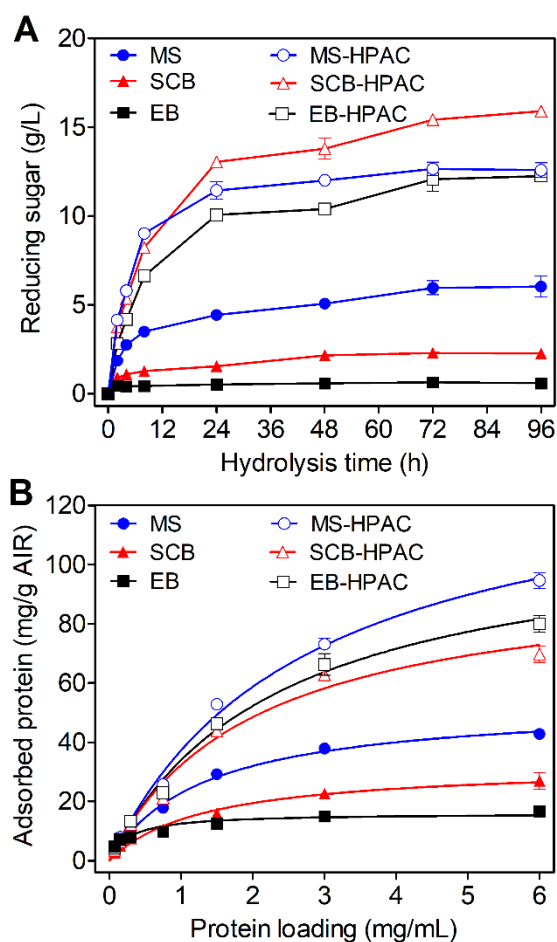


Fig. 2. Reducing sugar yields of enzymatic hydrolysis (A) and adsorption isotherms of proteins on untreated and HPAC-pretreated biomasses (B). Lines indicate the predicted amounts of adsorbed proteins well fitted with the Langmuir isotherm. Mean values \pm SEM ($n = 4$).

This probably occurs because delignification exposes the polysaccharides to the access of hydrolytic enzymes (Li et al., 2016). Compared to pretreatments with hydrogen peroxide, acetic acid, peracetic acid and sulphuric acid under the same conditions, HPAC pretreatment is more effective in improving the enzymatic saccharification of pine, oak woods, and rice straw (Wi et al., 2015). Our results indicate that HPAC is an efficient pretreatment for lignocellulosic materials of contrasting types of cell walls.

3.3 HPAC pretreatment enhances the enzyme adsorption

Due to the interference of lignin in the hydrolysis of polysaccharides by the impeding of enzyme accessibility to the substrates, we evaluated the effect of selective

HPAC-delignification on enzyme adsorption. The adsorption isotherms were generated using untreated and HPAC-pretreated biomasses incubated with different enzyme loadings (75 to 6,000 $\mu\text{g/mL}$). Representative predicted and experimental protein adsorption data are shown in **Fig. 2B**, and adsorption parameters were well fitted with the Langmuir isotherm, with $R^2 \geq 0.90$ (**Table 2**).

After pretreatment, the results revealed that adsorbed proteins were strongly increased (**Fig. 2B**). The maximum adsorption capacity (P_{max}) of MS increased 2.6-fold. In the same experimental condition, P_{max} of HPAC-pretreated SCB and EB were increased 3.0-fold and 7.0-fold, respectively. These findings show a nearly linear relationship between P_{max} vs. enzymatic hydrolysis ($r = 0.90$; $P < 0.05$) and P_{max} vs. lignin content ($r = -0.90$; $P < 0.05$). The high values of adsorption affinity (K_p) and adsorption strength (A) observed for untreated EB (3.61 mL/g protein and 57.05 mL/mg, respectively) may be related to the lower amount of reducing sugar released throughout the enzymatic hydrolysis (**Fig. 2A**). The HPAC pretreatment induced reductions in the K_p values of all the lignocellulosic materials (**Table 2**). As reported by Li et al. (2016), the lower K_p values suggest that delignified samples have more adsorption sites for proteins and, as expected, a possible relationship with the cell wall recalcitrance, as well as a higher efficiency for sugar yields. Instead, our analysis of pairwise correlations for K_p did not present clear relationships with enzymatic hydrolysis ($r = -0.69$; $P > 0.05$), lignin ($r = 0.58$; $P > 0.05$) or P_{max} ($r = -0.69$; $P > 0.05$), suggesting no evident correlation between K_p values and biomass recalcitrance.

Table 2. Maximum enzyme adsorption capacity (P_{max}), adsorption affinity (K_p) and adsorption strength (A) constants for different lignocellulosic biomass. Mean values \pm SEM ($n = 4$).

Samples	P_{max} (mg protein/ g biomass)	K_p (mL/mg protein)	$A = P_{\text{max}} \times K$ (mL/mg)	R^2
MS	53.33 \pm 0.80	0.75 \pm 0.03	39.90	0.98
MS-HPAC	138.80 \pm 2.65	0.37 \pm 0.02	50.85	0.99
SCB	32.34 \pm 1.04	0.75 \pm 0.07	24.30	0.93
SCB-HPAC	97.13 \pm 2.26	0.50 \pm 0.03	48.36	0.98
EB	15.79 \pm 0.56	3.61 \pm 0.28	57.05	0.90
EB-HPAC	111.50 \pm 4.75	0.44 \pm 0.04	49.61	0.98

The removal of lignin exposes more cellulose for protein adsorption (Kumar & Wyman, 2009). Delignification caused by HPAC had a strong positive effect on protein

adsorption to the pretreated biomasses, suggesting relevant changes in the substrate accessibility. Pretreatments affect enzyme adsorption to the lignocellulose material altering its physicochemical properties (Pareek et al., 2013). After HPAC pretreatment, the reduction in lignin content led to a higher surface area of cell wall polysaccharides, which contributed to enhance productive enzyme adsorption on pretreated substrates and, consequently, to enzymatic hydrolysis rate.

3.4. HPAC pretreatment avoids the production of furfurals

Taking into account the pretreatment conditions (acidic solution at 80 °C for 2 h), the production of furfurals was expected (Jönsson & Martin, 2016). However, after HPAC pretreatment, no furfural (FURF) or 5-hydroxymethylfurfural (HMF) accumulated in the liquor (**Fig. 3A**).

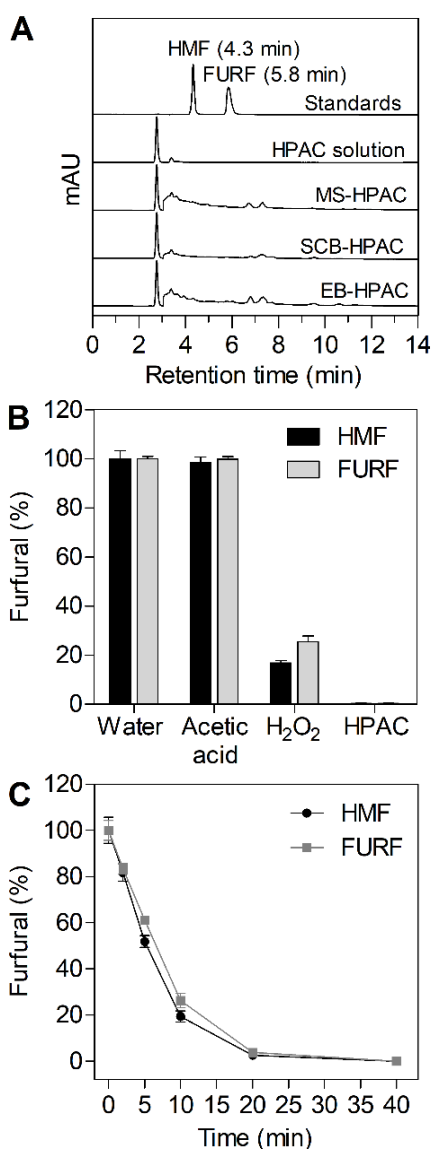


Fig. 3. Furfural analysis. (A) Chromatogram profile of liquor from different HPAC-pretreated biomass, standards and HPAC solution; (B) incubation of furfurals (at 0.25 mM) in water, acetic acid, hydrogen peroxide and HPAC solution, and (C) degradation of furfurals (at 0.25 mM) by HPAC after incubation in different times. HMF, 5-hydroxymethylfurfural; FURF, furfural. Mean values \pm SEM ($n = 3$).

Therefore, we hypothesized that HPAC solution degrades furfurals in these pretreatment conditions. To strengthen this hypothesis, FURF and HMF standards (at 0.25 mM) were incubated with HPAC solution, deionized water, acetic acid and hydrogen peroxide in the same conditions used for the pretreatment (**Fig. 3B**). After 20 min, only 2.6% of initial HMF and 3.7% of FURF concentrations were detected, and after 40 min, both furfurals were completely degraded (**Fig. 3C**). In brief, this property of HPAC is an advantage for pretreatment of lignocellulose, since it avoids the accumulation of furfurals in the reaction medium.

4. Conclusions

Our results showed the potential of maize straw, sugarcane bagasse and eucalyptus bark as sources of fermentable sugars for bioethanol production after HPAC pretreatment. The HPAC pretreatment efficiently removed lignin from lignocellulosic materials with different cell wall types (types I and II). The delignification exposed cellulose and hemicellulose leading to more efficient saccharification of lignocellulose materials, without accumulation of furfurals, inhibitors of ethanol fermentation by yeasts. Furthermore, HPAC increased the adsorption of hydrolytic enzymes onto lignocellulose with potential to maximize sugar yields. Based on our results, HPAC pretreatment may be applied in feedstocks with different cell wall types focusing on cellulosic ethanol production. Altogether, these findings suggest that HPAC treatment is a valuable strategy to decrease the costs of second-generation bioethanol processing in the industry.

Acknowledgements

The authors thank Eglee S. G. Igarashi for the technical assistance, the Coordination of Enhancement of Higher Education Personnel (CAPES) and the National Council for Scientific and Technological Development (CNPq). T. R. Mota is a recipient of CAPES fellowship, D. M. Oliveira is a recipient of CNPq fellowship. R. Marchiosi, M.S. Buckeridge and O. Ferrarese-Filho are research fellows of CNPq. This work was partially supported by the National Institute of Science and Technology of Bioethanol (INCT-Bioethanol) (FAPESP 2008/57908-6 and 2014/50884-5) and (CNPq 574002/2008-1 and 465319/2014-9).

Conflict of interests

The authors declare no conflicts of interest.

References

- Almeida, J.R.M., Runquist, D., Nogu , V.S., Lid n, G., Gorwa-Grausland, M.F. 2011. Stress-related challenges in pentose fermentation to ethanol by the yeast *Saccharomyces cerevisiae*. *Biotechnol. J.*, 6, 286-299.
- Alvira, P., Tomas-Pejo, E., Ballesteros, M., Negro, M.J. 2010. Pretreatment technologies for an efficient bioethanol production process based on enzymatic hydrolysis: A review. *Bioresour. Technol.*, 101(13), 4851-61.
- Amorim, H.V., Lopes, M.L., Oliveira, J.V.C., Buckeridge, M.S., Goldman, G.H. 2011. Scientific challenges of bioethanol production in Brazil. *Appl. Microbiol. Biotechnol.*, 91(5), 1267.
- Bekiaris, G., Lindedam, J., Peltre, C., Decker, S.R., Turner, G.B., Magid, J., Bruun, S. 2015. Rapid estimation of sugar release from winter wheat straw during bioethanol production using FTIR-photoacoustic spectroscopy. *Biotechnol. Biofuels*, 8, 85.
- de Souza, A.P., Leite, D.C.C., Pattathil, S., Hahn, M.G., Buckeridge, M.S. 2012. Composition and Structure of Sugarcane Cell Wall Polysaccharides: Implications for Second-Generation Bioethanol Production. *Bioenerg. Res.*, 6(2), 564-579.
- Ferrarese, M.L.L., Zottis, A., Ferrarese-Filho, O. 2002. Protein-free lignin quantification in soybean (*Glycine max*) roots. *Biologia*, 57, 541-543.
- Gatt, E., Rigal, L., Vandebossche, V., 2018. Biomass pretreatment with reactive extrusion using enzymes: A review. *Ind. Crops Prod.* 122, 329-339.
- G rio, F., Marques, S., Pinto, F., Oliveira, A.C., Costa, P., Reis, A., Moura, P., 2017. Biorefineries in the World, in: Raba al, M., Ferreira, A.F., Silva, C.A.M., Costa, M. (Eds.), *Biorefineries: Targeting Energy, High Value Products and Waste Valorisation*. Springer International Publishing, Cham, pp. 227-281.
- J nsson, L.J., Martin, C. 2016. Pretreatment of lignocellulose: Formation of inhibitory by-products and strategies for minimizing their effects. *Bioresour. Technol.*, 199, 103-112.
- Ko, J.K., Ximenes, E., Kim, Y., Ladisch, M.R. 2015. Adsorption of enzyme onto lignins of liquid hot water pretreated hardwoods. *Biotechnol. Bioeng.*, 112(3), 447-56.
- Kumar, R., Wyman, C.E. 2009. Cellulase adsorption and relationship to features of corn stover solids produced by leading pretreatments. *Biotechnol. Bioeng.*, 103(2), 252-67.

- Li, Y., Sun, Z., Ge, X., Zhang, J. 2016. Effects of lignin and surfactant on adsorption and hydrolysis of cellulases on cellulose. *Biotechnol. Biofuels*, 9, 20.
- Lima, M.A., Gomez, L.D., Steele-King, C.G., Simister, R., Bernardinelli, O.D., Carvalho, M.A., Rezende, C.A., Labate, C.A., Azevedo, E.R., McQueen-Mason, S.J., Polikarpov, I. 2014. Evaluating the composition and processing potential of novel sources of Brazilian biomass for sustainable biorenewables production. *Biotechnol. Biofuels*, 7(1), 10.
- Lima, M. A., Lavorente, G. B., da Silva, H. K., Bragatto, J., Rezende, C. A., Bernardinelli, O. D., Azevedo, E.R., Gomez, L.D., McQueen-Mason, S.J., Polikarpov, I. 2013. Effects of pretreatment on morphology, chemical composition and enzymatic digestibility of eucalyptus bark: a potentially valuable source of fermentable sugars for biofuel production—part 1. *Biotechnol. Biofuels*, 6(1), 75.
- Lin, X., Wu, Z., Zhang, C., Liu, S., Nie, S., 2018. Enzymatic pulping of lignocellulosic biomass. *Ind. Crops Prod.* 120, 16-24.
- Marques, F. 2018. Obstacles in the way. *Pesquisa FAPESP*, 268, 1-1.
- Miller, G.I. 1959. Use of dinitrosalicylic acid reagent for determination of reducing sugar. *Anal. Chem.* 31 (3), 426-428.
- Moreira-Vilar, F.C., Siqueira-Soares, R.C., Finger-Teixeira, A., Oliveira, D.M., Ferro, A.P., da Rocha, G.J., Ferrarese, M.L.L., dos Santos, W.D., Ferrarese-Filho, O. 2014. The acetyl bromide method is faster, simpler and presents best recovery of lignin in different herbaceous tissues than klason and thioglycolic acid methods. *PLOS ONE*, 9(10), e110000.
- Mota, T.R., Oliveira, D.M., Marchiosi, R., Ferrarese-Filho, O., dos Santos, W.D. 2018. Plant cell wall composition and enzymatic deconstruction. *AIMS Bioeng.*, 5(1), 63-77.
- Oliveira, D.M., Finger-Teixeira, A., Mota, T.R., Salvador, V.H., Moreira-Vilar, F.C., Molinari, H.B., Mitchell, R.A., Marchiosi, R., Ferrarese-Filho, O., dos Santos, W.D. 2015. Ferulic acid: a key component in grass lignocellulose recalcitrance to hydrolysis. *Plant Biotechnol. J.*, 13(9), 1224-32.
- Oliveira, D.M., Mota, T.R., Oliva, B., Segato, F., Marchiosi, R., Ferrarese-Filho, O., Faulds, C.B., dos Santos, W.D., 2019a. Feruloyl esterases: Biocatalysts to overcome biomass recalcitrance and for the production of bioactive compounds. *Bioresour. Technol.*, 278, 408-423.

- Oliveira, D.M., Mota, T.R., Salatta, F.V., Marchiosi, R., Gomez, L.D., McQueen-Mason, S.J., Ferrarese-Filho, O., dos Santos, W.D., 2019b. Designing xylan for improved sustainable biofuel production. *Plant Biotechnol. J.* DOI: 10.1111/pbi.13150
- Oliveira, D.M., Salvador, V.H., Mota, T.R., Finger-Teixeira, A., Almeida, R.F., Paixão, D.A.A., de Souza, A.P., Buckeridge, M.S., Marchiosi, R., Ferrarese-Filho, O., Squina, F.M., dos Santos, W.D. 2016. Feruloyl esterase from *Aspergillus clavatus* improves xylan hydrolysis of sugarcane bagasse. *AIMS Bioeng.*, 4(1), 1-11.
- Pagliuso, D., Grandis, A., Igarashi, E.S., Lam, E., Buckeridge, M.S. 2018. Correlation of Apiose Levels and Growth Rates in Duckweeds. *Front. Chem.*, 6, 291.
- Pareek, N., Gillgren, T., Jonsson, L.J. 2013. Adsorption of proteins involved in hydrolysis of lignocellulose on lignins and hemicelluloses. *Bioresour. Technol*, 148, 70-7.
- Pereira, S.C., Maehara, L., Machado, C.M.M., Farinas, C.S. 2016. Physical–chemical–morphological characterization of the whole sugarcane lignocellulosic biomass used for 2G ethanol production by spectroscopy and microscopy techniques. *Renew. Energ.*, 87, 607-617.
- Rahikainen, J.L., Martin-Sampedro, R., Heikkinen, H., Rovio, S., Marjamaa, K., Tamminen, T., Rojas, O.J., Kruus, K. 2013. Inhibitory effect of lignin during cellulose bioconversion: The effect of lignin chemistry on non-productive enzyme adsorption. *Bioresour. Technol*, 133, 270-278.
- Reina, L., Botto, E., Mantero, C., Moyna, P., Menéndez, P. 2016. Production of second generation ethanol using *Eucalyptus dunnii* bark residues and ionic liquid pretreatment. *Biomass Bioenerg.*, 93, 116-121.
- Song, Y., Wi, S.G., Kim, H.M., Bae, H.J. 2016. Cellulosic bioethanol production from Jerusalem artichoke (*Helianthus tuberosus* L.) using hydrogen peroxide-acetic acid (HPAC) pretreatment. *Bioresour. Technol.*, 214, 30-36.
- Tan, H., Yang, R., Sun, W., Wang, S. 2010. Peroxide–Acetic Acid Pretreatment To Remove Bagasse Lignin Prior to Enzymatic Hydrolysis. *Ind. Eng. Chem. Res.*, 49(4), 1473-1479.
- Wi, S.G., Cho, E.J., Lee, D.S., Lee, S.J., Lee, Y.J., Bae, H.J. 2015. Lignocellulose conversion for biofuel: a new pretreatment greatly improves downstream biocatalytic hydrolysis of various lignocellulosic materials. *Biotechnol. Biofuels*, 8, 228.

CHAPTER 3

Suppression of a BAHD acyltransferase decreases *p*-coumaroyl on arabinoxylan and improves biomass digestibility in the model grass *Setaria viridis*

Thatiane R. Mota^{1,*}, Wagner R. de Souza^{2,3}, Dyoni M. Oliveira¹, Polyana K. Martins², Bruno L. Sampaio², Felipe Vinecky², Ana P. Ribeiro², Karoline E. Duarte², Thályta F. Pacheco², Norberto K. V. Monteiro^{4,6}, Raquel B. Campanha², Rogério Marchiosi¹, Davi S. Vieira⁴, Adilson K. Kobayashi², Patrícia A. O. Molinari², Osvaldo Ferrarese-Filho¹, Rowan A. C. Mitchell⁵, Hugo B. C. Molinari^{2,*}, Wanderley D. dos Santos¹

¹Department of Biochemistry, State University of Maringá, Maringá, PR, Brazil.

²Embrapa Agroenergy, Brasília, DF, Brazil.

³Center for Natural and Human Sciences, Federal University of ABC, São Bernardo do Campo, SP, Brazil.

⁴Institute of Chemistry, Federal University of Rio Grande do Norte, Natal, RN, Brazil.

⁵Plant Sciences, Rothamsted Research, Harpenden, Hertfordshire, UK.

⁶Department of Analytical and Physical Chemistry, Federal University of Ceará, Fortaleza, CE, Brazil.

***Corresponding author:**

Hugo B. C. Molinari

Thatiane R. Mota

E-mail: hugo.molinari@embrapa.br; thatianermota@gmail.com

Type of chapter:	Research article
Journal:	The Plant Journal
Impact factor:	5.726
Current status:	Under review

Running title

Acyltransferase suppression reduces *p*CA onto AX.

Significance statement

A BAHD acyltransferase was studied and revealed that its suppression causes reduction of ester-linked *p*CA in the cell walls of *Setaria viridis*. RNAi silenced lines had higher biomass saccharification efficiency with no alteration in the biomass production. Molecular dynamics simulation reinforced the evidences that *SvBAHD05* is mainly responsible for the incorporation of *p*-coumaric acid onto arabinoxylan, the main hemicellulose in grass cell walls.

Summary

Grass cell walls have hydroxycinnamic acids attached to arabinosyl residues of arabinoxylan and certain BAHD acyltransferases are involved in their addition. In this study, we characterized one of these *BAHD* genes in the cell wall of the model grass *Setaria viridis*. RNAi silenced lines of *S. viridis* (*SvBAHD05*) presented a decrease of up to 42% of ester-linked *pCA* and 50% of *pCA-Araf*, across three generations. Biomass from *SvBAHD05* silenced plants exhibited up to 32% increase in biomass saccharification efficiency after acid pretreatment, with no change in total lignin. Molecular dynamics simulations suggested that *SvBAHD05* is a *p*-coumaroyl coenzyme A transferase mainly involved in the addition of *pCA* to the arabinofuranosyl units of arabinoxylan, the main hemicellulose in grass cell walls, in *Setaria*. Our results provide a strong evidence of *p*-coumaroylation of arabinoxylan promoted by *BAHD05* acyltransferase gene in cell wall biosynthesis of monocot plants, thus, *SvBAHD05* is a promising biotechnological target to engineer crops for improved biomass saccharification for biofuels, biorefineries and animal feeding.

Keywords

Cell wall acylation, *p*-coumaric acid, hydroxycinnamic acids, grass xylan, lignin, lignocellulose, saccharification.

1. Introduction

Renewable biofuels are environment-friendly and can replace petrochemical products in a sustainable economy. Currently, ethanol production utilizes crops like maize and sugarcane, which competes with food production (Oakey *et al.*, 2013). Given this, bioethanol from the lignocellulosic biomass has been receiving special attention. Understanding the plant cell wall architecture, the acylation patterns and its biosynthesis is an efficient way to accelerate the development of technologies for cellulosic ethanol production.

The high content of *p*-coumaric (*p*CA) and ferulic (FA) acids, known as hydroxycinnamic acids (HCA), is a distinctive structural feature of grass cell walls when compared to eudicots (Harris and Trethewey, 2010, Hatfield *et al.*, 2017). FA is involved in grass cell walls cross-linking through the acylation of arabinofuranosyl residues (Araf) that are 1→2- or 1→3-linked to the xylan backbone of arabinoxylan or glucuronoarabinoxylan (AX; for simplicity we refer to all grass xylans here as AX although they mostly have numerous decorations in addition to arabinose) (de Oliveira *et al.*, 2015). Extensive cross-linkages among the cell wall polymers inhibit the access of hydrolytic enzymes to cellulose microfibrils; since AX is the main hemicellulose in grass cell walls, forming the interface between cellulose microfibrils and lignin (Terrett and Dupree, 2019), decreasing FA on AX is a means to increase the digestibility of grass lignocellulose (Oliveira *et al.*, 2019a).

*p*CA mostly acylates the lignin polymer, and a small fraction also acylates the AX, by the action of a *p*-coumaroyl coenzyme A transferase (PAT) with the addition of *p*CA to the arabinofuranosyl residues of arabinoxylan (see putative route in Figure 1). The lignin γ -acylation in grass cell walls mainly arise from the incorporation of γ -*p*-coumaroylated monolignols, the sinapyl- and coniferyl *p*-coumarates. The formation of the γ -*p*-coumaroylated monolignols, using *p*-coumaroyl coenzyme A (*p*CA-CoA) as an acyl-donor, is catalyzed by *p*-coumaroyl-CoA:monolignol transferase (PMT) (Withers *et al.*, 2012, Petrik *et al.*, 2014). Although the activity of PMT has been demonstrated *in vitro* (Withers *et al.*, 2012, Bouvier d'Yvoire *et al.*, 2013) explaining the role of PMTs in lignin acylation by *p*CA (Marita *et al.*, 2014, Petrik *et al.*, 2014), no equivalent activity was demonstrated for AX acylation by *p*CA promoted by the PAT neither for FA promoted by FAT enzyme (feruloyl coenzyme A transferase). However, it has been

shown that overexpressing the gene *OsAT10* of the same clade as PMT in the BAHD superfamily, led to increased acylation of AX by *pCA* in rice (Bartley *et al.*, 2013).

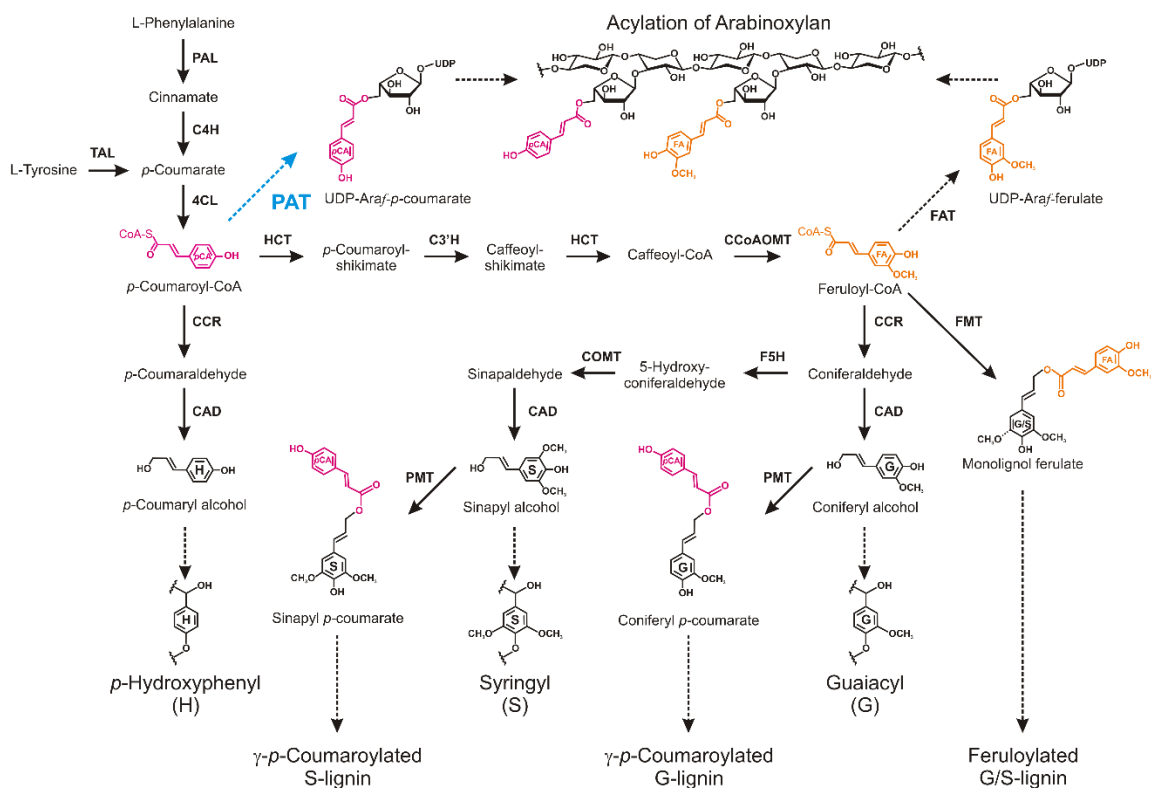


Figure 1. Overview of phenylpropanoid and monolignol pathways, and acylation of arabinoxylan and monolignols. Blue dotted arrow is highlighting the putative *p*-coumaroyl:CoA transferase (PAT) encoded by *BAHD05* gene. PAT and FAT are putative enzymes without direct evidence on their activity – UDP-Araf-*pCA* and UDP-Araf-FA are theoretical metabolites that have not been observed experimentally. PAL, L-phenylalanine ammonia-lyase; C4H, cinnamate 4-hydroxylase; TAL, L-tyrosine ammonia-lyase; 4CL, 4-hydroxycinnamate: CoA ligase; PAT, *p*-coumaroyl:CoA transferase; HCT, hydroxycinnamoyl-CoA: shikimate/quinate hydroxycinnamoyltransferase; C3'H, *p*-coumarate 3'-hydroxylase; CCoAOMT, caffeoyl-CoA O-methyltransferase; CCR, cinnamoyl-CoA reductase; FAT, feruloyl:CoA transferase; FMT, feruloyl-CoA:monolignol transferase; F5'H, ferulate 5'-hydroxylase/coniferaldehyde 5'-hydroxylase; COMT, caffeate/5-hydroxyferulate 3-O-methyltransferase; CAD, cinnamyl alcohol dehydrogenase; PMT, *p*-coumaroyl-CoA:monolignol transferase. Arrows with dashed lines designate putative routes.

Recent studies have highlighted that lowering *pCA* and FA in grass cell walls decrease biomass recalcitrance (Li *et al.*, 2018, de Souza *et al.*, 2019). Thus, decreasing *pCA* or FA contents of grass biomass is a promising strategy for increasing digestibility for biofuels production or animal feeding (Oliveira *et al.*, 2019b). The functional comprehension of the BAHD acyltransferases is therefore pivotal to identify new targets

for grass crop improvement and elucidate the evolutionary role of *p*-coumaroylation and feruloylation in economic important grasses as sugarcane, maize, rice, miscanthus, and switchgrass.

Plant BAHD acyltransferases belong to a large family of acyl CoA-utilizing enzymes named according to the first letter of the first four characterized enzymes (BEAT, AHCT, HCBT and DAT) (St-Pierre and De Luca, 2000). Their catalytic versatility makes it very difficult to do functional predictions based solely on the primary sequence and additional biochemical analyses are important to predict the protein function (D'Auria, 2006). A particular clade of genes (Mitchell Clade) within the BAHD superfamily was first proposed as involved in the addition of *p*CA and FA to AX in grasses, based on a bioinformatics analysis showing expansion of the number of genes and greater expression of these in grasses compared to dicots orthologs, and some co-expression with cell wall genes (Mitchell *et al.*, 2007). This clade contains the PMT gene responsible for *p*-coumaroylation of lignin, but there is now evidence that other genes in the clade are indeed responsible for the acylation of AX side chains present in grass cell walls (by PAT and FAT enzymes).

Suppression and overexpression of BAHD acyltransferase genes are respectively correlated with decreased and increased cell wall *p*CA or FA in different monocot species (Bartley *et al.*, 2013, Buanafina *et al.*, 2016, de Souza *et al.*, 2018, de Souza *et al.*, 2019) and some of these studies confirmed that these changes are on AX by direct measurement of HCA-Araf conjugates (Bartley *et al.*, 2013, de Souza *et al.*, 2018, de Souza *et al.*, 2019). This additional measurement is essential for distinguishing between *p*CA ester-linked to AX and *p*CA ester-linked to lignin, in contrast to cell wall FA which is derived mostly or entirely from that linked to AX, since acylation of monolignols by FA becomes incorporated into the lignin polymer and is not detected by standard methods so far (Karlen *et al.*, 2016).

Whereas clear evidence was obtained for the role of *OsAT10* in addition of *p*CA to AX (Bartley *et al.*, 2013), the effects on FA of manipulating *BAHD* gene expression tended to be smaller (Piston *et al.*, 2010, Bartley *et al.*, 2013, Buanafina *et al.*, 2016). However, in our previous study of the *BAHD01* gene in *Setaria viridis* (de Souza *et al.*, 2018), an emerging monocot plant model for molecular and genetic studies (Brutnell *et al.*, 2010), we achieved large and consistent effects (Brutnell *et al.*, 2010, de Souza *et al.*, 2018). By silencing *BAHD01* in *S. viridis* (*SvBAHD01*), we induced decreases by ~60%

in the levels of FA in cell walls of RNAi plants, improving the biomass saccharification (de Souza *et al.*, 2018). These results suggest that *SvBAHD01* is a feruloyl transferase responsible for the addition of FA onto arabinosyl residues linked to AXs. Furthermore, we recently showed that silencing of *SvBAHD01* ortholog in sugarcane (*SacBAHD01*) led to similar results to those demonstrated in *S. viridis* (de Souza *et al.*, 2019). We were interested in characterizing the other *BAHD* gene in *S. viridis* and for that, we selected *SvBAHD05*, the ortholog of *BdAT1* that appears to act in the addition of FA to AX in *Brachypodium distachyon* (Buanafina *et al.*, 2016). Thus, *SvBAHD05* might be functionally redundant with *SvBAHD01* in *S. viridis*.

Here we demonstrate the effects of suppressing *SvBAHD05* by RNAi. Surprisingly, we found that *SvBAHD05* silenced lines have decreased *pCA* levels, but not FA levels, on AX in leaves, stems, and roots of *S. viridis*. Molecular dynamics simulations of *SvBAHD05* suggested that both *pCA* and FA can bind to a specific *SvBAHD05* domain, indicating a substrate versatility of the enzyme. Moreover, the study also demonstrated that the presence of arabinosyl residues linked to *pCA* and FA stabilizes the ligands in the *SvBAHD05* catalytic domain, reinforcing the hypothesis that *SvBAHD05* is responsible for the addition of hydroxycinnamates to arabinosyl residues of AX in grasses. Our results contribute to a greater understanding of the *BAHD* acyltransferases role in cell wall biosynthesis of monocot plants, and *SvBAHD05* is a promising target in grasses for increasing biomass saccharification in biorefineries and animal feeding.

2. Results

2.1 Generation of *SvBAHD05* silencing lines in *Setaria viridis*

We previously analyzed the phylogeny of *BAHD* genes in the ‘Mitchell Clade’ (Mitchell *et al.*, 2007, Bartley *et al.*, 2013), identifying 10 members of *BAHD* orthologs in *S. viridis* (de Souza *et al.*, 2018). In the present work, we selected *Sevir.5G233700* (*SvBAHD05*) as target for suppression because this gene is among the most expressed in tissues of *Setaria* and other grasses (Bartley *et al.*, 2013, Molinari *et al.*, 2013, Buanafina *et al.*, 2016, de Souza *et al.*, 2018). We obtained 10 independent lines of *S. viridis* transgenic plants transformed with a construct containing an RNA hairpin designed to suppress *SvBAHD05* under control of a constitutive maize ubiquitin (Figure S1a) with 247 bp sequence (Figure S1b). The levels of *SvBAHD05* silencing ranged by 48-98% in

leaves, stems, and roots in T₃ generation plants of *S. viridis* (Table S1). We then selected three transgenic lines presenting low (1.1), intermediate (2.1) and high (3.1) levels of silencing for further biochemical studies (Figure 2a-2c).

In addition, we analyzed the transcript levels of other *BAHD* genes in leaves of RNAi lines 1.1 and 3.1, to check for pleiotropic effects on different members of this gene family. In agreement with *SvBAHD05* expression in transgenic lines estimated by qRT-PCR (Figure 2a), we observed lower FPKM values for *SvBAHD05* in RNAi lines 1.1 (65%) and 3.1 (71%) compared to NT plants (Figure S2). We found no evidence of compensatory effect in the expression of other *BAHD* genes triggered by *BAHD05* suppression. Both *SvBAHD09* and *SvBAHD08*, which are orthologues of *BdPMT1* and *BdPMT2* (de Souza et al., 2018), were slightly downregulated in transgenic line 1.1 (Figure S2). These genes were also slightly down-regulated in *SvBAHD01* RNAi plants (de Souza et al., 2018) and may reflect a response in expression to changed HCA-CoA or monolignol levels (the substrates for PMT) in the RNAi plants.

2.2 *SvBAHD05* silencing lines present reduced content of ester-linked *pCA* and *pCA* linked to the AX

To evaluate the effects of *SvBAHD05* silencing in cell walls of *S. viridis*, we measured the levels of esterified ferulates, dehydrodimers and *p*-coumarates from the alcohol insoluble residues (AIR) of the reproductive developmental stage. Our analysis demonstrated that suppression of *SvBAHD05* reduced the ester-linked *pCA* levels in all tissues of silenced lines compared with non-transformed (NT) plants (Figure 2d-2f). Silenced lines of leaves had lower content of *pCA*, with reductions of 35–39%, while roots showed reductions of 22% to 42%, compared to NT plants. In contrast, stems had a slight reduction of 12% in *pCA* content only in the transgenic line 2.1. We also found that ester-linked FA did not show significant differences in all tissues of silenced lines, although only line 3.1 had a significant decrease of FA (14%) in roots compared to NT plants (Figure 2f). In addition, absolute abundance of cell wall *pCA* was higher in stems and roots than in leaves (Table S2).

Ferulic acid ester-linked to AX can form dehydrodimers (DiFA), which can cross-link adjacent AX chains to one another (Hatfield *et al.*, 2017). To assess whether *SvBAHD05* RNAi silencing led to altered proportion of DiFA, we quantified the six most abundant DiFA. Overall, the individual amounts (Figure S3a-S3c) and the sum of the

dimers (TOTdiFA; Figure 2d-2f) of RNAi *SvBAHD05* lines had no changes compared to NT plants. The exception was a slight alteration in the levels of 8–5 DiFA coupled forms (8–5'-DiFA and 8–5'-DiFA benzofuran form) in leaves and stems of RNAi lines 1.1 and 2.1 (insert on the Figure 2d-2e and Figure S3a-S3b).

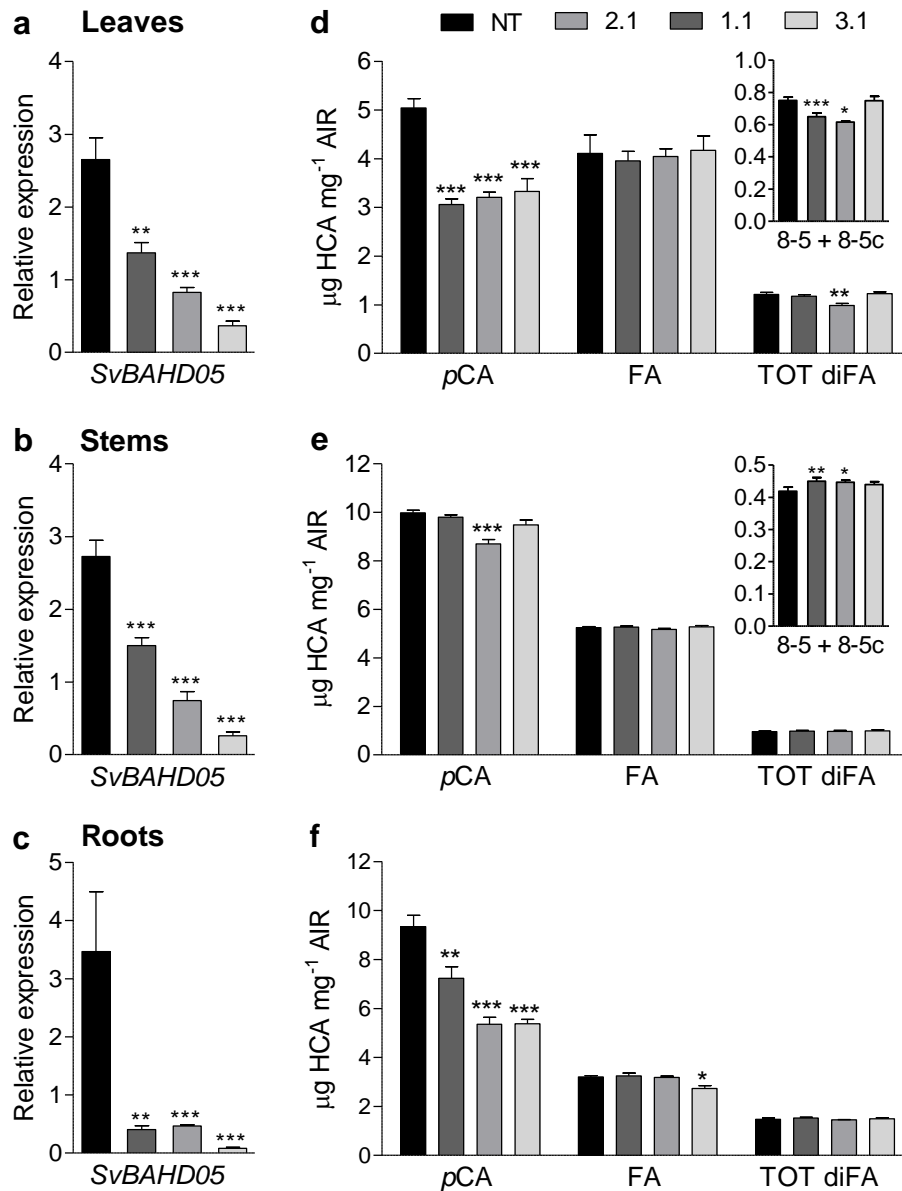


Figure 2. Relative expression, ester-linked HCA and dehydrodimer contents of *SvBAHD05* silencing lines. Leaves, stems and roots of *Setaria viridis* from the non-transformed (NT) plants and transgenic lines 1.1, 2.1 and 3.1. (a-c) qRT-PCR assays of *SvBAHD05* (T_3 generation). Expression is relative to the high expressed reference genes *EF1a* and *eIF4a* for leaves and stems, *CAC* and *CUL* for roots. ($n = 3$). (d-f) Ester-linked HCA contents of *p*-coumarate (*pCA*), ferulate (FA) and the sum of FA dimers (TOTdiFA) in the alcohol insoluble fraction (AIR) of cell walls. ($n = 4$). Error bars \pm SEM; statistical differences of transgenic lines compared to NT are with (*) from ANOVA at $*P < 0.05$, $**P < 0.01$, $***P < 0.001$. Three technical replicates were used for each biological replicate.

The total ester-linked HCA content of cell walls is comprised of *pCA* and FA esterified at *O*-5 position of α -(1,2)- or α -(1,3)-arabinofuranosyl (*Araf*) residues of AX backbone and that esterified to lignin (Hatfield et al., 2017). To determine whether the effects in silenced lines were on HCA-lignin or on HCA-AX, we measured *Araf*-HCA conjugates released from *pCA*-AX or FA-AX by mild acidolysis according to the methodology previously described (de Souza et al., 2018). We observed a decrease in *pCA*-*Araf* in all tissues of transgenic lines when compared with NT (Figure 3a-3c). The levels of *pCA*-*Araf* were ~50% lower in leaves of RNAi lines, whereas stems presented 26–50% less *pCA*-*Araf*. We also found that roots exhibited reductions of 14–42% in *pCA*-*Araf* levels.

Overall, the greater relative effects of *SvBAHD05* suppression on *pCA*-*Araf* (Figure 3a-3c) than on total ester-linked *pCA* (Figure 2d-2f) are consistent with a decrease in *pCA*-AX. The greater effect in leaves than in stems also fits with our previous finding that *pCA*-AX makes up a greater proportion of total ester-linked *pCA* in *Setaria* leaves than in stems (de Souza *et al.*, 2018). As mentioned above, total FA is expected to be derived all from FA-AX and relative effects on total FA and FA-*Araf* were similar in our previous work (de Souza *et al.*, 2018). Here however, despite no significant effects on total FA (Figure 2d-2f), leaves of the transgenic lines had significantly lower FA-*Araf* levels compared to NT (18-25% reduction), whereas stems and roots exhibited slight reductions of ~15% only in silenced line 2.1 (Figure 3d-3f). These combined observations of reductions in cell wall ester-linked *pCA* and *pCA*-*Araf* in the RNAi lines support that *SvBAHD05* gene is involved in *p*-coumaroylation of AX with lesser effect on feruloylation in grass cell walls, suggesting a versatile activity of the protein.

2.3 Composition of cell wall polysaccharides in RNAi silencing lines

We analyzed the monosaccharide composition of the cell walls in *SvBAHD05* RNAi plants. Compared to NT plants, the amounts of glucose of transgenic plants were significantly reduced in leaves (~15%), stems (5% to 8%) and roots (6% to 15%) (Figure S4). Similarly, lower amounts of xylose were observed in leaves (10% to 16%), stems (~5%) and roots (~8%) of silenced plants. We also observed a reduction in arabinose of leaves by 4% to 14%, whereas a slightly increase of ~6% was observed in stems and roots. Our results demonstrated that, compared to NT plants, the content of cell wall

acetate was decreased by 5% to 15% in all the tissues of *SvBAHD05* silenced plants (Figure S4).

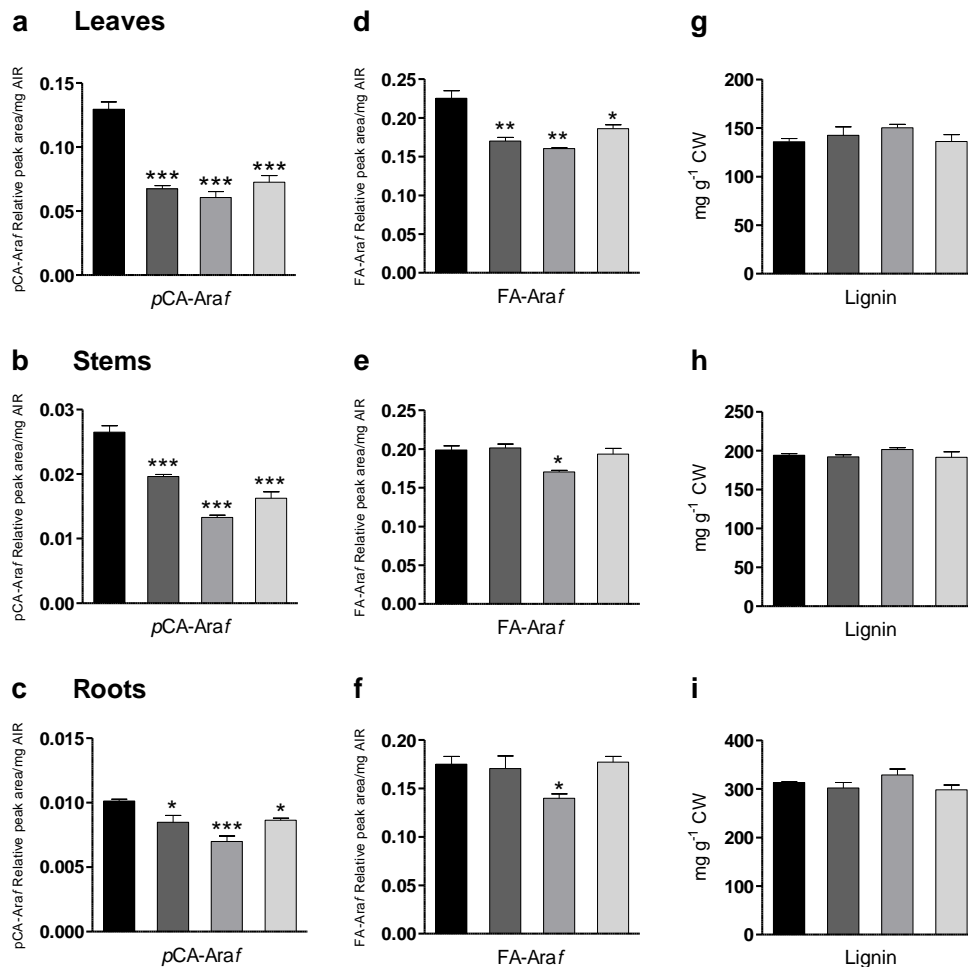


Figure 3. HCA conjugates in supernatant following mild acidolysis of the AIR and acetyl bromide-soluble lignin of *SvBAHD05* RNAi lines. (a-f) Relative peak areas of major peaks of *p*-coumarate, *pCA-Araf* in leaves (a), stems (b), and roots (c); and ferulate, *FA-Araf* in leaves (d), stems (e), and roots (f), previously identified by LC–MS as described by de Souza et. al. (2018) ($n = 4$). (g-i) Acetyl bromide-lignin of cell walls in leaves (g), stems (h), and roots (i) ($n = 5$). NT (non-transformed plants), 1.1, 2.1, and 3.1 (transgenic lines). Error bars \pm SEM; asterisks indicate significant differences using ANOVA (* $P < 0.05$, ** $P < 0.01$, *** $P < 0.001$).

2.4 Effects of *SvBAHD05* suppression on lignin content and structure

To further investigate the extent of cell wall changes in *SvBAHD05* silenced lines, we analyzed lignin content and structure. Leaves, stems and roots of transgenic lines had no significant differences in the content of acetyl bromide-lignin compared to NT plants (Figure 3g-3i). We examined lignin composition using alkaline nitrobenzene oxidation to determine relative amounts of monomers and two-dimensional heteronuclear single

quantum coherence NMR (2D-HSQC-NMR) spectroscopy to estimate overall distributions of lignin and HCA in whole cell walls (Mansfield *et al.*, 2012).

By nitrobenzene oxidation, we observed that the relative frequency of S-lignin was altered in leaves and stems but not roots of silenced lines (Figure S3g-S3h). Leaf lignin of the transgenic lines showed reduction in S-lignin compared to NT plants (16% to 37%). Stem lignin of 1.1 line presented a reduction in S-lignin (18%) and a small increase in G-lignin (7%), while the line 3.1 had higher S-lignin (8%). In roots, no differences in relative abundances of S- and G-lignin were observed between NT and transgenic lines (Figure S3d-S3i).

To investigate the changes in lignin structural components, unfractionated *S. viridis* cell walls were analyzed using 2D-NMR spectroscopy at the solution-state (Kim and Ralph, 2010). As observed in Figure 4, there is a good agreement between the biochemical analysis and 2D-NMR data in leaves of *Setaria*. As expected, we observed reductions in *pCA* in cell walls of transgenic lines of 40-50% (Figure 4) comparable with the biochemical assessment of 35-39% (Figure 2d). The 2D-NMR analysis revealed that leaves, but not stems, of transgenic plants had lower levels of FA, compared to NT, in agreement with effects observed for FA-Araf (Figure 3d). Moreover, the *pCA*/FA ratio from 2D-NMR also corroborated the biochemical data (Table S2), decreasing in transgenic lines as observed in 2D-NMR analysis (Figure 4). The lower S/G ratio observed in leaves of *SvBAHD05* RNAi silenced lines determined by 2D-NMR also agreed with that those estimated by alkaline nitrobenzene oxidation (Figure S3j). Therefore, the NMR results largely corroborated the findings obtained by biochemical assessment, indicating a lower incorporation of *pCA* in silenced plants.

2.5 Molecular dynamics simulations of BAHD05 and BdAT1

In contrast to our results, suppressing the ortholog of *SvBAHD05* in *B. distachyon*, *BdAT1*, reduces the levels of cell wall FA but not *pCA* (Buanafina *et al.*, 2016). We therefore decided to subject the *SvBAHD05* (*Sevir.5G233700*) and *BdAT1* (*Bradi2g43520*) protein sequences to molecular modeling analysis. Firstly, we predicted the tridimensional structures of *SvBAHD05* and *BdAT1* proteins (Figure 5a-5b).

The two models, validated through the MolProbity and Ramachandran plot (Figure S5a-S5b), were submitted to the molecular dynamics (MD) simulations for refinement and equilibration of these structures under thermal and solvent effects

(Machado *et al.*, 2016, Melo *et al.*, 2017). The ligands structures (pCA, FA, pCA-Araf and FA-Araf) had their geometries optimized (Figure 5c-5f) in order to perform molecular docking near the HXXXD motif (Figure 5g-5n) into SvBAHD05 and BdAT1 proteins.

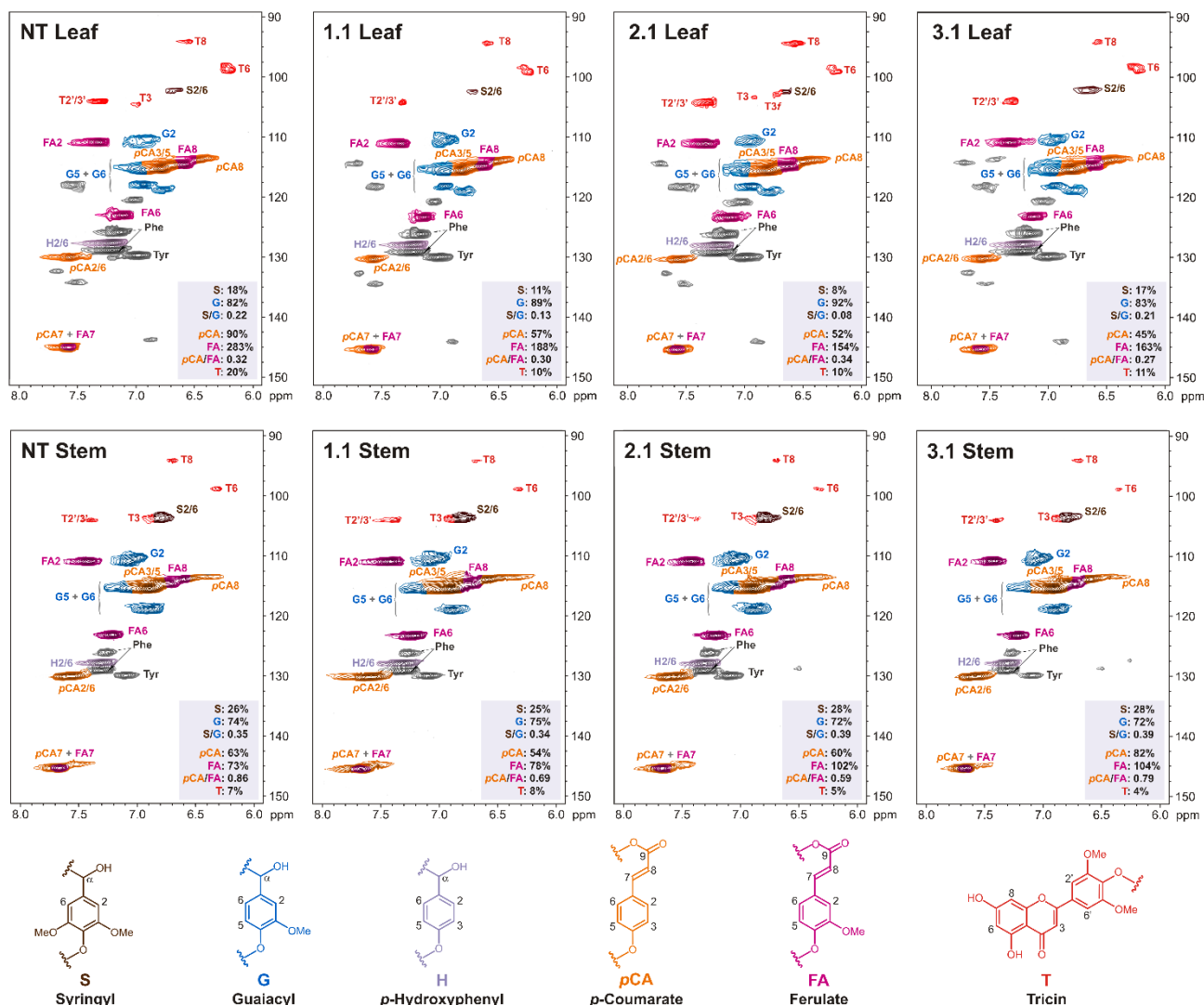


Figure 4. 2D-NMR single-quantum coherence (HSQC) partial spectra of leaves and stems tissues from the non-transformed (NT) and the three transgenic lines (1.1, 2.1 and 3.1) of *Setaria viridis*. Color-coding of the contours matches that of the assigned structures; where contour overlap occurs, the colorization is only approximate. The analytical data are from volume integrals of correlation peaks representing reasonably well-resolved (except for H) C/H pairs in similar environments; thus, they are from S2/6, G2, H2/6, FA2, pCA2/6 and T2/6, with correction for those units that have two C/H pairs per unit. All relative integrals are on a G + S = 100% basis; H-units are over-quantified due to an overlapping peak from protein phenylalanine units.

The final structure of all complexes was used in the PM7 semi empirical analysis in order to calculate the binding energy, E_{bind} (Table 1). These conformations were used

to conduct a structural analysis of the catalytic site (Figure S6), so we could verify the linkages that allow the stabilization of the complexes and how those interactions occurred. A single interaction involving charged residues was identified in the complexes. This interaction is formed by the residue of 160 His (SvBAHD05) or 161 His (BdAT1) with the carboxylate groups of the complexes without Araf or with carbonyl groups of Araf-complexes.

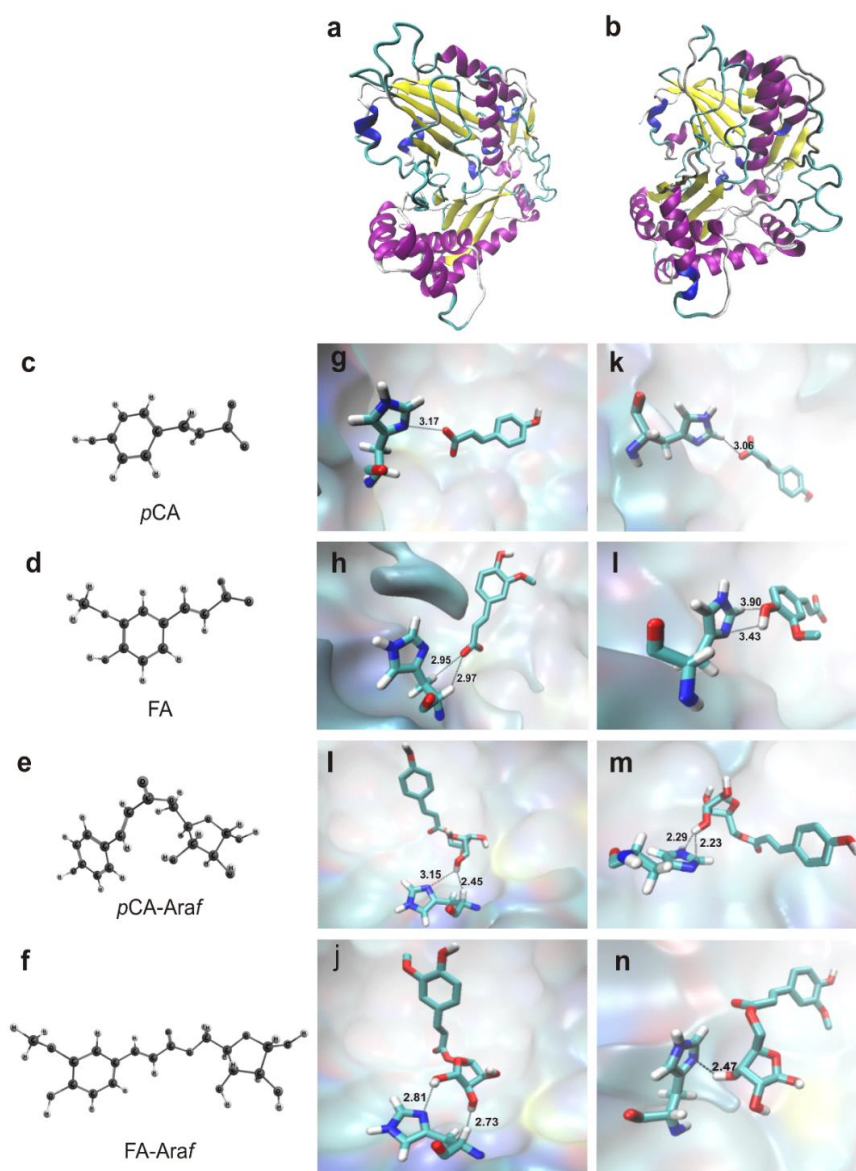


Figure 5. Tridimensional structures, conformations by molecular docking and HCA geometries of BAHD acyltransferases of *Setaria viridis* (SvBAHD05) and *Brachypodium distachyon* (BdAT1). (a,b) Tridimensional structures of BAHD acyltransferase in ribbon representation. SvBAHD05 (a) and BdAT1 (b). α -helices are depicted in purple and β -sheets are depicted in yellow. SvBAHD05 and BdAT1 presented a TM-score of 0.945 and 0.948, respectively. (c-f) Structures of pCA (c), FA (d), pCA-Araf (e) and FA-Araf (f) from optimized geometries. (g-n) Conformations obtained from molecular docking procedures. pCA-Sv (g), FA-Sv (h), pCA-Araf-Sv (i), FA-Araf-Sv (j), pCA-Bd (k), FA-Bd (l), pCA-Araf-Bd (m), FA-Araf-Bd (n). The highlighted residue corresponds to the histidine of the HXXXD motif.

Modeling the structures of SvBAHD05 and BdAT1 revealed that both enzymes present higher affinity for the arabinosyl residue linked to *pCA* and FA than to arabinosyl-free HCAs. The binding energies differences ($\Delta E_{bind} = E_{bind(pCA-Araf)} - E_{bind(pCA)}$) for *pCA* complexes were $-27 \text{ kcal.mol}^{-1}$ for SvBAHD05 protein and $-52 \text{ kcal.mol}^{-1}$ for BdAT1 protein. Comparing the binding energies of *pCA-Araf* and FA-Araf to each enzyme ($E_{bind(FA-Araf)} - E_{bind(pCA-Araf)}$), the data indicated that arabinosyl residue confers approximately $-13 \text{ kcal.mol}^{-1}$ of stability in favor of FA-Araf in BdAT1 complex and -7 kcal.mol^{-1} in SvBAHD05.

We found that whilst SvBAHD05 was predicted to bind *pCA* and FA equally well, BdAT1 was predicted to bind FA much more stably than *pCA* (Table 1). This therefore supports the hypothesis that these orthologous proteins have differing substrate specificities.

Table 1. Binding energies. E_{bind} , computed by PM7 semiempirical method from the last configuration generated by MD simulations.

SvBAHD05		BdAT1	
<i>pCA</i>	FA	<i>pCA</i>	FA
$E_{bind} \text{ (kcal/mol)}$	$E_{bind} \text{ (kcal/mol)}$	$E_{bind} \text{ (kcal/mol)}$	$E_{bind} \text{ (kcal/mol)}$
-21.99	-36.52	-2.68	-61.59
<i>pCA-Araf</i>	FA-Araf	<i>pCA-Araf</i>	FA-Araf
$E_{bind} \text{ (kcal/mol)}$	$E_{bind} \text{ (kcal/mol)}$	$E_{bind} \text{ (kcal/mol)}$	$E_{bind} \text{ (kcal/mol)}$
-49.00	-56.51	-54.98	-68.58

2.6 Saccharification, plant biomass, and seed yield of SvBAHD05 RNAi plants

To evaluate the effects of reducing *p*-coumaroylation of AX promoted by the suppression of *BAHD05* gene on cell wall recalcitrance, we performed saccharification assays of leaves and stems from SvBAHD05 RNAi plants. An increase in biomass saccharification compared with NT plants was observed in both tissues of silenced lines after 6 h and 48 h of enzymatic hydrolysis (Figure 6a-6b).

Glucose released from untreated leaves and stems at 6 h of enzymatic hydrolysis increased $\sim 15\%$ in silenced lines compared to NT plants. In acid-pretreated leaves at 6 h of saccharification, we observed an increase in glucose yields in RNAi silenced lines 2.1 (10%) and 3.1 (32%), whereas at 48 h of hydrolysis the line 3.1 increased by 15%

compared to NT (Figure 6a). In addition, pretreated stems of RNAi lines 2.1 and 3.1 exhibited ~12% higher saccharification at 6 h of hydrolysis, followed of an increase of ~10% after 48 h of hydrolysis for 3.1 line (Figure 6b). These data demonstrate that saccharification levels of transgenic plants were higher compared to NT before and after acid pretreatment, indicating that decreased levels of *pCA* promoted by *SvBAHD05* silencing led to reduced recalcitrance and improved biomass digestibility.

Moreover, seed yield from *SvBAHD05* suppression lines was unaffected (Figure 6c-6e). We observed no significant alterations in the plant biomass production (Figure 6c), nor in the thousand-grain weight (Figure 6d) nor in the seed number per plant associated with *SvBAHD05* RNAi plants (Figure 6e).

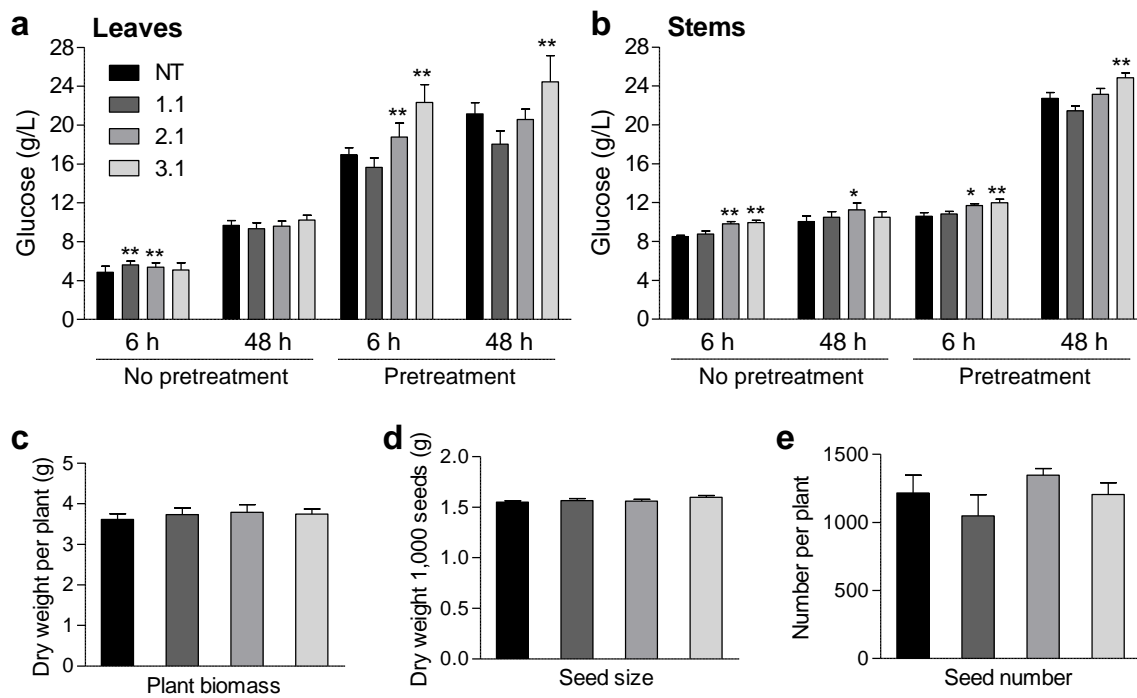


Figure 6. Saccharification, biomass production and seed yield of *SvBAHD05* RNAi lines. (a,b) Glucose released of transgenic lines of leaves (a) and stems (b) of biomass pretreated and not pretreated with 0.5% H₂SO₄. (c-e) Productivity data from plant biomass (c), thousand-grain weight (d), and seed number per plant (e). NT indicates the non-transformed line. 1.1, 2.1 and 3.1 are three independently transformed lines overexpressing *SvBAHD05*. Means ± SEM from three (a, b), 10 (c, d) or five (e) replicate plants. *, *P* < 0.05; **, *P* < 0.01; ***, *P* < 0.001 (ANOVA).

3. Discussion

There is evidence that BAHD acyltransferases are involved in the incorporation of *pCA* and FA in arabinosyl moieties of AX in grass cell walls (Mitchell *et al.*, 2007, Piston *et al.*, 2010, Bartley *et al.*, 2013, Molinari *et al.*, 2013, Buanafina *et al.*, 2016, de Souza *et al.*, 2018, Li *et al.*, 2018, de Souza *et al.*, 2019). The only experimental evidence to date has come from suppression or overexpression of *BAHD* genes affecting the levels of cell wall-bound HCAs in grasses. Here, we present results showing that RNAi suppression of *SvBAHD05* plants decrease the incorporation of *pCA* to the *Araf* residues of xylan and our MD simulations support that *SvBAHD05* has strong PAT activity related to the *p*-coumaroylation of AX.

Previously, we identified the *BAHD* genes in the “Mitchell clade” (Mitchell *et al.*, 2007) of *S. viridis* genome. We found 10 gene members within this family, which were named *SvBAHDs* (*SvBAHD01* - *SvBAHD10*). Gene expression analysis showed that the most expressed *BAHD* genes in *Setaria* tissues were *SvBAHD01*, *SvBAHD04* and *SvBAHD05* (de Souza *et al.*, 2018). Using an RNAi approach, we previously silenced *SvBAHD01*, showing that its suppression decreased cell wall ester-linked FA in stems and leaves (de Souza *et al.*, 2018). The large and consistent effects of *SvBAHD01* suppression on FA content, allowed us to hypothesize that *SvBAHD01* is responsible for feruloylation of AX in *Setaria* cell walls.

We assumed that all *pCA* and FA released by mild acid hydrolysis from AIR came from ester linkages of *Araf*-AX. Here, we demonstrate that silencing *SvBAHD05* gene decreases cell wall ester-linked *pCA* in cell walls of *S. viridis* (Figure 2d-2f). Moreover, suppression of *SvBAHD05* had no or little effects on FA content (Figure 2d-2f). The effects on *pCA*-*Araf* were conspicuous in all tissues (Figure 3a-3c), however there were also some smaller but significant reductions in FA-*Araf* in leaves (Figure 3d). Reductions in *pCA*-*Araf* (Figure 3a-3c) were generally greater than the decreases in ester-linked *pCA*, especially in stems (Figure 2d-2f), consistent with a much greater effect of *SvBAHD05* silencing on *pCA* linked to AX than on *pCA* linked to lignin. Taken together, our results strongly support the hypothesis that *SvBAHD05* is responsible for AX acylation by incorporation of *pCA* to the *Araf* residues by the activity of PAT enzyme.

By comparing the biochemical results (Figure 2d-2f) with 2D-NMR data (Figure 4), we observed similar trends for *pCA* levels with decreases in leaves and little effect in stems. The 2D-NMR values are based on lignin without chemical degradation (Mansfield

et al., 2012, de Souza *et al.*, 2018), and do not distinguish between *pCA* on lignin and *pCA* on AX so it is expected that they agree better with effects on total cell wall *pCA* (Figure 2d-2e) than those on *pCA-Araf* (Figure 3a-3b). Overall, the 2D-NMR revealed only small differences in S- and G-lignin in stems in transgenic lines when compared to NT plants. In nitrobenzene oxidation, we observed decrease in S/G ratio for all silenced lines in leaves (Figure S3j) and these results are in concordance with 2D-NMR.

Genetic and biochemical evidence have demonstrated that suppression of genes related to lignin biosynthesis, with the consequent reduction in lignin content, is compensated by an increase in cellulose content in some plant species (Takeda *et al.*, 2018). By contrast, in *Arabidopsis thaliana*, the reduced lignin content was compensated for by increased matrix polysaccharide content rather than by cellulose content (Van Acker *et al.*, 2013). Here, the lignin content assessed by acetyl bromide of silenced *SvBAHD05* plants was unchanged compared to NT plants and we found no compensatory effects between lignin and the matrix polysaccharides (Figure 3g-3i and Figure S4).

As observed in Figure 5a and 5b, both *SvBAHD05* and *BdAT1* possess ten β -sheets and seven α -helix, but the conformations of the tertiary structures and the folding of these proteins are different. We performed MD simulations to verify the interaction of *SvBAHD05* and *BdAT1* with the possible substrates *pCA* and FA, and it was demonstrated that, in fact, *BdAT1* protein interacts more favorably with FA, corroborating the hypothesis that *BdAT1* is responsible for cell wall feruloylation (Table 1). Conversely, *SvBAHD05* presented energetically favored interactions with both *pCA* and FA, the energy bindings of *SvBAHD05-FA* and *SvBAHD05-pCA* are not so different as the free substrates with *BdAT1* (Table 1). It is known that many plant BAHD acyltransferases demonstrate catalytic versatility and present wide substrate specificity for *in vitro* assays, whereas the products formed by BAHD acyltransferases *in planta* are determined when relative concentrations of substrates are available (D'Auria, 2006). Our MD simulation-based analyses support the hypothesis that *SvBAHD05* is a possible PAT enzyme, performing the addition of *pCA* to arabinosyl residues *in planta*.

Interestingly, the computational studies also demonstrated that the presence of arabinosyl residue around the conserved motif HLVFDG is responsible to stabilize the complex BAHD-*pCA/FA* (Table 1 and Figure S7a), as the binding energies in the presence of arabinosyl residue are more favorable when compared to the E_{bind} of the complex of BAHD with free *pCA* or FA. Currently, the proposed model for *p*-

coumaroylation/feruloylation of AX by BAHDs has UDP-Araf as the acceptor for *p*CA-CoA or FA-CoA substrates (de O. Buanafina, 2009, de Oliveira *et al.*, 2015). According to this model, UDP-Araf, which is generated in the cytosol by UDP-arabinose mutase, is acylated by *p*CA and FA due to BAHD activity. Acylated UDP-Araf would then pass into the Golgi by a transporter (UDP-Araf transporters were recently identified in *Arabidopsis* by (Rautengarten *et al.*, 2017). The *p*CA-Araf and FA-Araf would then be transferred onto AX, probably by GT61 enzymes that are responsible for arabinosylation of xylan (Anders *et al.*, 2012). This model is further supported by studies on RNAi *Brachypodium* lines with decreased mutase activity (Rancour *et al.*, 2015) and the rice *xax1* mutant that carries a knockout for a GT61 family gene (Chiniquy *et al.*, 2012), both showing a substantial decrease in cell wall *p*CA and FA. The predicted stabilization of BAHD-*p*CA and BAHD-FA complexes by arabinosyl residue that we found in our modelling and the decrease of *p*CA levels in cell walls of RNAi *SvBAHD05* for *Setaria* plants, further the understanding of how grasses incorporate *p*CA in their cell walls and reinforce this model.

The suppression of RNAi lines reduced esterified *p*CA levels and *p*CA-Araf. The data of MD simulations and the results obtained from FA-Araf analysis do not exclude the hypothesis that *SvBAHD05* enzymes could also incorporate FA in the cell walls, but to a smaller extent, in line with the known substrate versatility of BAHD superfamily. This possibility contrasts sharply with our finding for *SvBAHD01*, where the effect of silencing was a strong decrease in FA-Araf with an accompanying increase in *p*CA-Araf (de Souza *et al.*, 2018), suggesting complete substrate specificity for *SvBAHD01*.

We also assessed the saccharification for leaves and stems before and after pretreatment with 0.5% H₂SO₄. Biomass saccharification of stems and leaves was higher in *SvBAHD05* RNAi lines and the glucose released in pretreated leaves was 32% higher at 6 h of enzymatic hydrolysis for the line 3.1 compared to NT plants. Overall, saccharification efficiency was increased after acid pretreatment in 2.1 and 3.1 lines for leaves and stems (Figure 6a-6b), indicating that *SvBAHD05*, similarly to *SvBAHD01* and *SacBAHD01* (de Souza *et al.*, 2018, de Souza *et al.*, 2019) is a promising target to increase the yields of sugar fermentation in the bioethanol processing or animal feeding. Overall, the biomass productivity and seed yield from *SvBAHD05* RNAi suppressed lines remains unchanged (Figure 6c-6e).

The suppression of *SvBAHD05*, in *S. viridis*, revealed consistent reduction in *p*-coumaroylation associated to the matrix polysaccharide of arabinoxylan in all tissues, and

a small decrease in feruloylation of leaves. The results were validated following three generations of transgenic plants, showing reductions of up to 42% of the ester-linked *pCA* and 50% of *pCA-Araf* compared to NT. Suppressed lines exhibited no change in total lignin and increased sugar yields after *in vitro* saccharification, without affecting biomass and plant productivity. The comprehension of the role of BAHD acyltransferases in plants is pivotal to identify new targets for grass crop improvement intended for biofuels, biorefineries and animal feeding. Additionally, the present study describes new insights into cell wall *p*-coumaroylation of grasses. We described a new function of *SvBAH05* gene to *S. viridis* and our data strongly support the hypothesis that *SvBAH05* is mainly responsible for the addition of *pCA* to the *Araf* residues onto AX in grass cell walls.

4. Experimental Procedures

4.1 Growth conditions for *Setaria viridis*

Seeds of *S. viridis* were treated with concentrated sulfuric acid to break dormancy. After, the mature seeds were germinated in MS medium in Fitotron[®] under 16 h of photoperiod, 500 $\mu\text{mol m}^{-2}\text{s}^{-1}$ of light intensity and 26 ± 2 °C. The relative humidity was 65% and the plants were maintained until the reproductive developmental stage, with approximately 45 days-old plants, when they were harvested. The plants were separated into leaf, stem and root tissues and they were immediately transferred to liquid nitrogen and stored at -80 °C until grinding the material for analyzes. Pools of 10 plants of the tissues were harvested comprising one biological sample. All analyses were performed at the reproductive phase, except seed data, which was collected at maturity phase. In all experiments, non-transformed (NT) plants were produced via calli embryo culture, grown and harvested at the same time as transformed plants.

4.2 Plasmid construct and generation of transgenic plants

For silencing of *BAHD05* gene in *S. viridis*, an inverted repeat of 247 bp sequence was cloned into the binary vector A780p6iA-UB5 (Figure S1a-S1b) containing a cassette flanking the maize *Adh2* intron, driven by *ZmUbi1* constitutive promoter and the *hpt* gene selection marker (hygromycin resistance). The vector was synthesized by DNA Cloning Service, Germany. The genetic transformation of *S. viridis* accession 10.1 by *Agrobacterium tumefaciens* was performed as previously described (Martins *et al.*, 2015). Briefly, mature seeds were used for embryogenic callus induction and after 4-5 weeks the

induced calli were co-cultivated with *A. tumefaciens* containing the binary vector. The putative transgenic calli, resistant to hygromycin B, were transferred to selective regeneration medium (SRM). The surviving regenerated plants were submitted to PCR analysis in order to confirm the presence of the transgene.

4.3 Determination of transcript abundance

RT-qPCR was carried out in a 96-well optical plate with a StepOnePlus Real-Time PCR Systems (Applied Biosystems). Leaf, stem and root tissues of *S. viridis* (T₃ generation) were harvested at the reproductive phase. About 200 mg of starting material was used for RNA isolation. Total RNA from leaf and stem was isolated using TRIzol Reagent (Thermo Scientific), according to the manufacturer's instructions. RNA from roots was extracted using a CTAB-LiCl method (Chang *et al.*, 1993). Genomic DNA was removed using RQ1 RNase-free DNase (Promega), according to the manufacturer's instructions. Reverse transcription reaction was carried out with 1 µg of total RNA and oligo (dT) using RevertAid First Strand cDNA Synthesis Kit (Thermo Scientific), following the manufacturer's recommendations. cDNA samples were diluted (1:25) prior to use in RT-qPCR assays. The RT-qPCR was carried out using Platinum SYBR Green PCR SuperMix-UDG with ROX (Invitrogen) using the protocol recommended by the StepOnePlusReal-Time PCR Systems (Applied Biosystems). Total RNA was quantified using a NanoDrop ND-1000 Spectrophotometer (Uniscience), and RNA integrity was verified in agarose gel electrophoresis. Background-corrected raw fluorescence data were imported into LinRegPCR version 2016.0 software for primer efficiency estimation (Ramakers *et al.*, 2003). Relative quantities (RQs) for *BAHD05* were calculated using the q-Gene (Muller *et al.*, 2002). The expression of the genes were normalized with the geometrical mean of the RQs of the reference genes *EF1α* (elongation factor 1-alpha) and *IF4α* (eukaryotic initiation factor 4-alpha) for leaves and stems, *CAC* (clathrin adaptor complex), and *CUL* (cullin) for roots (Martins *et al.*, 2016). The primers used in the RT-qPCR are described in Table S4. All assays were performed using three biological replicates with three technical replicates each and a non-template control.

4.4 Determination of pCA, FA, pCA-Araf, FA-Araf and DiFA

The content of the cell wall ester-linked hydroxycinnamates (pCA and FA) and dehydrodiferulates (DiFA) obtained by alkaline hydrolysis were determined according to

the method described by (de Souza *et al.*, 2018), with modifications. The relative proportion of *p*-coumaroyl-Arabinose (*p*CA-Araf) and feruloyl-Arabinose (FA-Araf) were determined essentially as described by (Freeman *et al.*, 2017), slightly modified.

First, the biomass was frozen in liquid N₂, then grinded in an ultra-centrifugal mil (Rerstch[®] model ZM 200) using a 0.5 mm pore size sieve to obtain a fine powder, and freeze-dried. The determination of ester-linked *p*CA and FA was performed using 20 mg freeze-dried ground tissue after procedure of extraction to obtainment of alcohol insoluble residue (AIR), washing the biomass three times with 80% ethanol (v/v). For the analysis of the *p*CA and FA from alkaline hydrolysis, it was used the following gradient system: 0 min (10% B), 5 min (20% B), 7.5 min (25% B), 12.5 min (45% B), 14 to 17 min (100% B), 17.5 to 21 min (10% B).

For the determination of *p*CA-Araf and FA-Araf, the AIR obtained from 10 mg of freeze-dried ground tissue (prepared using extractions as described for cell wall-bound HCA) was treated with 1.2 mL of 50 mM trifluoroacetic acid for 4 h at 99 °C with agitation at 750 rpm. After centrifugation for 10 min at 16,000g, 2 aliquots of 500 µL of supernatant were freeze-dried. Released HCA-conjugates from a dried aliquot of supernatant were dissolved in 1 mL of a mixture of water/acetonitrile (1:1 v/v) for analysis of cell wall bound HCA, and analyzed by HPLC-DAD in an equipment Agilent[®] model 1290 using a binary gradient system of 0.1% formic acid in water (solvent A) and acetonitrile (solvent B), using an Waters[®] Acquity UPLC HSST3 column (2.1 mm I.D. × 150 mm L., particle size 1.8 µm), with the temperature of column oven at 40 °C. For the analysis of *p*CA-Araf and FA-Araf from mild acidolysis, it was used the following gradient system: 0 min (10% B), 5 to 7.5 min (13% B), 12.5 min (45% B), 14 to 17 min (100% B), 17.5 to 21 min (10% B).

The results for *p*CA, FA, and DiFA from alkaline hydrolysis obtained samples were expressed as µg HCA mg⁻¹ AIR. The areas for the peaks corresponding to the *p*CA-Araf and FA-Araf that were previously identified by mass spectrometry-based approach by (de Souza *et al.*, 2018), were divided by the peak area of the internal standard (IS) added to the samples (20 µL of 3,5-dichlorobenzoic acid 1,5 mg.mL⁻¹) and the peak area ratios at 280 nm (*p*CA-Araf/IS and FA-Araf/IS) were used to compare the proportion of HCA conjugates among samples.

4.5 Transcriptome analysis of transgenic *SvBAHD05*

For *S. viridis* (accession 10.1), the total RNA of leaves was extracted from plants in the fourth stage. To each library, the RNA was extracted using ReliaPrepTM RNA Tissue Miniprep System®. RNA concentration and integrity were checked with Nanodrop ND 1000 spectrophotometer (Nanodrop Technologies Inc., Rockland, DE, USA), and Agilent 2100 Bioanalyzer (Agilent Technologies, Santa Clara, CA, USA), respectively. The prepared mRNA-seq libraries of NT and transformed lines of *SvBAHD05* (1.1 and 3.1 lines) were constructed for sequencing on the Illumina HiSeq 2500 sequencing platform using Illumina's TruSeq RNA Sample Preparation Kit (Illumina Inc, San Diego, CA, USA) by Novogene Technology. Sequencing quality of each library was assessed using FastQC v0.11.3. For all libraries, high-quality reads were mapped into *S. viridis* genome v.2.1 from Phytozome 11.0 using TopHat (<http://tophat.cbcb.umd.edu/>) and Bowtie v.2.2.5 (Langmead *et al.*, 2009), and unigenes were annotated on genome sequence. To analyze the transcript levels of *SvBAHD* genes, it was used the FPKM (fragments per kilobase of exon per million mapped reads) method. Cuffdiff (<http://cufflinks.cbcb.umd.edu/>) (Trapnell *et al.*, 2013) was used for differential expression analysis using a threshold for FDR (false discovery rate) < 0.05 and the fold change of two to determine significant differences in gene expression.

4.6 Monosaccharide composition

The chemical composition (monosaccharide and acetyl composition) of AIR samples was determined by a two-step acid hydrolysis method following the protocol described by the National Renewable Energy Laboratory of the US Department of Energy, with modifications (Sluiter *et al.*, 2008). The quantification of structural carbohydrates was performed by high performance anion-exchange chromatography with pulsed amperometric detection (HPAEC-PAD), according to the method describe by (Rohrer *et al.*, 2013), slightly modified.

4.7 Cell wall characterization by solution-state 2D NMR

Cell walls of *S. viridis* samples were characterized without fractionation and using solution-state two-dimensional (2D) ¹H-¹³C heteronuclear single quantum coherence nuclear magnetic resonance (HSQC-NMR) spectroscopy as described by (Kim and Ralph, 2010). Briefly, 500 mg of tissue (leaf and stem) were freeze-dried ground tissue

and overnight extracted with acetone/water (95:5) on the Soxhlet at 70 °C. After the extraction, the samples were dried at 50 °C for 48 h. 200 mg of each sample were ball-milled in 20 mL jars with 10 x 10 mm ball bearing in a Fritsch® Planetary micro mill Pulverisette 7 premium line equipment. The milling procedure was 8 x 5 min with 5 min pauses. After milling, 100 mg of the samples were gelled into a 5 mm NMR tube by adding 500 µL of DMSO-d₆ without derivatization and performed the NMR analysis were carried out on a 600 MHz Bruker® AVANCE III spectrometer system equipped with a 5 mm TCI cryoprobe with ATMA® (Automatic Tuning and Matching). The data obtained as FID (Free Induction Decay) were processed in the software MestReNova version 9, using the following parameters: F2 (proton frequency co-ordinates) – Gaussian apodization (GB = 0.01); F1 (carbon frequency co-ordinates) – Sine Bell apodization (90.00°); Smoothing applied to all dimensions by wavelets method (Parameters: scales = 4; fraction = 1.00%; universal threshold). The spectra obtained after processing was used to calculate the proportion of monolignols, tricin, *p*CA, and FA in plant cell wall (*p*CA, FA, and tricin are expressed as percentage in relation to the sum of syringyl and guaiacyl – S+G = 100%).

4.8 Lignin quantification and monomers composition

For lignin quantification, a 150 mg aliquot of biomass from all tissues were washed sequentially with: 50 mM potassium phosphate buffer pH 7.0, 1% (v/v) triton X-100 in pH 7.0 buffer, 1 M NaCl in pH 7.0 buffer, distilled water, and acetone. The pellet was oven-dried (55°C, 24 h). After drying, we obtained the protein-free cell wall fraction and 20 mg of this fraction was used to quantify the total lignin. Screw cap tubes containing 20 mg of biomass and 0.5 mL of 25% acetyl bromide (v/v in glacial acetic acid) were incubated (70 °C, 30 min). After, the samples were cooled and mixed with 0.9 mL of 2 M NaOH, 0.1 mL of 5 M hydroxylamine-HCl, and 6 mL of acetic acid. The samples were centrifuged, and the absorbance of the supernatant was measured at 280 nm (Moreira-Vilar *et al.*, 2014).

For the lignin monomer composition, an aliquot of 50 mg of protein-free cell wall fraction was sealed in a Pyrex® ampule containing 0.9 mL of 2 M NaOH and 0.1 mL of nitrobenzene and heated at 170 °C for 150 min. The sample was cooled to room temperature, washed twice with chloroform, acidified to pH 3–4 with 5 M HCl and extracted twice with chloroform. The organic extracts were combined, dried, and

resuspended in 1 mL of methanol. All of the samples were filtered in a 0.45- μ m disposable syringe filter and analyzed by HPLC. The mobile phase used was methanol/acetic acid 4% (20:80, v/v), with a flow rate of 1.2 mL/min for an isocratic run. Quantification of the monomer aldehyde products (vanillin and syringaldehyde) released by the nitrobenzene oxidation was performed at 290 nm using the corresponding standards. All measurements were performed on five biological replicates. Each biological replicate is a pool of ten plants.

4.9 Computational details of protein modeling

The prediction of 3D BdAT1 and SvBAHD05 structures were performed using the Iterative Threading Assembly Refinement (I-TASSER) server (Zhang, 2008, Roy *et al.*, 2010, Yang *et al.*, 2015). The quality of initial models generated was validated by MolProbity (<http://molprobity.biochem.duke.edu/>) and Ramachandran plot. Protonated states of *pCA* and FA at physiological pH (~7.4) were evaluated by MarvinSketch software Version 17.24.0 at 300K. From the protonation states at pH 7.4, the *pCA*, FA, *pCA-Araf*, and FA-Araf were subjected to an energy minimization using Gaussian 09 package. All torsions of *pCA*, FA, *pCA-Araf* and FA-Araf were allowed to rotate during docking. 35 Å-Sized grid box was centered on the HXXXD motif of BAHD structures.

Nine conformations for each ligand were obtained from molecular docking (Table S3), and the geometries with lower binding energies (configurations 1 from Table S3) were selected to perform the MD simulations. The *pCA*, FA, *pCA-Araf* and FA-Araf complexes with SvBAHD05 were named of *pCA-Sv*, FA-Sv, *pCA-Araf-Sv*, and FA-Araf-Sv, respectively. The *pCA*, FA, *pCA-Araf* and FA-Araf complexes with BdAT1 were named of *pCA-Bd*, FA-Bd, *pCA-Araf-Bd*, and FA-Araf-Bd, respectively. The molecular docking was carried out using AutoDockVina 1.1.2 and the conformations with lowest docked energy were submitted to molecular dynamics (MD) simulations. A total time of 20 ns simulations was enough to equilibrate the complexes (Figure S5c-S5d) and structural equilibration of complexes occurred up to 10 ns for all complexes. Before the MD simulations, the ligand structures was optimized and we performed the investigation of the protonated state of the ligands in different pHs (Figure S7b). Therefore, the structures were selected by the minimization steps and the *pCA*, FA, *pCA-Araf*, and FA-Araf optimized geometries are depicted in the Figure 5c-5f, respectively.

Classical MD simulations were employed to equilibrate the protein and the complexes protein-ligands. MD simulations were performed by the GROMACS 5.1.4 program (Van Der Spoel *et al.*, 2005) using the High-Performance Computing Center facilities at UFRN (NPAD/UFRN). The root-mean-square deviation (RMSD) was calculated to evaluate the structural stability of the complexes of acids (*pCA* and *FA*) and esters (*pCA-Araf* and *FA-Araf*) with BAHD structures. Equilibrated structures from MD simulations were used for the quantum mechanics calculation. For the energy analysis, PM7 semi empirical method was used to study the interaction energies of the 4 Å cut-off radius from *pCA*, *FA*, *pCA-Araf* or *FA-Araf* with BAHD proteins structures. The interaction energy (de Morais *et al.*, 2016), E_{bind} , or binding energy, is defined as:

$$E_{bind} = H_f(\text{complex}) - [H_f(\text{BAHD}) + H_f(\text{ligand})]$$

Where $H_f(\text{complex})$ is the enthalpy of formation of complex, $H_f(\text{ligand})$ is the enthalpy of formation of the isolated ligands (*pCA*, *FA*, *pCA-Araf* or *FA-Araf*) and $H_f(\text{BAHD})$ is the enthalpy of formation of isolated BAHD structures.

4.10 Pretreatment and enzymatic saccharification assay

Pretreatment of lignocellulosic materials increases the saccharification yield (Mota *et al.*, 2019), therefore we carried out the saccharification analysis with Cellic[®] CTec3 enzyme cocktail using leaves and stems tissues of NT, 1.1, 2.1, and 3.1 pretreated or not with 0.5% diluted sulfuric acid and the glucose released from the silenced lines was compared with those from NT. The liquid ratio of the biomass was 1:10 (w/v) and the biomass was mixed with 0.5% (v/v) H₂SO₄ and submitted to 121 °C for 15 minutes. Pretreated biomass was recovered by filtration, washed with 30 mL of deionized water and dried in an oven overnight at 40 °C. Enzymatic saccharification assays were performed in 2 mL tubes with 5% (w/v) dry biomass in 100 mM citrate buffer, pH 5.0 using the Cellic[®] CTec 3 enzyme cocktail (Novozymes, Lyngby, Denmark) at 10 filter paper activity units FPU/g biomass. Samples were incubated in a Thermomixer microplate incubator (Eppendorf, Germany), at 50 °C and 800 rpm. Samples were withdrawn after 6 h and 48 h, followed by centrifugation at 10000 *g* for 15 min. Sugars in enzyme hydrolysates were analyzed by high-performance liquid chromatography (HPLC) system (Agilent, Palo Alto, CA-USA), equipped with a refractive index detector

and Aminex HPX-87H ion exchange column (Bio-Rad, Hercules, CA-USA). The mobile phase contained 5 mM H₂SO₄, at a flow rate of 0.6 mL min⁻¹, heated at 45°C. The experiments were carried out with three biological replicates each of them with three technical ones. Each biological replicate is a pool of ten plants.

4.11 Biomass and seed measurement

For the biomass measurement, 10 plants were selected for each *SvBAHD05* silencing lines (1.1, 2.1 and 3.1), and for NT. The plant organs (excluding roots) were completely dried in an oven at 65 °C for 72 h to obtain the dry biomass at maturity. The seeds were collected after 90 days and the weight of the total seeds and the weight of one thousand seeds were estimated. Additionally, five plants were selected of each *SvBAHD05* RNAi plants to determine the seed number per plant and the values were compared to the NT.

4.12 Statistical Analyses

Statistical analyses were conducted using GraphPad Prism (version 5.00 for Windows). The experimental design was completely randomized and conducted using technical replicates. The biological sample in this study consisted of a bulk containing 10 plants. Statistical analyses consisted of Dunnett's test for comparisons of non-transformed plants (NT) and transgenic lines (1.1, 2.1 and 3.1), and statistical significance was defined as * 0.05 ≥ *P* > 0.01, ** 0.01 ≥ *P* > 0.001, and *** *P* ≤ 0.001.

4.13 Gene identifiers

The genes can be accessed at <https://phytozome.jgi.doe.gov/pz/portal.html>.

The gene IDs are *SvBAHD01*:Sevir.5G130000; *SvBAHD02*: Sevir.5G124000; *SvBAHD03*: Sevir.5G233600;*SvBAHD04*: Sevir.3G107300;*SvBAHD05*: Sevir.5G233700.

Acknowledgments

T.R.M. and D.M.O. gratefully acknowledge the doctoral scholarship granted by Coordination of Enhancement of Higher Education Personnel (CAPES) and the Brazilian National Council for Scientific and Technological Development (CNPq). We thank the Instituto Metr pole Digital (IMD) at Federal University of Rio Grande do Norte for the computer cluster facility.

Funding

This work was supported by grants from the Coordination of Enhancement of Higher Education Personnel (CAPES) and EMBRAPA Macroprogram SEG (02.12.01.008.00.00).

Author contributions

H.B.C.M. conceived the project. T.R.M., W.R.S., D.M.O., P.K.M., B.L.S., F.V., A.P.R., K.E.D., T.F.P., N.K.V.M., R.B.C., R.M., D.S.V., A.K.K., P.A.O.M., and O.F.F. performed research and/or analyzed the data. T.R.M and W.R.S. wrote the original draft of the manuscript, and T.R.M. wrote the final version of the manuscript. W.R.S., R.A.C.M., H.B.C.M., and W.D.S. revised and edited the manuscript. All authors read and approved the final manuscript.

Conflict of interest

The authors declare that they have no conflicts of interest.

References

- Anders, N., Wilkinson, M.D., Lovegrove, A., Freeman, J., Tryfona, T., Pellny, T.K., Weimar, T., Mortimer, J.C., Stott, K., Baker, J.M., Defoin-Platel, M., Shewry, P.R., Dupree, P. and Mitchell, R.A.C. (2012) Glycosyl transferases in family 61 mediate arabinofuranosyl transfer onto xylan in grasses. *Proc. Natl. Acad. Sci. USA*, **109**, 989.
- Bartley, L.E., Peck, M.L., Kim, S.-R., Ebert, B., Manisseri, C., Chiniquy, D.M., Sykes, R., Gao, L., Rautengarten, C., Vega-Sánchez, M.E., Benke, P.I., Canlas, P.E., Cao, P., Brewer, S., Lin, F., Smith, W.L., Zhang, X., Keasling, J.D., Jentoff, R.E., Foster, S.B., Zhou, J., Ziebell, A., An, G., Scheller, H.V. and Ronald, P.C. (2013) Overexpression of a BAHD acyltransferase, *OsAt10*, alters rice cell wall hydroxycinnamic acid content and saccharification. *Plant Physiol.*, **161**, 1615.
- Bouvier d'Yvoire, M., Bouchabke-Coussa, O., Voorend, W., Antelme, S., Cézard, L., Legée, F., Lebris, P., Legay, S., Whitehead, C., McQueen-Mason, S.J., Gomez, L.D., Jouanin, L., Lapiere, C. and Sibout, R. (2013) Disrupting the cinnamyl alcohol dehydrogenase 1 gene (BdCAD1) leads to altered lignification and improved saccharification in *Brachypodium distachyon*. *Plant J.*, **73**, 496-508.
- Brutnell, T.P., Wang, L., Swartwood, K., Goldschmidt, A., Jackson, D., Zhu, X.-G., Kellogg, E. and Van Eck, J. (2010) *Setaria viridis*: a model for C₄ photosynthesis. *Plant Cell*, **22**, 2537.
- Buanafina, M.M.d.O., Fescemyer, H.W., Sharma, M. and Shearer, E.A. (2016) Functional testing of a PF02458 homologue of putative rice arabinoxylan feruloyl transferase genes in *Brachypodium distachyon*. *Planta*, **243**, 659-674.
- Chang, S., Puryear, J. and Cairney, J. (1993) A simple and efficient method for isolating RNA from pine trees. *Plant Mol. Biol. Rep.*, **11**, 113-116.
- Chiniquy, D., Sharma, V., Schultink, A., Baidoo, E.E., Rautengarten, C., Cheng, K., Carroll, A., Ulvskov, P., Harholt, J., Keasling, J.D., Pauly, M., Scheller, H.V. and Ronald, P.C. (2012) XAX1 from glycosyltransferase family 61 mediates xylosyltransfer to rice xylan. *Proc. Natl. Acad. Sci. USA*, **109**, 17117.
- D'Auria, J.C. (2006) Acyltransferases in plants: a good time to be BAHD. *Curr. Opin. Plant Biol.*, **9**, 331-340.

- de Morais, C.d.L.M., Silva, S.R.B., Vieira, D.S. and Lima, K.M.G.** (2016) Integrating a smartphone and molecular modeling for determining the binding constant and stoichiometry ratio of the iron(II)–phenanthroline complex: an activity for analytical and physical chemistry laboratories. *J. Chem. Educ.*, **93**, 1760-1765.
- de O. Buanafina, M.M.** (2009) Feruloylation in grasses: current and future perspectives. *Mol. Plant*, **2**, 861-872.
- de Oliveira, D.M., Finger-Teixeira, A., Rodrigues Mota, T., Salvador, V.H., Moreira-Vilar, F.C., Correa Molinari, H.B., Craig Mitchell, R.A., Marchiosi, R., Ferrarese-Filho, O. and Dantas dos Santos, W.** (2015) Ferulic acid: a key component in grass lignocellulose recalcitrance to hydrolysis. *Plant Biotechnol. J.*, **13**, 1224-1232.
- de Souza, W.R., Martins, P.K., Freeman, J., Pellny, T.K., Michaelson, L.V., Sampaio, B.L., Vinecky, F., Ribeiro, A.P., da Cunha, B.A.D.B., Kobayashi, A.K., de Oliveira, P.A., Campanha, R.B., Pacheco, T.F., Martarello, D.C.I., Marchiosi, R., Ferrarese-Filho, O., dos Santos, W.D., Tramontina, R., Squina, F.M., Centeno, D.C., Gaspar, M., Braga, M.R., Tiné, M.A.S., Ralph, J., Mitchell, R.A.C. and Molinari, H.B.C.** (2018) Suppression of a single BAHD gene in *Setaria viridis* causes large, stable decreases in cell wall feruloylation and increases biomass digestibility. *New Phytol.*, **218**, 81-93.
- de Souza, W.R., Pacheco, T.F., Duarte, K.E., Sampaio, B.L., de Oliveira Molinari, P.A., Martins, P.K., Santiago, T.R., Formighieri, E.F., Vinecky, F., Ribeiro, A.P., da Cunha, B.A.D.B., Kobayashi, A.K., Mitchell, R.A.C., de Sousa Rodrigues Gambetta, D. and Molinari, H.B.C.** (2019) Silencing of a BAHD acyltransferase in sugarcane increases biomass digestibility. *Biotechnol. Biofuels*, **12**, 111.
- Freeman, J., Ward, J.L., Kosik, O., Lovegrove, A., Wilkinson, M.D., Shewry, P.R. and Mitchell, R.A.C.** (2017) Feruloylation and structure of arabinoxylan in wheat endosperm cell walls from RNAi lines with suppression of genes responsible for backbone synthesis and decoration. *Plant Biotechnol. J.*, **15**, 1429-1438.
- Harris, P.J. and Trethewey, J.A.K.** (2010) The distribution of ester-linked ferulic acid in the cell walls of angiosperms. *Phytochem. Rev.*, **9**, 19-33.
- Hatfield, R.D., Rancour, D.M. and Marita, J.M.** (2017) Grass cell walls: a story of cross-linking. *Front. Plant Sci.*, **7**, 2056.

- Karlen, S.D., Zhang, C., Peck, M.L., Smith, R.A., Padmakshan, D., Helmich, K.E., Free, H.C.A., Lee, S., Smith, B.G., Lu, F., Sedbrook, J.C., Sibout, R., Grabber, J.H., Runge, T.M., Mysore, K.S., Harris, P.J., Bartley, L.E. and Ralph, J.** (2016) Monolignol ferulate conjugates are naturally incorporated into plant lignins. *Sci. Adv.*, **2**, e1600393.
- Kim, H. and Ralph, J.** (2010) Solution-state 2D NMR of ball-milled plant cell wall gels in DMSO-d₆/pyridine-d₅. *Org. Biomol. Chem.*, **8**, 576-591.
- Langmead, B., Trapnell, C., Pop, M. and Salzberg, S.L.** (2009) Ultrafast and memory-efficient alignment of short DNA sequences to the human genome. *Genome Biol.*, **10**, R25.
- Li, G., Jones, K.C., Eudes, A., Pidatala, V.R., Sun, J., Xu, F., Zhang, C., Wei, T., Jain, R., Birdseye, D., Canlas, P.E., Baidoo, E.E.K., Duong, P.Q., Sharma, M.K., Singh, S., Ruan, D., Keasling, J.D., Mortimer, J.C., Loqué, D., Bartley, L.E., Scheller, H.V. and Ronald, P.C.** (2018) Overexpression of a rice BAHD acyltransferase gene in switchgrass (*Panicum virgatum* L.) enhances saccharification. *BMC Biotechnol.*, **18**, 54.
- Machado, R.J.A., Estrela, A.B., Nascimento, A.K.L., Melo, M.M.A., Torres-Rêgo, M., Lima, E.O., Rocha, H.A.O., Carvalho, E., Silva-Junior, A.A. and Fernandes-Pedrosa, M.F.** (2016) Characterization of TistH, a multifunctional peptide from the scorpion *Tityus stigmurus*: structure, cytotoxicity and antimicrobial activity. *Toxicon*, **119**, 362-370.
- Mansfield, S.D., Kim, H., Lu, F. and Ralph, J.** (2012) Whole plant cell wall characterization using solution-state 2D NMR. *Nat. Protoc.*, **7**, 1579-1589.
- Marita, J.M., Hatfield, R.D., Rancour, D.M. and Frost, K.E.** (2014) Identification and suppression of the p-coumaroyl CoA:hydroxycinnamyl alcohol transferase in *Zea mays* L. *Plant J.*, **78**, 850-864.
- Martins, P.K., Mafra, V., de Souza, W.R., Ribeiro, A.P., Vinecky, F., Basso, M.F., da Cunha, B.A.D.B., Kobayashi, A.K. and Molinari, H.B.C.** (2016) Selection of reliable reference genes for RT-qPCR analysis during developmental stages and abiotic stress in *Setaria viridis*. *Sci. Rep.*, **6**, 28348-28348.
- Martins, P.K., Ribeiro, A.P., Cunha, B.A.D.B.d., Kobayashi, A.K. and Molinari, H.B.C.** (2015) A simple and highly efficient *Agrobacterium*-mediated transformation protocol for *Setaria viridis*. *Biotechnol. Rep.*, **6**, 41-44.

- Melo, M.M.A., Daniele-Silva, A., Teixeira, D.G., Estrela, A.B., Melo, K.R.T., Oliveira, V.S., Rocha, H.A.O., Ferreira, L.d.S., Pontes, D.L., Lima, J.P.M.S., Silva-Júnior, A.A., Barbosa, E.G., Carvalho, E. and Fernandes-Pedrosa, M.F.** (2017) Structure and *in vitro* activities of a copper II-chelating anionic peptide from the venom of the scorpion *Tityus stigmurus*. *Peptides*, **94**, 91-98.
- Mitchell, R.A.C., Dupree, P. and Shewry, P.R.** (2007) A novel bioinformatics approach identifies candidate genes for the synthesis and feruloylation of arabinoxylan. *Plant Physiol.*, **144**, 43.
- Molinari, H., Pellny, T., Freeman, J., Shewry, P. and Mitchell, R.** (2013) Grass cell wall feruloylation: distribution of bound ferulate and candidate gene expression in *Brachypodium distachyon*. *Front. Plant Sci.*, **4**, 50.
- Moreira-Vilar, F.C., Siqueira-Soares, R.C., Finger-Teixeira, A., Oliveira, D.M., Ferro, A.P., da Rocha, G.J., Ferrarese, M.d.L.L., dos Santos, W.D. and Ferrarese-Filho, O.** (2014) The acetyl bromide method is faster, simpler and presents best recovery of lignin in different herbaceous tissues than klason and thioglycolic acid methods. *PloS one*, **9**, e110000.
- Mota, T.R., Oliveira, D.M., Morais, G.R., Marchiosi, R., Buckeridge, M.S., Ferrarese-Filho, O. and dos Santos, W.D.** (2019) Hydrogen peroxide-acetic acid pretreatment increases the saccharification and enzyme adsorption on lignocellulose. *Ind. Crop. Prod.*, **140**, 111657.
- Muller, P.Y., Janovjak, H., Miserez, A.R. and Dobbie, Z.** (2002) Processing of gene expression data generated by quantitative real-time RT-PCR. *Biotechniques*, **32**, 1372-1374, 1376, 1378-1379
- Oakey, H., Shafiei, R., Comadran, J., Uzrek, N., Cullis, B., Gomez, L.D., Whitehead, C., McQueen-Mason, S.J., Waugh, R. and Halpin, C.** (2013) Identification of crop cultivars with consistently high lignocellulosic sugar release requires the use of appropriate statistical design and modelling. *Biotechnol. Biofuels*, **6**, 185.
- Oliveira, D.M., Mota, T.R., Oliva, B., Segato, F., Marchiosi, R., Ferrarese-Filho, O., Faulds, C.B. and dos Santos, W.D.** (2019a) Feruloyl esterases: Biocatalysts to overcome biomass recalcitrance and for the production of bioactive compounds. *Bioresour. Technol.*, **278**, 408-423.
- Oliveira, D.M., Mota, T.R., Salatta, F.V., Marchiosi, R., Gomez, L.D., McQueen-Mason, S.J., Ferrarese-Filho, O. and dos Santos, W.D.** (2019b) Designing

- xylan for improved sustainable biofuel production. *Plant Biotechnol. J.*, **17**, 2225-2227.
- Petrik, D.L., Karlen, S.D., Cass, C.L., Padmakshan, D., Lu, F., Liu, S., Le Bris, P., Antelme, S., Santoro, N., Wilkerson, C.G., Sibout, R., Lapierre, C., Ralph, J. and Sedbrook, J.C.** (2014) *p*-Coumaroyl-CoA:monolignol transferase (PMT) acts specifically in the lignin biosynthetic pathway in *Brachypodium distachyon*. *Plant J.*, **77**, 713-726.
- Piston, F., Uauy, C., Fu, L., Langston, J., Labavitch, J. and Dubcovsky, J.** (2010) Down-regulation of four putative arabinoxylan feruloyl transferase genes from family PF02458 reduces ester-linked ferulate content in rice cell walls. *Planta*, **231**, 677-691.
- Ramakers, C., Ruijter, J.M., Deprez, R.H.L. and Moorman, A.F.M.** (2003) Assumption-free analysis of quantitative real-time polymerase chain reaction (PCR) data. *Neurosci. Lett.*, **339**, 62-66.
- Rancour, D.M., Hatfield, R.D., Marita, J.M., Rohr, N.A. and Schmitz, R.J.** (2015) Cell wall composition and digestibility alterations in *Brachypodium distachyon* achieved through reduced expression of the UDP-arabinopyranose mutase. *Front. Plant Sci.*, **6**, 446.
- Rautengarten, C., Birdseye, D., Pattathil, S., McFarlane, H.E., Saez-Aguayo, S., Orellana, A., Persson, S., Hahn, M.G., Scheller, H.V., Heazlewood, J.L. and Ebert, B.** (2017) The elaborate route for UDP-arabinose delivery into the golgi of plants. *Proc. Natl. Acad. Sci. USA*, **114**, 4261.
- Rohrer, J.S., Basumallick, L. and Hurum, D.** (2013) High-performance anion-exchange chromatography with pulsed amperometric detection for carbohydrate analysis of glycoproteins. *Biochem. (Mosc)* **78**, 697-709.
- Roy, A., Kucukural, A. and Zhang, Y.** (2010) I-TASSER: a unified platform for automated protein structure and function prediction. *Nat. Protoc.*, **5**, 725-738.
- Sluiter, A., Hames, B., Ruiz, R., Scarlata, C., Sluiter, J., Templeton, D. and Crocker, D.** (2008) Determination of structural carbohydrates and lignin in biomass. *Lab. Anal. Proc.*, **1617**, 1-16.
- St-Pierre, B. and De Luca, V.** (2000) Evolution of acyltransferase genes: origin and diversification of the BAHD superfamily of acyltransferases involved in

- secondary metabolism. In *Recent Adv. Phytochem.* (Romeo, J.T., Ibrahim, R., Varin, L. and De Luca, V. eds): Elsevier, pp. 285-315.
- Terrett, O.M. and Dupree, P.** (2019) Covalent interactions between lignin and hemicelluloses in plant secondary cell walls. *Curr. Opin. Biotechnol.*, **56**, 97-104.
- Trapnell, C., Hendrickson, D.G., Sauvageau, M., Goff, L., Rinn, J.L. and Pachter, L.** (2013) Differential analysis of gene regulation at transcript resolution with RNA-seq. *Nat. Biotechnol.*, **31**, 46-53.
- Van Acker, R., Vanholme, R., Storme, V., Mortimer, J.C., Dupree, P. and Boerjan, W.** (2013) Lignin biosynthesis perturbations affect secondary cell wall composition and saccharification yield in *Arabidopsis thaliana*. *Biotechnol. Biofuels*, **6**, 46.
- Van Der Spoel, D., Lindahl, E., Hess, B., Groenhof, G., Mark, A.E. and Berendsen, H.J.C.** (2005) GROMACS: fast, flexible, and free. *J. Comput. Chem.*, **26**, 1701-1718.
- Withers, S., Lu, F., Kim, H., Zhu, Y., Ralph, J. and Wilkerson, C.G.** (2012) Identification of grass-specific enzyme that acylates monolignols with *p*-coumarate. *J. Biol. Chem.*, **287**, 8347-8355.
- Yang, J., Yan, R., Roy, A., Xu, D., Poisson, J. and Zhang, Y.** (2015) The I-TASSER suite: protein structure and function prediction. *Nat. Methods*, **12**, 7-8.
- Zhang, Y.** (2008) I-TASSER server for protein 3D structure prediction. *BMC Bioinformatics*, **9**, 40.

Supporting Material

CHAPTER 3. Suppression of a BAHD acyltransferase decreases *p*-coumaroyl on arabinoxylan and improves biomass digestibility in the model grass *Setaria viridis*

Thatiane R. Mota, Wagner R. de Souza, Dyoní M. Oliveira, Polyana K. Martins, Bruno L. Sampaio, Felipe Vinecky, Ana P. Ribeiro, Karoline E. Duarte, Thályta F. Pacheco, Norberto K. V. Monteiro, Raquel B. Campanha, Rogério Marchiosi, Davi S. Vieira, Adilson K. Kobayashi, Patrícia A. O. Molinari, Osvaldo Ferrarese-Filho, Rowan A. C. Mitchell, Hugo B. C. Molinari, Wanderley D. dos Santos

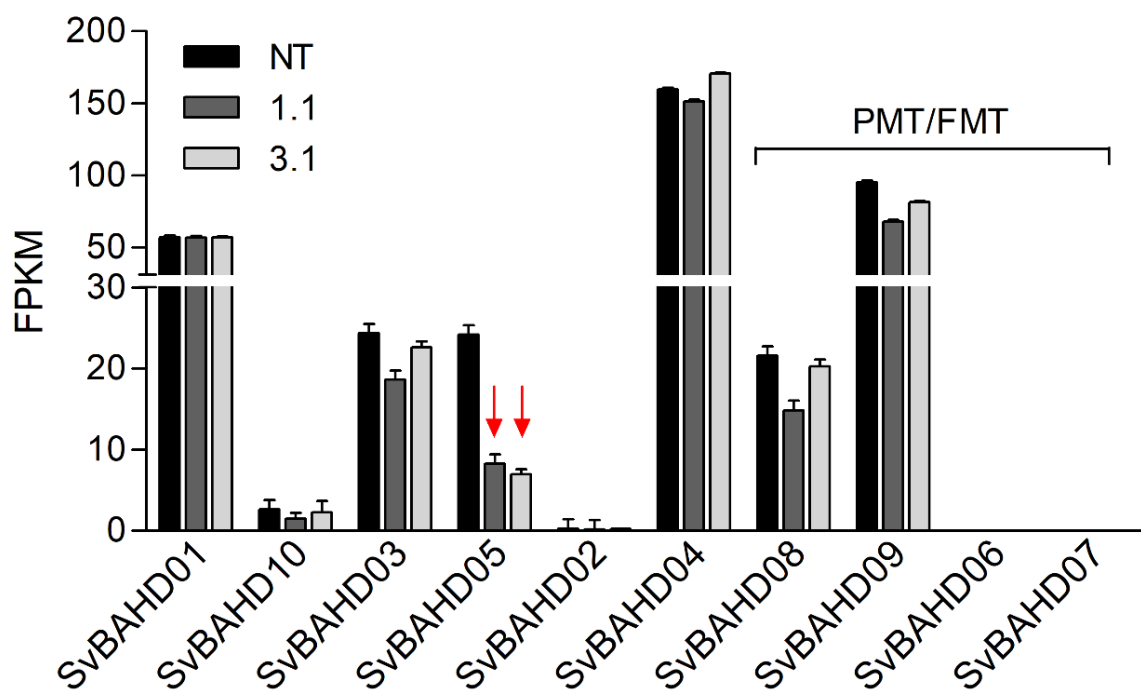


Fig. S2. RNA-seq analysis of BAHD gene expression in *Setaria viridis* SvBAHD05 RNAi lines. Genes associated with monolignol acylation (PMT and FMT) are indicated. Transcript abundance is measured as fragment per kilobase per million mapped reads.

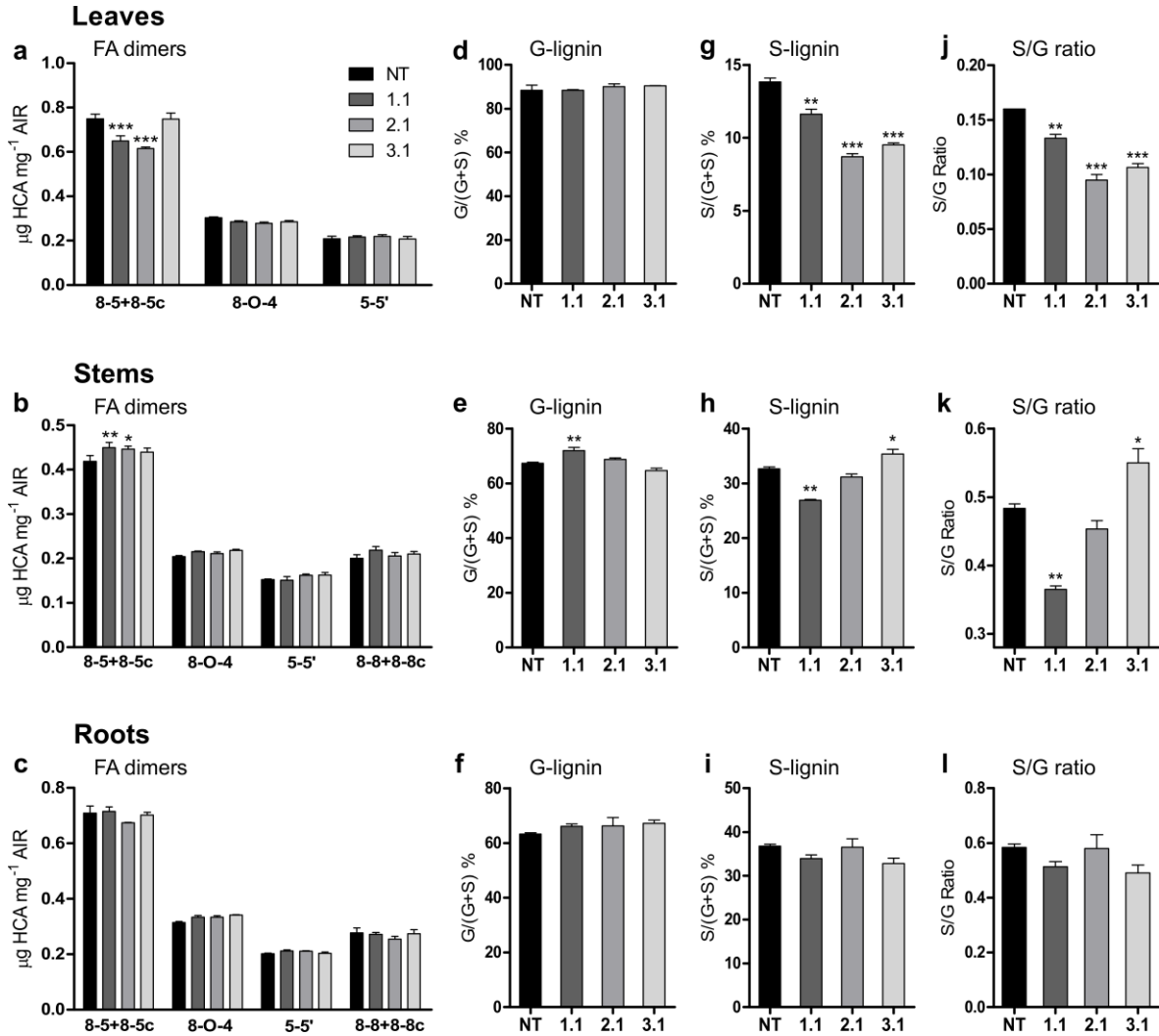


Fig. S3. Dehydrodimers (DiFAs) and lignin monomers. (a-c) Dehydrodimers of ferulic acid (FA) in leaves (a), stems (b), and roots (c) of cell walls of *Setaria viridis* from non-transformed (NT) and plants from the 1.1, 2.1 and 3.1 RNAi silenced lines ($n = 4$). (d-l) Lignin monomers: guaiacyl – G (d-f), syringyl – S (g-i), and S/G ratio (j-l) released by nitrobenzene oxidation of cell walls in leaves, stems and roots of the non-transformed (NT) and transgenic lines 1.1, 2.1 and 3.1 ($n = 4$). Statistical differences of transgenic lines compared to NT are with (*) from ANOVA at $*P < 0.05$, $**P < 0.01$, $***P < 0.001$.

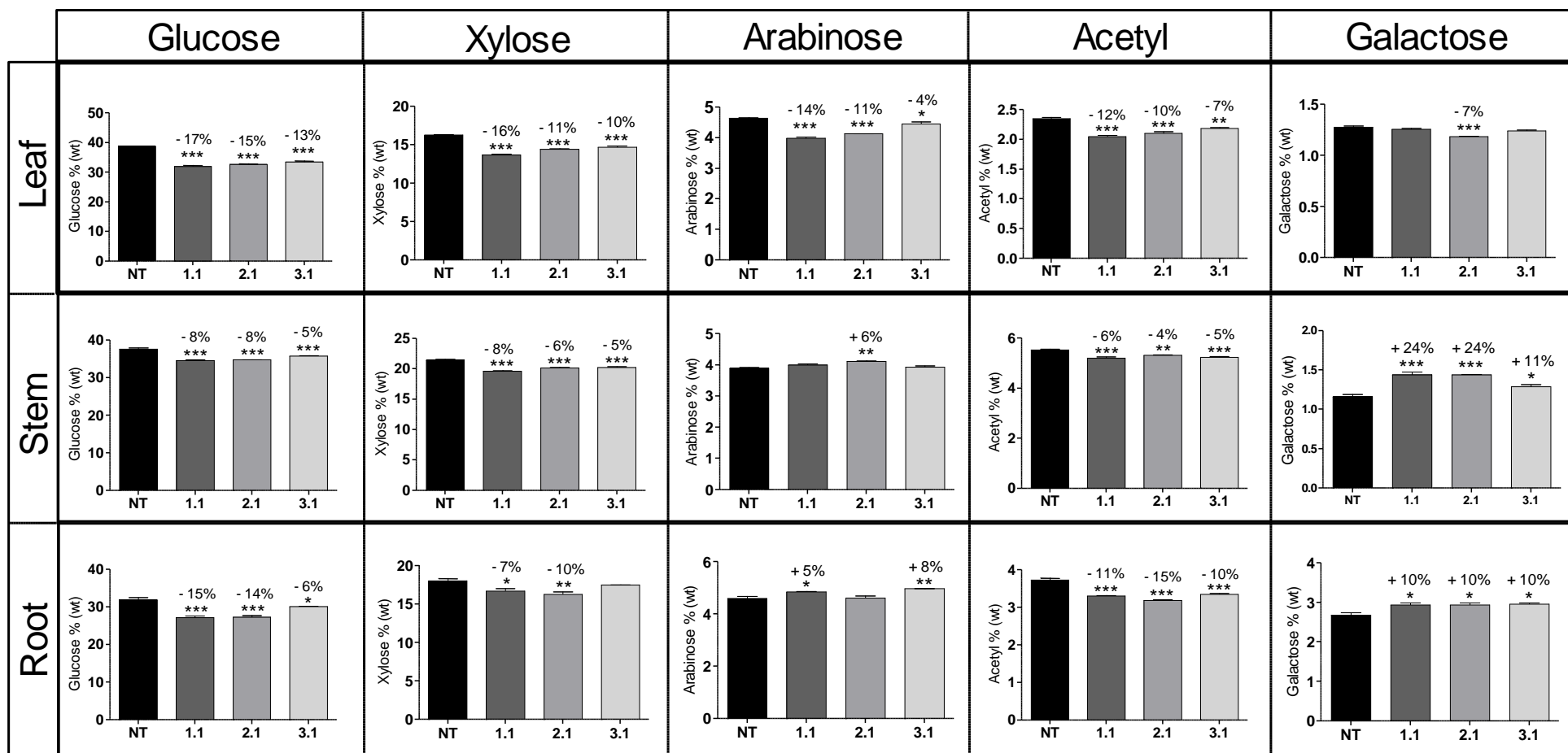


Fig. S4. Monosaccharide and acetyl composition. Monosaccharide and acetyl composition of alcohol insoluble residue (AIR) from leaves, stems, and roots of non-transformed (NT) and *SvBAHD05* RNAi transgenic plants descended from the lines 1.1, 2.1 and 3.1. Values are means (%) \pm SEM from 4 different replicates of transgenic lines compared to NT. Statistical differences are with (*) from ANOVA at $*P < 0.05$, $**P < 0.01$, $***P < 0.001$.

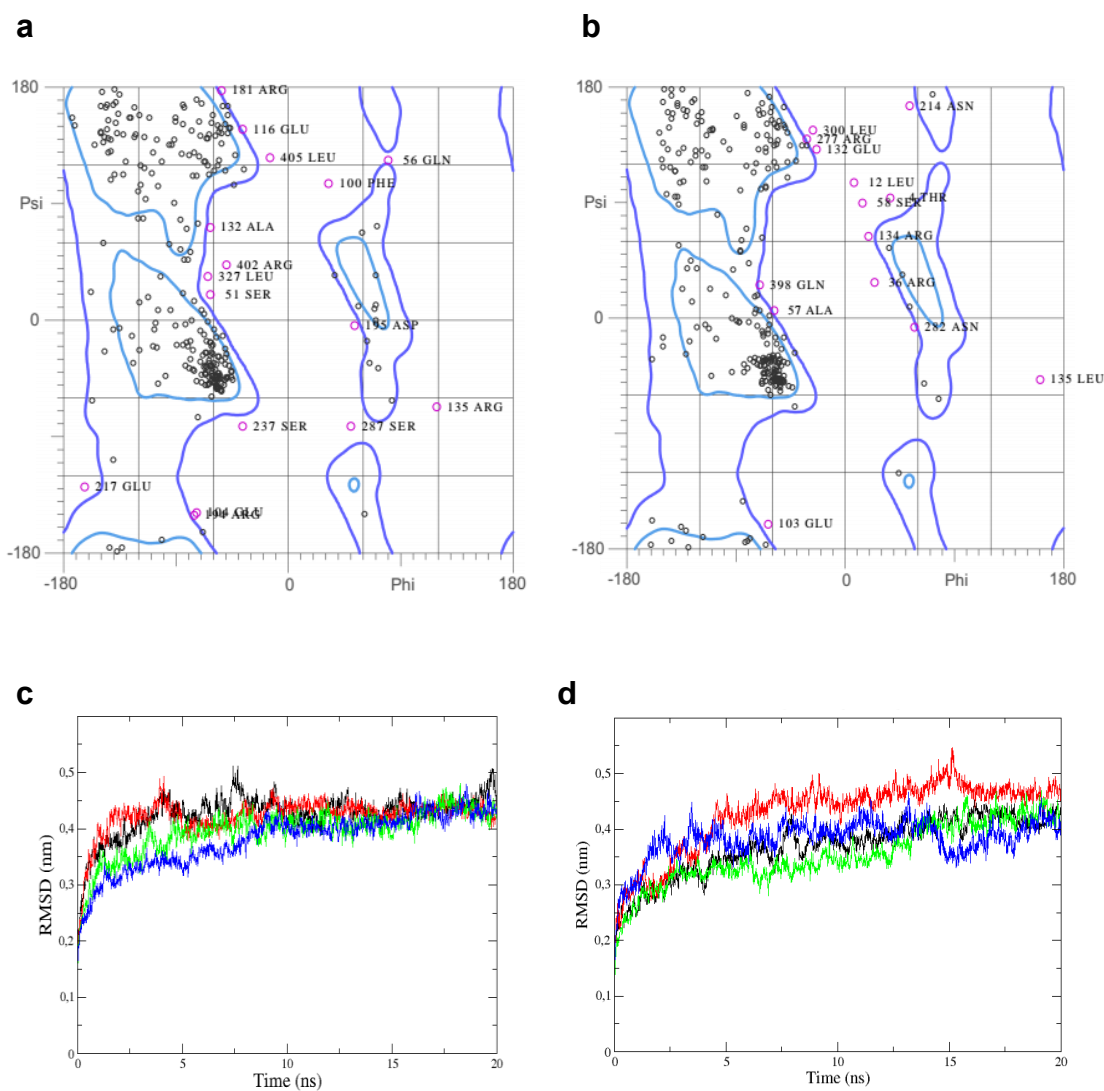


Fig. S5. Ramachandran plots and RMSD analysis. (a,b) Ramachandran plots of molecular modeling of SvBAHD05 from *Setaria viridis* (a) and BdAT1 from *Brachypodium distachyon* (b). (c,d) RMSD analysis of MD simulations from: the pCA and FA complexes with SvBAHD05 and BdAT1 were named of pCA-Sv (red), FA-Sv (black), pCA-Bd (blue), and FA-Bd (green), respectively (c), and the pCA-Araf and FA-Araf complexes with SvBAHD05 and BdAT1 were named of pCA-Araf-Sv (red), FA-Araf-Sv (black), pCA-Araf-Bd (blue), and FA-Araf-Bd (green), respectively (d).

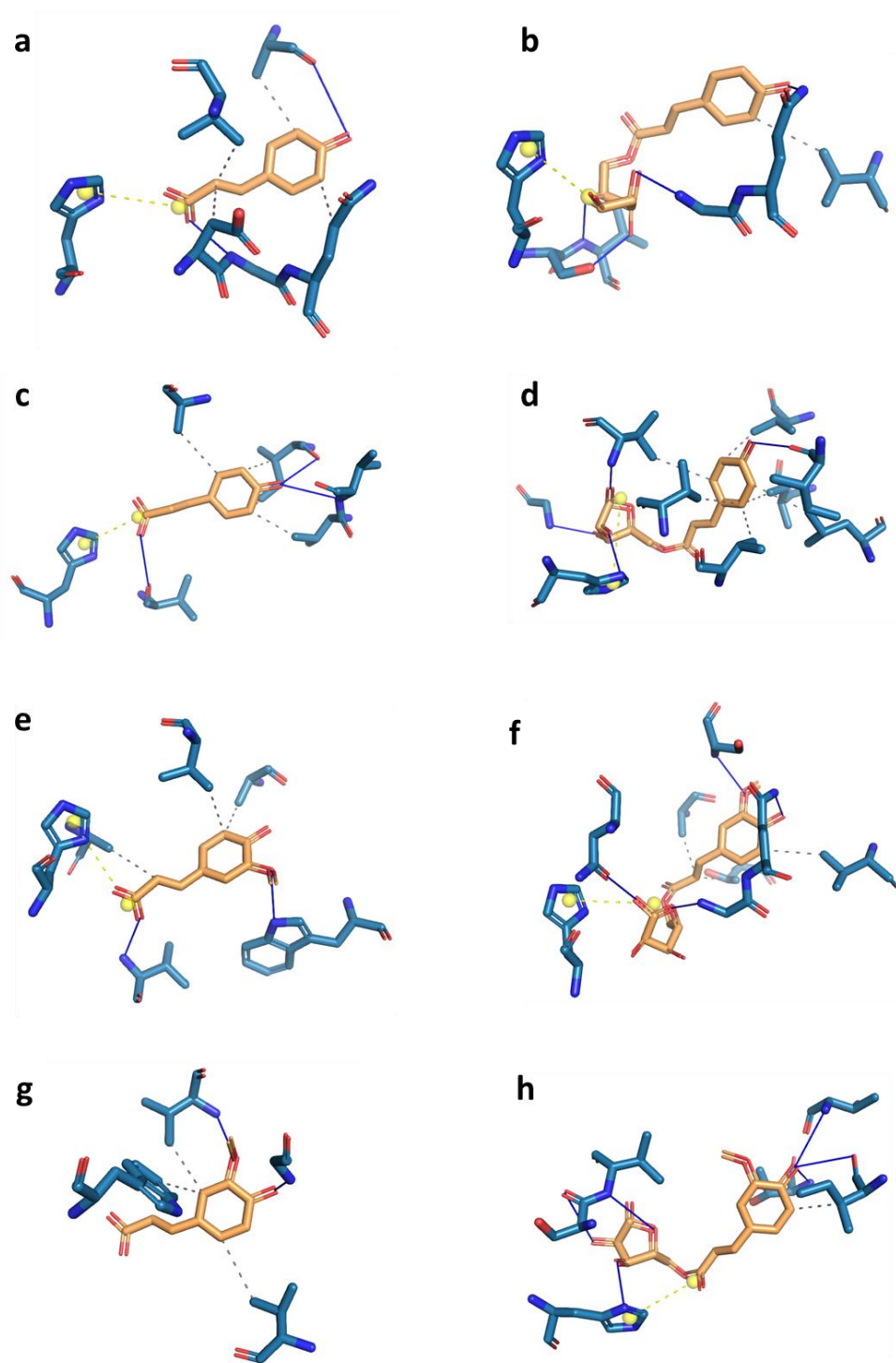


Fig. S6. Structural analysis of the catalytic site. (a-h) Interaction between protein and the ligand with the more stable conformation from *pCA-Sv* (a), *pCA-Araf-Sv* (b), *pCA-Bd* (c), *pCA-Araf-Bd* (d), *FA-Sv* (e), *FA-Araf-Sv* (f), *FA-Bd* (g), *FA-Araf-Bd* (h).

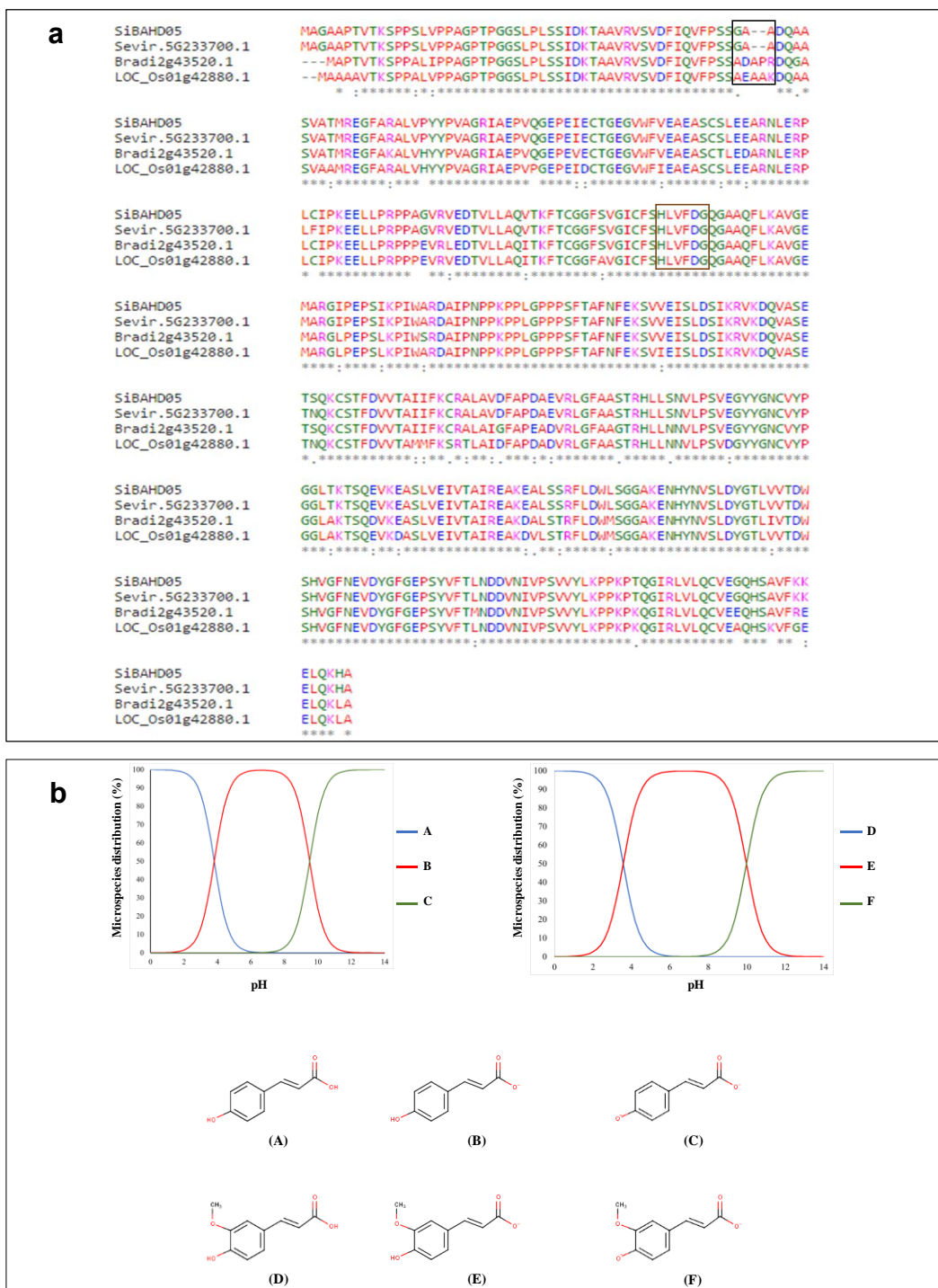


Fig. S7. Alignment comparison and microspecies distribution. (a) Alignment comparison of region targeted by BAHD05 from *Setaria viridis* with other phylogenetically related grasses *Setaria italica* (Si), *Brachypodium distachyon* (Bradi) and *Oryza sativa* (LOC_Os). Only a few amino acids distinguish SvBAHD05 and BdAT1, the conserved motif represented by HXXXDG, typical of BAHD acyltransferases, is present in the proteins, with XXX indicating leucine (L), valine (V) and phenylalanine (F). (b) Microspecies distribution as a function of pH for *p*-coumaric acid (lines A, B and C) and ferulic acid (lines D, E and F) in the protonation states.

Table S1. Percentage of silencing for *SvBAHD05* transgenic RNAi lines.

Tissue	Line	% Silencing
Leaf	1.1	48.4
	2.1	68.8
	3.1	86.2
	4.4	75.8
	5.4	57.6
Stem	1.1	44.9
	2.1	72.8
	3.1	90.4
	4.4	83.2
	5.4	68.1
Root	1.1	88.4
	2.1	86.5
	3.1	97.7
	4.4	93.2
	5.4	84.5

Table S2. *pCA/FA* ratio by biochemical data of cell walls of *Setaria viridis* from non-transformed (NT) and transgenic plants from the lines 1.1, 2.1 and 3.1 ($n = 4$; error bars \pm SEM; statistical differences of transgenic lines compared to NT are with (*) from ANOVA at $*P < 0.05$, $**P < 0.01$, $***P < 0.001$).

	Ratio <i>pCA/FA</i>			
	NT	1.1	2.1	3.1
Leaf	1.206	0.782***	0.801**	0.801**
Stem	1.922	1.875	1.712***	1.797*
Root	2.887	2.159*	1.687***	1.860***

Table S3. All configurations predicted by molecular docking of *pCA*, *FA*, *pCA-Araf* and *FA-Araf* to SvBAHD05 and BdAT1 at HXXXD motifs and their binding energy.

<i>pCA-Sv</i>		<i>FA-Sv</i>		<i>pCA-Bd</i>		<i>FA-Bd</i>	
Configuration	Energy (Kcal/mol)	Configuration	Energy (Kcal/mol)	Configuration	Energy (Kcal/mol)	Configuration	Energy (Kcal/mol)
1	-6.5	1	-6.5	1	-6.1	1	-6.5
2	-6.4	2	-6.4	2	-6.1	2	-6.2
3	-6.1	3	-6.1	3	-6.0	3	-6.0
4	-5.9	4	-6.0	4	-5.8	4	-6.0
5	-5.9	5	-6.0	5	-5.6	5	-5.9
6	-5.7	6	-5.9	6	-5.6	6	-5.8
7	-5.5	7	-5.8	7	-5.5	7	-5.8
8	-5.5	8	-5.7	8	-5.5	8	-5.8
9	-5.4	9	-5.7	9	-5.4	9	-5.7

<i>pCA-Araf-Sv</i>		<i>FA-Araf-Sv</i>		<i>pCA-Araf-Bd</i>		<i>FA-Araf-Bd</i>	
Configuration	Energy (Kcal/mol)	Configuration	Energy (Kcal/mol)	Configuration	Energy (Kcal/mol)	Configuration	Energy (Kcal/mol)
1	-7.7	1	-7.7	1	-7.8	1	-7.9
2	-7.6	2	-7.6	2	-7.8	2	-7.7
3	-7.4	3	-7.5	3	-7.8	3	-7.4
4	-7.4	4	-7.5	4	-7.6	4	-7.4
5	-7.4	5	-7.5	5	-7.6	5	-7.4
6	-7.3	6	-7.4	6	-7.5	6	-7.4
7	-7.3	7	-7.4	7	-7.5	7	-7.3
8	-7.2	8	-7.3	8	-7.4	8	-7.3
9	-7.2	9	-7.3	9	-7.3	9	-7.2

Table S4. Primers used in the RT-qPCR. Reference genes: *EF α* (elongation factor 1-alpha) and *IF4 α* (eukaryotic initiation factor 4-alpha) for leaves and stems, *CAC* (clathrin adaptor complex), and *CUL* (cullin) for roots.

Gene symbol	Description	Phytozome ID	Primer sequences (5' - 3')
<i>EF1a</i>	Elongation factor 1-alpha	Sevir.3G272400	F:TGGTATGCTTGTCACCTTTGGT R:CTCGTGGTGCATCTCAACTGA
<i>eIF4a</i>	Eukaryotic initiation factor 4-alpha	Sevir.1G088000	F:GTCTGCTAAGGTGCTGGATAAA R:ACCACTCCTCCAGAACATAGA
<i>CAC</i>	Clathrin adaptor complex	Sevir.1G284400	F:CTGCTTCTGGTCTTCGTGTT R:GTATGATCCTGCTCTCGTGATG
<i>CUL</i>	Cullin	Sevir.3G038900	F: TCTCATCACGAGGGACTACTT R: CTTGCCAACAACCACCAATC
<i>BAHD05</i>	Acyltransferase	Sevir.5G233700	F: TGGTGCCAAGGAAAACCACT R: TTGGGTTC AACGAGGTGGAC